FAT AND FIT: METABOLIC CHANGES IN SKELETAL MUSCLE OF LIVER FATTY ACID-BINDING PROTEIN KNOCKOUT MICE

By

HELI XU

A dissertation submitted to the

School of Graduate Studies

Rutgers, The State University of New Jersey

In partial fulfillment of the requirements

For the degree of

Doctor of Philosophy

Graduate Program in Nutritional Sciences

Written under the direction of

Judith Storch

And approved by

_____

_____

_____

_____

New Brunswick, New Jersey

May, 2019

ABSTRACT OF THE DISSERTATION

Fat and Fit: Metabolic Changes in Skeletal Muscle

of Liver Fatty Acid-Binding Protein Knockout Mice

By HELI XU

Dissertation director:

Judith Storch

Liver fatty acid-binding protein (LFABP, FABP1) is abundantly expressed in the liver and small intestine, and thought to facilitate hepatic and intestinal lipid trafficking into various metabolic pathways with its high binding affinity for long chain fatty acids. Moreover, LFABP has also been implicated in regulating systemic energy homeostasis based on studies of LFABP null (LFABP$^{-/-}$) mice. We and others have previously reported that LFABP$^{-/-}$ mice exhibit greater body weight gain and body fat mass in response to high fat feeding compared with wild-type (WT) mice. Despite being more obese, however, LFABP$^{-/-}$ mice were protected from high fat feeding-induced decline in exercise capacity, showing an approximate doubling of running distance compared with WT mice on the high fat diet. In studies aimed at understanding the metabolic changes in skeletal muscle underlying this surprising exercise phenotype in LFABP$^{-/-}$ mice, we found significantly higher triglyceride and glycogen content, as well as increased mitochondrial enzyme activities and fatty acid oxidation capacity in the resting muscles of LFABP$^{-/-}$ mice, suggesting a greater substrate storage and mitochondrial function at resting state. During a low intensity exercise, LFABP$^{-/-}$ mice showed a preference for carbohydrate utilization in the first 10

min of the exercise and switched to a higher lipid utilization compared with WT during the rest 10 min of exercise, with greater exercise-dependent decreases in muscle glycogen stores and elevated free fatty acid in the plasma after exercise. Using cellular bioenergetics measurements, primary myoblasts from high fat-fed LFABP$^{-/-}$ mice showed a higher respiratory capacity compared with WT mice, supporting the increased exercise capacity of LFABP$^{-/-}$ mice. Interestingly, primary myotubes from chow-fed mice treated with fatty acids only showed modest difference between the genotypes, suggesting that apart from a high concentration of plasma FAs, other circulating mediators may be required for the improved muscle energy metabolism in high fat fed-LFABP$^{-/-}$ mice. In examining potential interorgan signaling possibilities, we found similar insulin sensitivity in skeletal muscle between the genotypes, suggesting an insulin-independent mechanism mediating the muscle metabolic changes in LFABP$^{-/-}$ mice. Moreover, we found decreased FGF21 expression levels in the liver and trending lower FGF21 levels in the plasma of LFABP$^{-/-}$ mice, despite our previous report that LFABP$^{-/-}$ mice showed trending higher plasma levels of adiponectin, a downstream target of FGF21. However, we found similar FGF21 sensitivity in epidydimal adipose tissues between the genotypes and trending lower expression levels of adiponectin in the epidydimal adipose tissues, suggesting that FGF21-meidated adiponectin production and secretion may be enhanced in other fat depots. Overall, muscle metabolic reprogramming in LFABP$^{-/-}$ mice underlies their resistance to high fat feeding-induced decline in exercise capacity, including increased substrate availability and improved mitochondrial function in response to high fat diets. Since LFABP is not expressed in the muscle, these alterations in muscle energy metabolism of LFABP$^{-/-}$ mice appear to be induced signaling molecules in the plasma, possibly involving adiponectin.

Acknowledgements

I would like to thank Dr. Judith Storch for being my Ph.D. advisor, offering me Graduate Assistantship and giving me tremendous support throughout my doctoral studies. I feel very grateful to have had the opportunity to work in her laboratory and learn from her and all the lab members. I am also thankful that Dr. Storch has always tried to create a very friendly work environment at the lab, as it has helped me a lot in stress management. I would also like to thank all my helpful and supportive committee members: I took my first nutrition class with Dr. Malcolm Watford and since then, he has provided a lot of helpful training and advice on metabolic regulation in my coursework and research project; Dr. Tracy Anthony has inspired me a lot with her drive and passion in research, and I have been very fortunate to have her helpful and specific guidance on my project; Dr. Gregory Henderson has been very helpful with his expertise on exercise physiology since our first observation of the exercise phenotype, and I have learned a lot from all the discussions via email and phone.

I would like to thank the wonderful group of people in the Storch Lab. I really appreciate the help from Yinxiu Zhou, our senior lab technician. She provided very thoughtful training when I first joined the lab, and has helped me a lot with many experiments in my project, especially those involving animal surgery. I would like to thank Atreju Lackey and Hiba Alhatim, two other PhD students, for their suggestions, support and friendly talks in the past few years. I really enjoyed working with them in the lab and talking with them as friends. I would like to thank Dr. Olga Ilnytska and Ran Li for their helpful discussions from different perspectives and training in cell culture techniques. I would also like to thank all the undergraduate students in the lab that I have had pleasure working with, including Anam Fatima, Cristina Panetta and Zoe Sifnakis. They have helped me with various parts of my project and working with them gave me the

opportunity to learn how to be a mentor. I hope the experience will help them in their future endeavors.

I have also been fortunate to receive help and support from other faculty members and staff in the Nutritional Sciences Graduate Program and Nutritional Sciences Department. I would like to thank Dr. Harini Sampath and Sai Santosh for their help in experiments on mitochondria and cellular bioenergetic analyses. I would like to thank Dr. Loredana Quadro and Dr. Youn-kyung Kim for the helpful discussion and suggestions on cellular bioenergetic analyses. I would like to thank Dr. David Cohen and Dr. Norihiro Imai for their help in primary myoblasts isolation procedures, Dr. Mike Verzi and Dr. Lei Chen for their help with cryosectioning, and Dr. Sue Shapses and Dr. Lihong Hao for giving me access to the LiCOR imaging system. I would like to thank Dr. Carol Byrd-Bredbenner, our graduate program director, for always making herself available for our questions, and introducing opportunities to improve our academic performance and career development. I am also thankful that many faculty members have invited speakers to give us seminars, lectures and workshops, from which I got to learn about pioneer research and interact with researchers from various background. I would like to thank DJ Polacik, Kevin McCarthy and Laura Amador for their assistance in ordering supplies, class registration and many other crucial administrative processes.

I would also like to thank the Rutgers Center for Lipid Research for not only hosting interesting seminars and symposiums, but also providing a platform for all the students and postdocs to present their research. I would like to especially thank Dr. George Carman for always being encouraging, and Dr. Grace Guo for the insightful discussion on liver metabolism.

In addition, I would like to thank the students that have been very friendly and supportive in our graduate program, especially Cheng Li, Qing Chen and Bryn Yeomans. I would also like to thank

the Graduate Student Organization in our graduate program for their work in bringing the students together, hosting the annual conference and introducing other activities in our campus life.

Last but not least, I would like to thank my parents for supporting my pursuit, even though it means we wouldn't be able to see each other very often. My gratitude towards them will always keep me moving forward. I would also like to thank Ran Li for his patience and support in the craziest times. None of this would have been possible without them.

Table of Contents

List of Tables

List of Figures

Chapter 1

Introduction and Literature Review

FABP introduction

Mammalian fatty acid binding proteins (FABPs) are abundant cytoplasmic proteins with high affinities for certain hydrophobic ligands, such as long-chain fatty acid, eicosanoids and monoacylglycerols[1,2]. FABPs are widely expressed in almost all tissues with many tissue-specific homologues, and some cell types have more than one FABP. So far, at least nine members of the FABP family have been identified, namely liver (L-), intestinal (I-), heart (H-), adipocyte (A-), epidermal (E-), ileal (Il-), brain (B-), myelin (M-) and testis (T-) FABPs.

Table 1-1. Family of fatty acid binding proteins (FABPs)[1,3].

Gene	Common name	Alternative names	Expression site(s)
Fabp1	Liver FABP	L-FABP	Liver, intestine
Fabp2	Intestinal FABP	I-FABP	Intestine
Fabp3	Heart FABP	H-FABP mammary-derived growth inhibitor (MDGI)	Heart, skeletal muscle, brain, kidney, adrenal gland, mammary gland
Fabp4	Adipocyte FABP	A-FABP, aP2	Adipocyte, macrophage
Fabp5	Epidermal FABP	E-FABP, mal1, KFABP	Skin, adipose tissue, mammary gland, brain, intestine, kidney, liver
Fabp6	Ileal FABP	Il-FABP, gastrotropin	Ileum, ovary
Fabp7	Brain FABP	B-FABP, MRG	Brain
Fabp8	Myelin FABP	M-FABP, PMP2	Peripheral nervous system
Fabp9	Testis FABP	T-FABP	Testis

(Adapted from Storch and Corsico, Ann Rev Nutr 2008)

FABPs have been proposed to modulate various aspects of cellular function. As intracellular lipid chaperones, FABPs are thought to escort fatty acids (FAs) into different lipid metabolizing pathways. In the meantime, by decreasing the unbound FA concentration inside the cell, FABPs also increase the FA concentration gradient and enhance FA uptake[4-6]. Moreover, FABPs also play an important role in transcriptional regulation of many genes involved in lipid metabolism, sometimes including their own expression levels. For example, liver FABP (LFABP, FABP1), adipocyte FABP (AFABP, FABP4) and epidermal FABP (EFABP, FABP5) have been found to interact with peroxisome proliferator-activated receptors (PPARs), facilitating FA-induced PPAR activation[7,8]. As part of the PPAR-mediated response, LFABP and AFABP expression have also been shown to be upregulated[9,10]. Interestingly, increased AFABP is also shown to mediate proteosomal degradation of PPARγ in adipocytes and macrophages and inhibit adipogenesis via a negative feedback mechanism[11]. In addition to coordinating lipid responses, certain FABPs have also been implicated in modulating cell growth and proliferation. For instance, LFABP is thought to be required in Caco-2 cell proliferation[12], as well as in carcinogen-induced mitogenesis in hepatocytes by interacting with the carcinogens and their metabolites[13,14]; Heart FABP (HFABP, FABP3) is shown to not only regulate cardiomyocyte differentiation in mouse neonatal heart, but also promote mammary gland differentiation and act as a breast tumor suppressor together with AFABP[15-18].

FABP content in a given cell type is thought to reflect the cellular capacity for lipid metabolism. In hepatocytes, enterocytes, adipocytes and cardiac myocytes, as active sites for fatty acid metabolism, the respective FABPs comprise 1-5% of all soluble cytosolic proteins[5]. On the other hand, the relationship between FABP content and lipid-metabolizing capacity depend on various physiological, pathological and pharmacological conditions in different tissues[19]. For example, high dietary fat was found to increase FABP content in liver, adipose and intestine, with no

effect on FABPs in muscle, heart and kidney[19,20]. However, the high fat feeding-induced peroxisomal proliferator response with upregulation in lipid-metabolizing genes has been observed not only in the liver, intestine and adipose, but also in the muscle, without alteration in FABP expression[21-26]. At postnatal development, FABP content and fatty acid oxidation capacity increased concomitantly in heart and skeletal muscle till up to 70 days after birth but not in liver or kidney[19]. Conditions with elevated circulating fatty acid could also lead to an increase in FABP expression in muscle, as found in endurance training[27]. Overall, the regulation of FABPs expression seems to be tissue-specific in response to environmental stimuli.

Recent studies of the roles of FABPs in metabolic disease also highlight their potentials as therapeutic targets for metabolic syndromes[28]. In particular, starting with the initial observation that AFABP null (AFABP$^{-/-}$) mice were protected from diet-induced insulin resistance[29], the development of high affinity and selective AFABP inhibitors has yielded promising effects on improving insulin sensitivity, fatty liver disease and atherosclerosis in both genetic and dietary mouse models of obesity and diabetes[30]. In addition, AFABP and EFABP are thought to play an important role in the formation of atherosclerosis by modulating cholesterol trafficking and inflammatory responses in macrophages[31]. Other members of the FABP family may also be targeted to treat metabolic disorders as their functions become better understood, and LFABP could be one of the important candidates. In response to high fat feeding, despite being more obese, LFABP$^{-/-}$ mice showed signs of being “metabolically healthy”, with similar glucose tolerance, insulin resistance, blood lipid profile and even an improved exercise capacity compared with the high fat-fed WT counterparts. A better understanding of the underlying alterations in energy metabolism and interorgan signaling associating with this phenotype will potentially promote development of pharmaceutical agents to manage or improve metabolic syndromes.

Lipid metabolism in liver

The liver plays a central role in lipid metabolism, including storage, synthesis and redistribution. Non-esterified fatty acids (NEFAs) from circulation enter the liver in proportion to their concentration via diffusion (short and medium chain FAs also directly enters the liver after absorption through portal vein), plasma membrane FABP, fatty acid transport protein (FATP) or fatty acid translocase (CD36)[32-34]. Within the hepatocytes, LFABP is thought to facilitate lipid trafficking into different metabolic or signaling pathways by binding not only NEFAs, but also acyl-CoAs and modulating acyl-CoA synthesis[35-39]. Several isoforms of long chain acyl-CoA synthase (ACSL) have also been identified to mediate compartmentalized fatty acid metabolism[40-42]. As a protective mechanism against fatty acid-induced lipotoxicity, intracellular levels of unbound NEFAs and fatty acyl-CoAs are usually kept very low with their rapid oxidation or incorporation into neutral and polar lipids[43]. On the other hand, de novo lipogenesis, where acetyl-CoA is converted to FAs, occurs in response to elevated plasma glucose and insulin signaling and may contribute to hepatic steatosis[44].

FA oxidation occurs in mitochondria and peroxisomes through the β-oxidation pathways. Long chain fatty acyl-CoAs (FA of 14-22 carbons) are imported into the mitochondria via carnitine palmitoyl transferase I (CPT1) on the outer mitochondrial membrane, forming acyl-carnitines, and further converted to acyl-CoA by CPT2 on the inner mitochondrial membrane. Under conditions of increased NEFAs uptake, incomplete mitochondrial FA oxidation in the liver induces ketogenesis, where acetyl-CoA are converted into ketone bodies, acetoacetate, β-hydroxybutyrate and acetone rather than entering the TCA cycle. Short and medium chain fatty acyl-CoAs (FA of 14 carbons or less) permeate the mitochondrial membranes and are activated by acyl-CoA synthetase in the mitochondrial matrix[45]. While mitochondria are responsible for the oxidation of short, medium and long chain FAs, peroxisomes are responsible for the

oxidation of very long chain FAs. However, due to the lack of the electron transfer chain present in mitochondria, peroxisomal β-oxidation is not coupled to ATP synthesis, but rather produces heat and hydrogen peroxide (H_2O_2). After the initial oxidation of very long chain FAs in peroxisome, octanoyl-CoA is generated and transported into mitochondria for further oxidation[46,47]. Peroxisomal FA oxidation is also important in handling long chain dicarboxylic acids, the product of hepatic FA ω-oxidation in endoplasmic reticulum that cannot metabolized directly by the mitochondria[48].

In addition to oxidation, many of the NEFAs are esterified to form glycerolipids including triglycerides (TGs) and glycerophospholipids on the microsomal membrane. Glycerophospholipids (and other polar lipids) are transferred to the membrane and incorporated into pre-HDL particles[49], whereas TGs are stored in the cytosolic pool as lipid droplets or secreted into circulation as VLDL[50]. The rate of VLDL production is not only affected by the synthesis and degradation of apoprotein B, a key component of VLDL, but also by the chain length, extent of saturation and source of FA substrates[51,52]. For example, while exogenous palmitate (16:0) and oleate (18:1 n-9) have been shown to increase TG-rich VLDL, an opposite effect has been observed with several medium chain FAs and n-3 polyunsaturated FAs such as octanoate (8:0) and docosahexaenoic acid (DHA, 22:6 n-3)[53-55], respectively. In contrast to the profound effects of exogenous (plasma) FAs on VLDL production and secretion, de novo lipogenesis in the liver does not affect the rate of VLDL export. Indeed, enhanced VLDL production induced by high carbohydrate diets has been shown to utilize exogenous FAs rather than endogenously synthesized FAs; inhibition of glucose-6-phosphatase leads to increased de novo lipogenesis without stimulating VLDL secretion, and the enhanced de novo lipogenesis in ob/ob mice is not associated with differences in the VLDL production rate[56-58]. As the only FABP abundantly expressed in the liver, LFABP play important roles in many of these metabolic

pathways, including transporting FAs and acyl-CoAs to different organelles, as well as interacting with and delivering FA and other ligands to transcription factors (e.g. PPARα) to regulate lipid metabolism.

LFABP in liver, intestine and beyond

Liver FABP (LFABP, FABP1) is abundant in the liver cytoplasm, and also highly expressed in intestine, and to a lower extent, in pancreas and kidney[6]. LFABP often co-expresses with other members of the FABP family, but it is the only FABP expressed in liver[8,59]. In contrast to other members of the FABP family, LFABP binds not only long chain FAs, but also acyl-CoAs, prostaglandins, bile acids, heme, hydroxyl metabolites of fatty acids, lysophosphatidic acids, monoacylglycerols, endocannabinoids such as N-acylethanolamide and 2-arachidonoylglycerol, as well as other hydrophobic ligands[2,6,60]. This extensive ligand binding property provides a structural basis for its pleiotropic biological function.

Early experiments measured the influence of enhanced L-FABP expression in mouse fibroblasts. Using cis-parinaric acid and radio-labeled fatty acid, LFABP-transfected fibroblasts showed a ~50% increase in fatty acid uptake, and rapid incorporation into triacylglycerols and phospholipids[61]. Using a nonesterifiable fluorescent fatty acid probe, NBD-stearate, L-FABP-expressing cells increased NBD-stearate uptake 1.7-fold compared with control cells in single-cell fluorescence imaging experiments, with increased cytoplasmic diffusion and lateral membrane mobility[62]. LFABP levels were also manipulated in HepG2 cells using peroxisome proliferators or antisense LFABP mRNA, where the net uptake of oleate was shown to correlate directly with the LFABP content of the cells[63].

To examine the function of LFABP in vivo, two independent laboratories generated LFABP$^{-/-}$ mice on the C57BL/6 background in 2003[64,65]. Chow-fed LFABP$^{-/-}$ mice showed a similar body weight and serum lipid profiles compared with their wild-type (WT) littermates. While fatty acid uptake into liver and the fatty acid-binding capacity of liver cytosol were drastically reduced in LFABP$^{-/-}$ mice, the overall hepatic levels of total lipids, non-esterified fatty acids, and triacylglycerols remained unchanged[64,65]. There was also a significant decrease in protein content in the 14kDa region, where almost all intracellular lipid-binding proteins should be, eliminating the possibility of a compensatory increase in other members of FABP family[5,65]. In response to fasting, LFABP$^{-/-}$ mice were observed to have a decreased accumulation of hepatic triglycerides and a blunted increase in fatty acid oxidation[64].

Further study also found lowered fatty acid oxidation rates in intact hepatocytes from LFABP$^{-/-}$ mice on standard, ketogenic and diabetogenic diets under fasting conditions, while the circulating free fatty acid was trending higher[66]. However, there were no differences in fatty acid oxidation rates when the liver homogenates from LFABP$^{-/-}$ mice were incubated with albumin-bound fatty acids, along with similar expression levels of enzymes in β-oxidation pathway (MCAD, ACO)[66] and membrane fatty acid transporters (CD36, FATP)[64]. These results support an intrahepatic defect in fatty acid uptake and trafficking in LFABP$^{-/-}$ mice, rather than restriction in substrate supply or decreased capacity in fatty acid oxidation.

Although mechanisms underlying LFABP-mediated modulation of fatty acid metabolism are not well understood yet, one of the most studied aspects is the interaction between LFABP and

peroxisome proliferator-activated receptors (PPARs), especially PPARa. PPARs are a family of ligand-activated nuclear receptors that induce transcription of multiple genes encoding proteins involved in fatty acid and glucose metabolism, and dysregulation of PPARa (the major PPAR isoform in liver) is associated with metabolic diseases like diabetes and obesity[67,68]. LFABP was shown to directly interact with PPARa using pull-down assay, immunocoprecipitation, altered circular dichroic spectra and altered fluorescence spectra[8,59], even without ligand binding[8]. When fatty acids and hypolipidemic drugs were applied to HepG2 cells with different LFABP content, there was a positive correlation between transactivation of PPARa and PPARγ with intracellular LFABP levels[8]. Moreover, the promoter of the LFABP gene contains a peroxisome-proliferator response element, and accordingly its mRNA levels are increased by fatty acids, dicarboxylic acids and retinoic acid[69]. This PPAR-mediated induction of LFABP was shown to be dependent on PPARa, as ablation of PPARa abolished the induction of LFABP by PPAR agonists[70]. LFABP expression seems also to be mediated by HNF1a in a PPARa-independent manner, as there was a reduced LFABP expression in HNF1a$^{-/-}$ mice despite unchanged PPARa levels. It was also confirmed in transfection studies that HNF1a was required for LFABP expression in liver[71].

In addition to the effects on hepatic lipid metabolism, LFABP has also been shown to mediate carcinogen-induced proliferation and liver regeneration and therefore could have broader implications in hepatocellular carcinoma and hepatectomy[72,73]. LFABP also acts as a cellular antioxidant by scavenging reactive oxygen species (ROS), as well as binding oxidative metabolites of unsaturated FAs and heme to regulate ROS production[74-78]. In rats with cholestasis, increased LFABP induced by PPAR agonist was found correlated with the reduction of oxidative stress in the liver[79]. LFABP$^{-/-}$ mice were found to be more susceptible to alcoholic liver disease with higher oxidative stress levels in response to ethanol ingestion[80].

Recently, our laboratory reported the first study examining the intestinal phenotypes of LFABP$^{-/-}$ mice[81]. By tracking 3H recovery in mucosal lipids in LFABP$^{-/-}$ and WT mice after [^{3}H]monoolein ingestion, it was suggested that LFABP is involved in the transport of MG away from PL synthesis and toward TG synthesis in enterocytes. In addition, LFABP$^{-/-}$ mice had an impaired oxidation of bloodstream-derived fatty acid in intestinal mucosa, suggesting a role of LFABP in trafficking fatty acids towards oxidative pathways in the enterocyte. Consistent with pattern found in liver, mucosal oxidative capacity was not affected in LFABP$^{-/-}$ mice, as their FA oxidation rate was similar to WT when a radiolabeled FA was added to mucosa homogenates.

Since the intestine delivers fat from the diets and the liver is the central processor of lipids, it is not surprising that LFABP is also involved in whole body energy homeostasis. Even though there was no difference in body weight on chow-fed LFABP$^{-/-}$ and WT mice, they showed phenotypic divergence on high fat diets. The Davidson group found that their LFABP$^{-/-}$ mice (male and female) were resistant to obesity and hepatic steatosis when fed high saturated fat diets (40 kcal% coconut oil or 41 kcal% milkfat), while no differences were observed in body weights when they were fed diets containing high levels of polyunsaturated FA (40 kcal% safflower oil)[82-84]. These differences in body weight were not due to food intake or lipid malabsorption or heat production.

In contrast, the Schroeder group found that LFABP$^{-/-}$ mice were prone to obesity with increases in fat mass relative to WT mice, and the effect was greater in female mice[85-87]. They also found a higher hepatic cholesterol accumulation in female LFABP$^{-/-}$ mice, suggesting that LFABP is involved in physiological regulation of cholesterol metabolism[87]. In our laboratory, we have

compared the phenotypes of male WT and LFABP$^{-/-}$ mice fed a low fat diet (10%kcal fat), a high saturated fat diet (45%kcal cocoa butter) and a high unsaturated fat diet (45%kcal safflower oil)[88]. Consistently with the Schroeder group's finding[85], LFABP$^{-/-}$ mice gained more body weight on both high fat diets than WT mice, with greater body fat mass and a lower 24h respiratory exchange ratio (RER). Despite the higher body fat mass of LFABP$^{-/-}$ mice, however, we observed a comparable insulin resistance level between WT and LFABP$^{-/-}$ mice, which is similar with the Davidson group's finding[84,88].

Interestingly and surprisingly, in our study on the phenotypic responses of LFABP$^{-/-}$ mice to high fat diets, we have also found increased levels of spontaneous activity in LFABP$^{-/-}$ mice, suggesting a possible modification in muscle activity[88]. Moreover, high fat-fed LFABP$^{-/-}$ mice showed greater exercise capacity compared with WT mice: In contrast to a drastic decrease in exercise capacity in high fat-fed WT mice compared with their low fat-fed littermates, LFABP$^{-/-}$ mice were able to maintain their exercise capacity after switching from low fat to high fat diets. Therefore we hypothesized that LFABP ablation is associated with alterations in skeletal muscle metabolism, protecting LFABP$^{-/-}$ mice from the high fat feeding-induced decline in exercise capacity. Little has been reported on the skeletal muscle metabolism in LFABP$^{-/-}$ mice. However, a microarray analysis of LFABP$^{-/-}$ soleus muscle showed increased expression levels of several genes involved in glucose uptake and metabolism[84], suggesting an effect of LFABP ablation on muscle energy homeostasis.

Muscle energy metabolism and exercise capacity

As one of the most metabolically active tissues, skeletal muscle produces energy in the form of ATP in both oxygen-dependent and -independent manners. First of all, the phosphagen system is oxygen-independent and the fastest way to synthesize ATP, where creatine phosphate stored in the skeletal muscle donates a phosphate group to ADP to generate ATP. With the limited storage of creatine phosphate, however, the phosphagen system only lasts for up to 10 seconds of muscle contraction before fatigue occurs[89,90]. Secondly, glycolysis is another oxygen-independent energy production pathway that lasts from 30 seconds to 2 minutes, with the major fuel source being glucose released from muscle glycogenolysis or taken up into the muscle cells from the circulation. During glycolysis, glucose undergoes a series of biochemical reactions to form pyruvate, generating three molecules of ATP per molecule of glucose[89]. When the demand for oxygen is greater than supply (anaerobic exercise), pyruvate produced from glycolysis converts to lactate, along with the decreased pH and accumulation of several metabolites such as ADP, Pi and reactive oxygen species. Consequently, calcium release from sarcoplasmic reticulum is impaired and muscle contraction is restricted[91-93].

Alternatively, when there is sufficient oxygen supply, pyruvate from glycolysis converts to acetyl-CoA, which then enters the aerobic metabolic system, or mitochondrial respiration. As the oxygen-dependent and the most complex energy production system, mitochondrial respiration includes the TCA cycle and electron transfer chain, with electrons produced from the TCA cycle transported to the electron transfer chain for oxidative phosphorylation. Complete oxidation of glucose, including glycolysis and mitochondrial respiration, generates 27 molecules of ATP per molecule of glucose. In addition to glucose, fatty acids (FAs) are also important substrates for acetyl-CoA production and mitochondrial respiration in muscle. After uptake into muscle cells from the blood, being released from circulating triglyceride via lipoprotein lipase or,

arising from lipolysis of intramuscular triglyceride, FAs are transported into mitochondria, where the carbon chains of FAs are shortened by β-oxidation and acetyl-CoA is produced to enter mitochondrial respiration[90]. Despite their relatively slow oxidation rate, FAs plays a major role in contributing to ATP production as a fuel source. For example, oxidation of one molecule of palmitate generates 129 molecules of ATP[89].

Due to the differences in the rate and capacity of the ATP production, the three energy production sources are activated in response to different types and stages of exercise. While the phosphagen system and glycolysis can quickly provide energy for short periods and are therefore more suitable for resistance training, mitochondrial respiration is the major limiting factor in ATP regeneration for endurance or prolonged exercise where sustained energy is required to maintain muscle contraction[94].

The biochemical reactions involved in mitochondrial respiration depend on continuous oxygen availability. That is why maximal oxygen uptake (VO_2max), the highest rate at which the body can take up and consume oxygen during intense exercise, has been viewed as one of the most important predictors of endurance exercise performance[95,96]. VO_2max is affected by both the cardiorespiratory system and the capacity of oxygen utilization in skeletal muscle[95,97]. As one of the important players determining the capacity of muscle oxygen utilization, mitochondrial function can be increased twofold by endurance training, and therefore endurance training has been considered an effective way to increase VO_2max[98].

Other than the metabolic machinery, adequate fuel supply, including lipids and carbohydrates, is also essential to endurance exercise performance. During low-intensity endurance exercise (≤

45% of VO_2max), lipids are the predominant fuel source and peripheral lipolysis in adipose tissues is highly stimulated for FA uptake into muscle (whereas muscle lipolysis is only stimulated at higher exercise intensity). With increasing exercise intensity, there is a shift toward more carbohydrate metabolism where plasma glucose uptake and muscle glycogen breakdown are increased[99,100]. Depletion of muscle glycogen stores results in fatigue, regardless of an adequate oxygen supply[94].

As skeletal muscle is one of the major metabolic engines of the body, obesity and associated conditions like metabolic syndrome had been shown to cause alterations in energy metabolism in skeletal muscles, such as reduction in glycogen synthesis and oxidative capacity[101]. Physical fitness and exercise capacity are generally low in obese patients[102,103], making it more challenging for the patients to follow a recommended exercise regimen. Moreover, the inactivity and poor aerobic fitness have been found to be more important than overweight and obesity as mortality predictors[104,105]. It has also been shown that even a short-term high fat diet could induce a significant decrease in exercise capacity without substantial weight gain[106,107].

In these studies, we found an unexpected resistance to high fat feeding-induced decline in exercise capacity in LFABP$^{-/-}$ mice. In order to understand the physiological basis associated with their exercise phenotype, we examined the metabolic machinery, focusing on the mitochondrial function, as well as the fuel supply in the skeletal muscle of LFABP$^{-/-}$ mice relative to WT mice.

Muscle fiber composition, function and obesity

Whole muscles are heterogeneous in their composition, consisting of different fiber types with distinct physiological properties (please see Table 1 below, modified from ref. 51). Skeletal muscle fibers are categorized as slow- (type I) or fast-twitch (type II) by the contractile property,

myofibrillar (myosin) ATPase staining and myosin heavy chain (MHC) protein expression. Type I muscle fibers are classically red in appearance, whereas type II muscle fibers are white (type IIb, glycolytic) or have an intermediate color (type IIa, oxidative). The difference in color reflects the abundance of the oxygen transport protein myoglobin, which is closely related to mitochondrial density and the oxidative capacity[108,109]. Since endurance exercise imposes a high-frequency, low-power output demand on muscular contraction, whereas resistance exercise imposes a low-frequency, high-resistance demand, type I muscle fibers are predominantly used to support endurance exercise and type II muscle fibers are more involved in resistance exercise[109].

Muscle fiber type is genetically determined during development, but the adaptive transformation of muscle fibers from one type to another is observed under certain conditions, such as exercise training or dietary changes[109,110]. Several animal models with specific genetic manipulations also showed dramatic muscle fiber switch from type II to type I, shedding light on the regulating pathways and possible targets for intervention in muscle fiber type determination[111,112]. Moreover, as one of the most highly plastic tissues, skeletal muscle may also exhibit changes in metabolic potential and morphology without a transformation of muscle fiber types, as measured by changes in MHC expression under certain stimuli[113,114].

Table 1-2. Contractile, Metabolic, and Morphological Characteristics of Skeletal Muscle Fiber Types{Zierath, 2004 #438}

	Type I muscle	**Type II**	
		IIa	**IIb**
Myosin heavy-chain isoform	MHC1	MHC2a	MHC2b
Appearance/myoglobin content	Red/High	Red/Intermediate	White/Low
Contractile characteristics	Slow twitch	Fast twitch	Fast twitch
Resistance to fatigue	High	Fairly high	Low
Force production (power output)	Weak	Intermediate	Strong
Endurance capacity	High	Intermediate	Low
Capillary density	High	Fairly high	Low
Mitochondrial density	High	Intermediate	Low
Oxidative capacity	High	Fairly high	Low
Glycolytic capacity	Low	Fairly high	High
Major storage fuel	Triglycerides, (creatine phosphate)	Glycogen, (creatine phosphate)	Glycogen, (creatine phosphate)
Exercise-type dominance	Prolonged low intensity	Moderate duration, high intensity	Short duration, maximal effort

Studies of human skeletal muscle have consistently shown that obesity is associated with a shift toward faster fiber types, with the proportions of slow fibers being inversely correlated with body fat levels[115-117]. These patterns have led to the general hypothesis that increased adipose tissue levels drive fundamental changes in muscle fiber composition and lead to impaired metabolic function. In contrast to human studies, mouse studies have shown less consistent associations between obesity and lower slow muscle fibers, but have provided interesting evidence on how excess energy intake can affect muscle-type specific metabolism. In response to high fat feeding, type I dominant muscle was less susceptible to intramyocellular lipid accumulation but more to fiber type shifting from type I fibers to type IIa fibers[118-120] with lower mitochondrial respiration[121], whereas type II dominant muscle showed higher intramyocellular lipid accumulation and oxidative capacity, with increase in type II oxidative muscle fiber[120,122-125]. Also, the genetic models of obesity, leptin knockout (*ob/ob*) mice and leptin receptor knockout (db/db) mice exhibited a possible switch from type IIb to IIa[126,127]. However, it is worth noting that these animal models displayed other phenotypes in addition to obesity that may contribute to muscle fiber change, including reduction in muscle mass[126,127], muscle atrophy and impaired neuromuscular signal transmission[128].

As key regulators of skeletal muscle fiber type differentiation, the master metabolic sensor AMP kinase (AMPK) and PPARγ coactivator 1α (PGC1α) play important roles in type I fiber type specification, mitochondrial biogenesis, and endurance adaptations during chronic exercise[129-131]. AMPK is activated in response to metabolic stress such as low energy, changes in intracellular Ca^{2+}, and exercise. Upon activation, AMPK helps maintain energy homeostasis by stimulating fatty acid oxidation and mitochondrial biogenesis, while inhibiting ATP consumption mediated by mammalian target of rapamycin (mTOR), a major regulator of cell growth and

protein synthesis[132]. In addition, AMPK regulates muscle metabolism and differentiation by modulating the expression and stability of the transcriptional regulator PGC1α, which further induces genetic programs involved in mitochondrial biogenesis, and drives formation of slow twitch muscle fiber[131,133].

In order to determine whether a muscle fiber switch is associated with the exercise phenotype in LFABP$^{-/-}$ mice, we examined markers for oxidative muscle fibers (slow-twitch) at the mRNA and protein levels in skeletal muscles of LFABP$^{-/-}$ mice. We analyzed AMPK activity due to its important role in energy sensing and muscle metabolism. In addition, bioenergetics analysis was used to examine the respiratory capacity of the myocytes of LFABP$^{-/-}$ relative to WT mice at the cellular level.

Metabolic regulation in liver and organ crosstalk

Based on the fact that LFABP is the only FABP highly expressed in the liver, and that liver plays a central role in lipid homeostasis on a whole body level, the systemic effects of LFABP ablation may be attributed to liver-derived interorgan signaling. As important regulators of lipid metabolism across different tissues, many transcription factors are present in the liver to integrate signals and orchestrate various metabolic pathways. In particular, PPARs and liver X receptors (LXRs), both forming obligate heterodimers with retinoid X receptors (RXRs), play important roles in regulating FA metabolism. As ligand-activated nuclear receptors, PPARs are activated by long chain FAs and involved in many aspects of FA metabolism. PPARα is the major isoform of PPAR in the liver that not only promotes FA uptake and oxidation, but also regulates the anti-inflammatory response[134,135]; PPARγ contributes to hepatic steatosis, TG clearance from circulation, as well as cellular differentiation especially in adipocytes[136,137]; PPARδ seems to be

only implicated in regulating FA uptake, β-oxidation and energy uncoupling in skeletal muscle and adipose[138]. Moreover, it is well established that LXRs, upon binding to their ligands, oxysterols, are activated to regulate hepatic cholesterol homeostasis by transactivating genes involved in cholesterol catabolism and conversion to bile acids, including the rate-determining enzyme in bile acid synthesis, cholesterol 7α-hydroxylase[139-141]. In other cell types, LXRs also regulates expression levels of cholesterol ester transfer protein and ATP-binding cassette transporter A1 (ABCA1) that control cholesterol efflux and reverse cholesterol transport[142,143]. In addition to their important role in cholesterol metabolism, LXRs have been shown to induce lipogenic pathways via upregulation in another transcription factor, sterol regulatory element-binding protein 1c (SREBP1c), and its downstream targets [144]. Due to the interactions among LXR, PPAR and RXR, PPARα activation has been shown to compete with LXR in forming heterodimers with RXRs, in turn suppressing LXR signaling and maintaining hepatic lipid homeostasis[145].

As indicated by the dramatic whole-body phenotype of high fat-fed LFABP$^{-/-}$ mice, the disturbance in lipid metabolism secondary to LFABP ablation is not limited to its expression sites (liver and intestine). Indeed, impaired lipid handling capacity in the liver not only leads to fuel substrate (FA) “overflow” into other tissues, but also may affect the FA-induced signaling pathways (e.g. PPARa) and energy metabolism in other tissues through organ crosstalk. Firstly, bi-directional communications between the brain and peripheral tissues, including liver, intestine, skeletal muscle and adipose tissues, are well established. Particularly, the gut-brain axis, consisting of enteric and central nervous systems, plays an important role in connecting gastrointestinal function, gut microbiota and higher cognitive function to regulate food intake, eating behaviors, and energy expenditure[146,147]. Moreover, crosstalk between liver and intestine has also been implicated in coordinating intestinal microbiota metabolism, gut barrier integrity,

bile acid synthesis, as well as hepatic lipid metabolism[148]. For example, as a major mediator for liver/intestine crosstalk in regulating bile acid and lipid homeostasis, FGF15/19 is induced by farnesoid X receptor (FXR) in the enterocytes in the presence of its ligand bile acid, and enters the liver via the portal vein, suppressing the bile acid synthesis[149,150]; oral administration of bile acid has also shown to reduce hepatic TG accumulation, VLDL secretion and plasma TG levels via activation of FXR and inhibition of LXR and SREBP1c in the liver[151]. Moreover, liver/adipose tissues crosstalk has recently gained a lot of attention due to the discovery of a promising anti-diabetic hepatokine, FGF21, that preferentially targets on adipose tissues; as a downstream target of FGF21 signaling, adiponectin is increased at the transcriptional level, and is released from the adipose tissue into circulation. Not only does adiponectin show antisteatotic, anti-fibrotic and anti-inflammatory effects in the liver[152-154], it ha

s also been shown to improve energy metabolism in the skeletal muscle[155-157].

FGF21-adiponectin signaling and obesity

As noted above, dynamic crosstalk between metabolic organs is important in systemic energy homeostasis. Since LFABP is not expressed in skeletal muscles, it is intriguing that *Lfabp* ablation in the liver and intestine leads to alterations in muscle energy metabolism. In considering a liver-derived signaling molecule with the potential to target skeletal muscle, fibroblast growth factor 21 (FGF21) has emerged as an important candidate, as it is a downstream target of PPARα.

As a member of the endocrine FGF family, FGF21 is predominantly produced in the liver and plays a key role in energy homeostasis[158]. Physiologically, FGF21 is induced directly by PPARα in liver in response to fasting, inducing hepatic expression of PGC1α and lipid oxidation,

gluconeogenesis and ketogenesis in liver[159-161]. After FGF21 is secreted into the circulation, adipose tissue is thought to be an essential target for FGF21 action[162,163], with elevated glucose uptake independent of insulin signaling, enhanced lipolysis and mitochondrial oxidative capacity in adipocytes[164-167]. Moreover, FGF21 knockout mice were observed to be slightly heavier and had an increased hepatic fat content when challenged with a ketogenic diet[167]. Consistently, mice with adenovirus-mediated knockdown of hepatic *Fgf21* also showed elevated hepatic and plasma triglyceride levels on a ketogenic diet[161].

Owing to its role in inducing metabolic adaptations to fasting, FGF21 has emerged as a therapeutic agent for obesity and metabolic disorders. In rodents and nonhuman primates, FGF21 therapies have been shown to improve insulin sensitivity, ameliorate hepatosteatosis and reduce adiposity[167-170]. Consistently, transgenic mice overexpressing FGF21 were viable although with stunted growth rate, and were resistant to diet-induced obesity and insulin resistance[167]. In order to circumvent the poor pharmacokinetic properties of native FGF21, the potential of FGF21 gene therapy is being explored, and a recent study successfully used adeno-associated viral vectors as a FGF21 delivery system, leading to reduced body weight, improved insulin resistance and alleviation of hepatic steatosis in genetic, diet-induced and aging-induced obese models[171].

Limited evidence has been reported on the direct effects of FGF21 on skeletal muscle, however it was recently found that in human myotubes, FGF21 exposure increased basal and insulin-stimulated glucose uptake and glycogen content[172,173], with increases in *Glut1* mRNA and and protein abundance at the plasma membrane. It was also shown that FGF21 facilitates insulin-

induced glucose transport without altering phosphorylation of Akt or AMP-activated protein kinase[173].

In addition to potential direct effects of FGF21 on skeletal muscle, adiponectin has been shown to couple FGF21 actions from adipocytes to liver and skeletal muscle: In adiponectin knockout mice, despite the unaffected FGF21-induced extracellular signal-regulated kinases1/2 (ERK1/2) activation in adipose tissues, the insulin-sensitizing effects of FGF21 liver and skeletal muscle were abrogated[174]. As an adipokine predominantly secreted from adipocytes, adiponectin bears many functional similarities with FGF21 in regulating glucose and lipid metabolism and improving insulin sensitivity. With its actions on major metabolic organs, adiponectin has been shown to alleviate fatty liver disorders[175,176], as well as enhance mitochondrial function and fatty acid oxidation in skeletal muscle[157,177]. Moreover, both FGF21 and adiponectin are downstream effectors of PPARγ and are shown to be important mediators for the therapeutic benefits of PPARγ agonists[178,179].

While FGF21 is considered a promising candidate for therapeutic treatments of metabolic disorders associating with obesity, a paradoxical increase in serum FGF21 levels has been found in obese mice, nonhuman primates and humans[161,180-182], along with impaired glucose tolerance and increased accumulation of lipid in the liver. Moreover, acute FGF21 administration was found to suppress hepatic glucose production, increased liver glycogen and improved glucose clearance in control mice while having no effect on obese *ob/ob* mice[183]. In examining the reason why FGF21 fails to exert its expected effects on energy homeostasis, Fisher et al. demonstrated that high fat-fed mice had increased endogenous FGF21 levels and respond poorly to exogenous FGF21, with attenuated phosphorylation of ERK1/2 and impaired induction

of FGF21 target genes in liver and white adipose tissue, as well as a blunted FGF21-induced decrease in plasma glucose. These results led to a conclusion that obesity is an FGF21-resistant state[184]. Consistent with this finding, Jeon et al. found that despite an increased plasma FGF21 level, there were decreased levels of phosphorylated FGF receptor (p-FGFR), phosphorylated FGFR substrates 2α (p-FRS2α), and phosphorylated ERK in the skeletal muscle of both type 2 diabetic patients and subjects with glucose intolerance[172]. Although impaired FGF21 signaling is consistently found in the liver and white adipose tissue, there is also evidence suggesting FGF21 sensitivity is maintained at the whole body level in obese mice, based on similar decreases in plasma glucose, insulin and triglyceride levels in lean and obese mice in response to chronic FGF21 treatment [185].

In my preliminary experiments of this study, we observed a lower FGF21 level in the liver and plasma of high fat-fed LFABP$^{-/-}$ mice, along with a trend of increased circulating adiponectin level, supporting alterations in FGF21 signaling[174]. Given the roles of FGF21 in maintaining whole body energy homeostasis, I hypothesized FGF21 may be a potential liver-derived signal leading to metabolic changes in skeletal muscles of LFABP$^{-/-}$ mice either directly or via adiponectin signaling. We examined FGF21 sensitivity in high fat-fed WT and LFABP$^{-/-}$ mice, and the effects of FGF21 and/or adiponectin on regulating myocyte respiration and substrate storage.

Summary

The Fatty Acid Binding Proteins (FABPs) are a family of intracellular proteins with high binding affinity for fatty acids and other related compounds. The first described FABP, liver FABP (LFABP, FABP1) is highly expressed in the liver and intestine, and thought to be involved in lipid metabolism both locally and systemically. In vitro studies have shown that LFABP facilitates

LCFA uptake and oxidation in the liver, and consistent results have been observed in isolated liver slices and primary hepatocytes from *Fabp1* gene ablated (LFABP$^{-/-}$) mice. Moreover, previous studies from our laboratory have revealed striking difference in whole body energy metabolism between LFABP$^{-/-}$ and WT mice fed high fat diets{Gajda, 2013 #123}. Compared with WT mice, LFABP$^{-/-}$ mice had a higher body weight and fat percentage. Nevertheless, they were able to maintain a similar glucose and insulin tolerance with WT mice, and surprisingly, were protected from high fat feeding-induced decline in exercise capacity. Therefore, in the present study, it is of great interest to understand the energy metabolism in skeletal muscle of high fat fed-LFABP$^{-/-}$ mice at rest and during exercise, and the possible mediators contributing to their improved exercise capacity, by undertaking the following aims:

Specific Aims

<u>Aim 1. To examine the energy metabolism in skeletal muscle of LFABP$^{-/-}$ mice associated with their improved exercise capacity on high fat diets.</u>

Our laboratory made the observation that LFABP$^{-/-}$ mice were protected from high fat feeding-induced decline in exercise capacity, despite their obese phenotype compared with WT mice. In the present study, we examined in depth the substrate storage and mitochondrial function in resting muscle, and substrate utilization in exercising muscle of LFABP$^{-/-}$ mice, and determined their potential contributions to the unimpaired exercise capacity.

<u>Aim 2. To determine the muscle fiber composition and cellular metabolism in skeletal muscle of LFABP$^{-/-}$ mice.</u>

Skeletal muscles consist of different types of muscle fibers with different functional characteristics, and they are subject to adaptive transformation in response to environmental

stimuli. We determined the muscle fiber composition in gastrocnemius muscle (mixture of oxidative and glycolytic muscle fibers) of high fat-fed LFABP$^{-/-}$ mice, which may provide structural basis for their more efficient energy metabolism. To determine the functional consequences of LFABP ablation, we also analyzed mitochondrial respiration capacity in primary myoblasts from LFABP$^{-/-}$ mice with cellular bioenergetic measurements.

Aim 3. To examine the role of FGF21 signaling in the metabolic changes in skeletal muscle of LFABP$^{-/-}$ mice.

To test the importance of circulating mediators apart from FAs, we examined whether primary myoblasts from LFABP$^{-/-}$ mice were protected from FA treatment-induced decline in mitochondrial respiration. As a stress hormone predominantly produced by the liver, FGF21 targets mainly extrahepatic tissues and regulates whole body energy homeostasis. We recently found lowered *Fgf21* levels in liver and plasma of high fat-fed LFABP$^{-/-}$ mice relative to WT, and therefore we examined the effects of FGF21 signaling on skeletal muscle. Moreover, we previously found that adiponectin, a coupler of FGF21 actions from adipocytes to skeletal muscle, was trending higher in LFABP$^{-/-}$ mice. Therefore we also determined potential indirect effects of FGF21 via adiponectin signaling, by analyzing the mRNA expression levels of adiponectin in adipose and its receptors on skeletal muscle.

Overall, our aims for the studies examined the metabolic alterations in skeletal muscle of LFABP$^{-/-}$ mice in the context of substrate availability, oxidative capacity and muscle fiber composition. In addition, we determined the effects of altered FGF21 signaling on muscle energy metabolism in LFABP$^{-/-}$ mice. The study provides new information about the systemic effect of LFABP on skeletal muscle metabolism, and reveals how FGF21 may facilitate interaction among metabolic organs, contributing to the improved exercise capacity of high fat-fed LFABP$^{-/-}$ mice.

Chapter 2

Energy Metabolism in Skeletal Muscle of *Lfabp* Null Mice Associated with their Protection Against High Fat Feeding-Induced Decline in Exercise Capacity

Abstract

Liver fatty acid-binding protein (LFABP, FABP1) binds long chain fatty acids with high affinity, and is abundantly expressed in the liver and small intestine. Although LFABP is thought to function in intracellular lipid trafficking, studies of LFABP null (LFABP$^{-/-}$) mice have also demonstrated a role in regulation of systemic energy homeostasis. We and others have reported that LFABP$^{-/-}$ mice become more obese than wild-type (WT) mice upon high fat feeding. Despite increased body weight and fat mass, however, LFABP$^{-/-}$ mice were protected from high fat feeding-induced decline in exercise capacity, showing an approximate doubling of running distance compared with the WT mice on the high fat diet. Therefore, to understand this surprising exercise phenotype, in the present studies we examined the fuel supply and substrate utilization in the skeletal muscle secondary to LFABP ablation. The results indicate significantly increased triglyceride (TG) content and glycogen content in the resting skeletal muscle of LFABP$^{-/-}$ mice. In addition, higher mitochondrial enzyme activities and an increased fatty acid oxidation rate suggest that LFABP$^{-/-}$ muscle has greater energy substrate availability and greater capacity for substrate oxidation compared with WT muscle at resting state. Moreover, substrate utilization during low intensity exercise showed different preference on different stage: compared with WT mice, LFABP$^{-/-}$ showed a higher respiratory exchange ratio (RER) during the first half of exercise, and a lower RER ratio during the second half, suggesting a greater carbohydrate utilization in the early stage of the exercise and a higher lipid utilization later on. Consistently, LFABP$^{-/-}$ mice were shown to have greater exercise-dependent decreases in muscle glycogen stores and elevated free fatty acid in the plasma after exercise. Overall, the improved exercise capacity in high fat-fed LFABP$^{-/-}$ mice is related to greater basal levels of energy substrate and mitochondrial function in skeletal muscle, as well as a more efficient muscle glycogen utilization and fatty acid availability during exercise. Since LFABP is not expressed in the skeletal muscle but rather in liver

and intestine, these muscle metabolic changes in LFABP$^{-/-}$ mice may be due, in part, to liver- and/or intestine- derived mediators contributing to the prevention of high fat feeding-induced impairment in the skeletal muscle.

Introduction

Fatty acids (FAs) are important metabolic fuels and signaling molecules that play a critical role in regulating energy homeostasis. As seen in the alarming obesity epidemic, disturbances in lipid homeostasis due to excessive energy intake often induce increased plasma free fatty acid levels and ectopic lipid accumulation in tissues such as liver and skeletal muscle, which in turn contribute to insulin resistance, atherosclerosis and metabolic syndrome[186,187]. Fatty acid binding proteins (FABPs) are a family of small cytosolic proteins accommodating fatty acids and other hydrophobic ligands, and are thought to be involved in intracellular lipid trafficking. Liver FABP (LFABP, FABP1) is the only FABP abundantly expressed in the liver, whereas in the proximal intestine LFABP is co-expressed with intestinal FABP (IFABP, FABP2)[6]. LFABP binds a variety of ligands including long-chain fatty acids, prostaglandins, heme, lysophosphatidic acid, monoacylglycerols (MGs), bile salts and certain lipophilic drugs[6,8,188,189]. Unlike other FABPs, LFABP can bind two fatty acids or MGs[188,189]. Moreover, LFABP has been shown to interact with peroxisome proliferator-activated receptors (PPARs), specifically PPARα and PPARγ[8,59,63]. Upon activation by micromolar concentrations of FAs and FA analogues, PPARs induce transcription of multiple genes encoding proteins involved in FA metabolism, and dysregulation of PPARs is associated with many metabolic diseases[67,190]. LFABP is thought to promote interaction between PPARs and many natural ligands, as well as synthetic agonists of PPARα (fibrates) and PPARγ (thiazolidinediones; TZDs) commonly used for treating type II diabetes[8].

Extensive research has provided evidence for both local and systemic functions of LFABP. In the liver, LFABP has been demonstrated in vitro and in vivo to facilitate hepatic FA uptake and trafficking[5,39,64,66] , as well as to regulate bile acid and cholesterol metabolism[87,191]. In the intestine, we have reported that LFABP is involved in directing MGs to triglyceride synthesis and FAs to oxidative pathways[88]. In addition to such local effects, we and others found that LFABP$^{-/-}$

mice became more obese on high fat diets than WT mice, with a lower respiratory exchange ratio (RER)[85,88] but a comparable level of insulin resistance [84,88], supporting an important role of LFABP in regulating whole body energy homeostasis.

Despite their obese phenotype, we found that LFABP$^{-/-}$ mice displayed higher levels of spontaneous activity than WT mice[88]. In the present studies we compared exercise tolerance in LFABP$^{-/-}$ vs. WT mice using a treadmill test; we observed a surprising difference in exercise capacity between the high fat-fed LFABP$^{-/-}$ and WT mice: In contrast to the drastic decrease in exercise capacity in high fat-fed WT mice compared with their low fat-fed littermates, high fat-fed LFABP$^{-/-}$ mice maintain their exercise capacity at the level found under low fat feeding conditions. Human obesity and diabetes are often associated with poor physical fitness and exercise capacity[102,103], which in turn limits the absolute intensity and duration of exercise that can be carried out; thus the potential benefits of regular exercise on insulin sensitivity and cardiovascular health in these patients could be limited. Therefore, an understanding of the physiological alterations in the skeletal muscle of LFABP$^{-/-}$ mice which underlie their resistance to high fat feeding-induced decline in exercise capacity may provide important information relevant to the maintenance of a healthful exercise capacity in the obese state.

Little has been reported on the effect of LFABP gene knockout on skeletal muscle metabolism, although a microarray analysis indicated higher muscle expression of several genes involved in glucose metabolism and fatty acid oxidation in LFABP$^{-/-}$ mice[82]. Given the importance of LFABP in FA metabolism and PPAR signaling, we hypothesized that the deficiency of LFABP and consequent restricted lipid handling capacity in liver and perhaps intestine, might shunt FAs to extrahepatic tissues, triggering interorgan signaling that would result in metabolic changes in skeletal muscle favoring more efficient energy production. To elucidate how LFABP deficiency protects exercise tolerance against high fat feeding, we analyzed substrate availability and

energy metabolism in the skeletal muscle of high fat-fed LFABP$^{-/-}$ mice in the resting state and during exercise. The results show that LFABP ablation leads to higher energy substrate storage levels (glycogen and IMTG) and mitochondrial respiratory capacity in resting muscles, and increased oxidation of circulating FAs during exercise, all of which contribute to preventing the decline in exercise performance that typically accompanies high fat feeding.

Experimental procedures

Animal and Diets

LFABP$^{-/-}$ mice on a C57BL/6N background were generously provided by B. Binas and coworkers[65]. The mice were back-crossed with wild type C57BL/6J mice from Jackson Laboratories (Bar Harbor, ME) to generate congenic C57BL/6 LFABP$^{-/-}$mice of mixed J/N background[17,81]; these were further back crossed 6 times to obtain LFABP$^{-/-}$ that are >99% /6J background. Wild type C57BL/6J mice obtained from Jackson Laboratories and bred in our facility were used as controls. Mice were maintained on a 12-h light/dark cycle and allowed *ad libitum* access to standard rodent chow (Purina Laboratory Rodent Diet 5015). At 2 months of age, male LFABP$^{-/-}$ and WT (C57BL/6J) mice were housed 2–3 per cage and fed a high saturated fat (45 kcal%) diet (HFS, Research Diets, Inc. #D10080402) for 12 weeks. A low fat diet containing 10 kcal % fat (LFD, Research Diets, Inc. #D10080401) was also used for the initial evaluation of exercise capacity. Diet composition was detailed previously and shown in Table 2-1 A and B[88].

Table 2-1A. Diet composition of low fat (LFD) and high saturated fat (HFS) diets

	LFD		HFS	
	grams	*kcal*	grams	*kcal*
Casein	200	*800*	200	*800*
L-Cystine	3	*12*	3	*12*
Corn starch	315	*1260*	72.8	*291*
Maltodextrin	35	*140*	35	*400*
Sucrose	350	*1400*	350	*691*
Cellulose	50	*0*	50	*0*
Soybean Oil	10	*90*	10	*90*
Lard	8.5	*77*	0	*0*
Cocoa Butter	26.5	*239*	192.5	*1733*
High Oleic Safflower Oil	0	*0*	0	*0*
Mineral mix	45	*0*	45	*0*
Vitamin mix	10	*40*	10	*40*
Choline Bitartrate	2	*0*	2	*0*
Total	1055.0	*4057*	858.1	*4057*

Table 2-1B. Fatty acid composition low fat (LFD) and high saturated fat (HFS) diets

	LFD	HFS
grams/4057 kcal		
C16	8.2	49.9
C16:1	0.1	0.4
C18	9.3	64.3
C18:1	17.7	65.2
C18:2	7.3	10.7
C18:3	0.8	1.0
%		
Saturated fatty acids	40.8	60.0
Monounsaturated fatty acids	40.9	33.9
Polyunsaturated fatty acids	18.1	6.1

Treadmill Test for exercise capacity

After 12 weeks of high fat feeding, mice were acclimatized to a motorized, speed-controlled treadmill with an electric shock stimulus (6 lanes, Columbus Instruments, Columbus, OH) one day prior to the test day, running for 5 min at 6m/min with 0 degree incline. On the test day, mice on fed state were run on the treadmill with a speed increased from 6m/min by 3m/min every 3 min and a constant 25-degree incline. Another groups of mice were fasted for 16 hours and run on the treadmill with a speed increased from 6m/min by 3m/min every 5 min and a 10-degree incline. The mice were run until they reached exhaustion, defined as when the mice remained on the shock grid for more than 5 seconds.

Energy expenditure during exercise

Energy expenditure during a low intensity exercise bout was assessed using the Oxymax system (Columbus Instrument, Columbus OH). At the end of 12 weeks of high fat feeding, mice were acclimatized to the treadmill as described above. On the test day, the mice were fasted for 16 hours, and each mouse was run individually on a treadmill positioned inside an indirect calorimetry chamber with rotating genotypes to minimize the effect of fasting time. The treadmill was set to a constant 10-degree incline throughout the test, and after one-minute settlement on a stationary treadmill and a 5-minute warm-up at 5m/min, the mice were run for 20min at 10m/min. Gas exchange and energy expenditure measurements were taken, with respiratory exchange ratio (RER) determined as VCO_2/VO_2, and energy expenditure calculated by $(3.815+1.232xRER)x\ VO_2$[192].

Glycerol tolerance test

At 11 weeks of high fat feeding, 19-week-old mice were fasted for 16 hours and intraperitoneally injected with glycerol (2 g/kg body weight)[193]. Blood glucose was measured before and within 3 hours after the injection every 30min with AlphaTRAK 2 blood glucose test strips.

Preparation of tissue and plasma

For pre-exercise (resting) state studies, mice were fasted for 16 hours before sacrifice by cervical dislocation at the end of the high fat feeding period. For post-exercise state studies, mice were fasted for 16 hours and sacrificed by cervical dislocation right after the low intensity exercise bout. At sacrifice, blood was drawn from the aorta and glucose was measured with AlphaTRAK 2 blood glucose test strips. Plasma was extracted after centrifugation at 4°C for 6 min at 6000 xg and stored at -80°C for further analysis. After the blood was taken, liver, epididymal white adipose tissue (WAT), and hind limb muscles (gastrocnemius, soleus and quadriceps) were removed, immediately processed for same-day assays or placed on dry ice and subsequently stored at -80°C for further analysis. For histochemical analyses, gastrocnemius muscle was removed, covered with OCT (optimal cutting temperature compound, Tissue-Tek; Sakura Finetek USA) and flash-frozen in liquid nitrogen-cooled isopentane for cryosectioning.

Plasma free fatty acid anaylsis

Plasma non-esterified fatty acid (NEFA) kit (Sigma, MAK044) was used to measure free fatty acid levels in plasma of post-exercise mice coloremitrically via a coupled enzyme assay.

Lipid extraction and triglyceride assay

Upon sacrifice, hind limb muscles (gastrocnemius, soleus and quadriceps) were diluted with 8x the weight of the samples of PBS (pH 7.4) per gram (wet weight), and homogenized for 2 min with a Potter-Elvejhem homogenizer on ice. Protein concentration was determined using the Bradford assay[81], and lipid extraction was performed on samples containing 1 mg of protein/ml using the Folch procedure[194]. Lipids were extracted twice with 10 ml of chloroform/methanol (2:1) and the aqueous phase nonlipid fractions discarded. The organic lipid layer was dried under a nitrogen stream and resuspended in chloroform/methanol (1:1), spotted onto Silica Gel G TLC plates along with authentic standards. The TLC plate was developed in a nonpolar solvent system consisting of hexane, diethyl ether, and acetic acid (70:30:1), visualized by iodine-staining and scanned with a Hewlett-Packard scanner. Absolute values for triglyceride mass were obtained by densitometric analysis with ImageJ software based on the standard curves using authentic standards.

Glycogen assay

Total glycogen content in hind limb muscles was measured as described by Xu et al. with minor modification[195,196]. Briefly, hind limb muscles were homogenized with a Polytron for 1 min on ice in 5X the weight of the samples of PBS (pH7.4) per gram (wet weight), and centrifuged at 14,000rpm for 5 min after heat-inactivation at 80°C for 10 min. 20µl of supernatant or standard solutions were mixed with amyloglucosidase (A1602-25MG, Sigma) to hydrolyze glycogen to glucose, and the glucose levels were measured colorimetrically with a glucose assay kit (GAGO-20, Sigma). Glycogen (G0885-1g, Sigma) standard was used to plot a standard curve and determine the amount of glucose broken down from glycogen in the homogenate.

Mitochondrial enzyme assays

Mitochondrial enzymatic acitivities for citrate synthase (CS), cytochome c oxidase (CCOX) and succinate dehydrogenase (SDH) were measured in fresh muscle homogenates as described[197,198]. Briefly, on the day of sacrifice, hind limb muscles were homogenized with a Potter-Elvejhem homogenizer (piston-type Teflon® pestle, clearance 0.1 to 0.15mm) for 2 min on ice in 20X the weight of the samples of Tris-sucrose buffer (20mM Tris, 100mM KCl, 70mM sucrose, 1mM EGTA, pH 7.4) per gram (wet weight) and centrifuged at 600 x g for 10 min at 4°C. Supernatant was collected, flash-frozen in liquid nitrogen and stored at -80°C. Protein concentration in the supernatant was determined by Bradford assay. All enzyme assays were performed within linear ranges for protein concentration and reaction time.

CS activity was determined by measuring the formation of thionitrobenzoate anion. Muscle homogenates was mixed with 200mM Tris (pH 8.0) with 0.2% Triton X-100 (vol/vol), 1mM dithionitrobenzoic acid (DTNB), and 10mM acetyl-CoA. The reaction was started by adding 9.0 mM oxaloacetate and absorbance was read at 412 nm every 30s for 3min. SDH activity was determined by the rate of reduction of coenzyme Q1 (ubiquinone). Muscle homogenates were incubated with 0.5M Potassium Phosphate buffer (pH 7.4) containing 0.01M succinate for 10 min at 37°C to activate complex II. Rotenone and antimycin A were added and baseline absorbance was recorded. The reaction was started by adding 5µl coenzyme Q1 and the absorbance was recorded at 280nm over 2 min. CCOX activity was determined by measuring the rate of oxidation of cytochrome c. Reduced cytochrome c was prepared freshly by addition of sodium dithionite, and added to Kpi buffer (100mM, pH7.4). Baseline absorbance at 550 nm was recorded for 2 min. Muscle homogenates were added to the mixture to start the reaction, and the absorbance at 550 nm was recorded for 3 min.

Fatty acid oxidation

Fatty acid oxidation rates in skeletal muscle homogenates were measured as detailed by Hirschey and coworkers[199,200]. Briefly, upon sacrifice, hind limb muscles were gently homogenized with a Potter-Elvejhem homogenizer for 15 strokes on ice in 6.5X the weight of the samples of sucrose-Tris-EDTA buffer per gram (wet weight), and the homogenates were incubated for 30 min with 400µl reaction mix containing 0.8µCi ^{14}C-Oleate solubilized in 0.7% bovine serum albumin(BSA)/500 µM palmitate. $^{14}CO_2$ generated from the reaction was released by addition of 200µl perchloric acid and absorbed onto a piece of filter paper in the tube cap soaked with 20µl 1M benzethonium hydroxide. The filter paper and ^{14}C-acid soluable metabolites (ASM) in the reaction mix were assesed for radioactivity by scitillation counting.

Quantitative RT-PCR for mRNA expression analysis

Total RNA was extracted from frozen muscles (Trizol, Invitrogen) and further purified using RNeasy cleanup kits along with DNase treatment to minimize genomic DNA contamination (Qiagen). cDNA was synthesized by using a reverse transcription kit (Invitrogen). Primer sequences were retrieved from Primer Bank (Harvard Medical School QPCR primer data base) and are shown in Table S1. Efficiency tests were performed for all primers to confirm similar amplification efficiency (100%±10%) between the genotypes. Real time PCR reactions were performed in triplicate using an Applied Biosystems StepOne Plus instrument. Each reaction contained 100ng of cDNA, 250nM of each primer, and 12.5µl of Power SYBR Green Master Mix (ThermoFisher) in a total volume of 25 µl. Relative expression of the target genes was calculated using the comparative Ct method and normalized to endogenous β-actin.

Table 2-2. Primer sequences in qPCR analysis of resting muscles of WT and LFABP$^{-/-}$ mice

Gene		Sequences (5' → 3')
Housekeeping		
β-actin	Forward	GGC TGT ATT CCC CTC CAT CG
	Reverse	CCA GTT GGT AAC AAT GCC ATG
Muscle fiber composition		
Mhc1	Forward	AAGGTCAAGGCCTACAAGC
	Reverse	CGGAACTTGGACAGGTTGGT
Mhc2a	Forward	AAGCGAAGAGTAAGGCTGTC
	Reverse	CTTGCAAAGGAACTTGGGCTC
Mhc2b	Forward	GAAGAGCCGAGAGGTTCACAC
	Reverse	CAGGACAGTGACAAAGAACGTC
Mb	Forward	TCCCAGTCCATTTTCTTCTG
	Reverse	GTGGGAGACTTGATGCTCAC
Tnnl	Forward	AGCTGCAGGAGATGATTGAC
	Reverse	TCCGTAATGGTCTCACCTGT
FA metabolism		
Cd36	Forward	CAACCACTGTTTCTGCACTG
	Reverse	CAGGCTTTCCTTCTTTGCAC
Fabp3	Forward	CATGACCAAGCCTACCACAAT
	Reverse	CCCCAACTTAAAGCTGATCTCTG
Acadl	Forward	AAGGATTTATTAAGGGCAAGAAGC
	Reverse	GGAAGCGGAGGCGGAGTC
Mcd	Forward	GCACGTCCGGGAAATGAAC
	Reverse	GCCTCACACTCGCTGATCTT
Cpt1	Forward	AGCACACCAGGCAGTAGCTT
	Reverse	AGGATGCCATTCTTGATTCG
Glucose metabolism		
Glut1	Forward	CAGTTCGGCTATAACACTGGTG
	Reverse	GCCCCCGACAGAGAAGATG
Pdhk4	Forward	AACGCAACACAAAACCAAGC
	Reverse	CATTGCCAAAGGAGAAGCAG
Mitochondrial function		
Cs	Forward	CCGTGCTCATGGACTTGGGCCTT
	Reverse	CCCCTGGCCCAACGTAGATGCTC
Sdh	Forward	CAT GAA CAT CAA CGG AGG CAA
	Reverse	CTC CTG GGA CTC ATC CTC TT
Transcriptional receptors		
Pparα	Forward	TCGGCG AAC TAT TCG GCT G
	Reverse	GCA CTT GTG AAA ACG GCA GT

Pparg	Forward	CATGACCAGGGAGTTCCTCAA
	Reverse	GCAAACTCAAACTTAGGCTCCATAA
Pgc1α	Forward	GCACCAGCCAACACTCA
	Reverse	TGGGTGTGGTTTGCTGCA
Lxrb	Forward	GAAGGCGTCCACCATTGAGAT
	Reverse	AGTCGTCCTTGCTGTAGGTGAAGT
BCAA metabolism		
Bcat	Forward	CGGACCCTTCATTCGTCAGA
	Reverse	CCATAGTTCCCCCCCAACTT-3
Bckdk	Forward	GATCCGAATGCTGGCTACTCA
	Reverse	GCCAACAAAATCAGGCTTGTC
LXR targets (lipogenesis)		
Scd1	Forward	CCGGAGACCCCTTAGATCGA
	Reverse	TAGCCTGTAAAAGATTTCTGCAAACC
Srebp1c	Forward	GG GCCATGGATTGCACATT
	Reverse	AGGAAGGCTTCCAGAGAGGA

Mitochondrial protein isolation

Mitochondria was isolated from gastrocnemius muscle as described [201]. Briefly, fresh gastrocnemius muscle was rinced and miced into small pieces in ice-cold PBS with 10mM EDTA, followed by resuspension in ice-cold PBS/EDTA with 0.05% Trypsin for 30 min. After centrifuging at 200 xg for 5 min and decarding supernatant, the pellet was homogenized in mitochondrial isolation buffer (250mM mannitol, 5mM HEPES, 0.5 mM EGTA, pH7.4) with a Potter-Elvejhem homogenizer. The homogenate was centrifuged at 600 xg for 5 min at 4°C to keep the supernatant, which was then centrifuged at 10,400 xg for 10 min at 4°C to get the pellet. The pellet was resuspended in mitochondrial isolation buffer and the mitochondrial protein concentration was measured by Bradford Assay[81].

Western blotting for protein analysis

Gastrocnemius muscles were homogenized in 12 volumes of RIPA buffer (Cell Signaling, 9806) with protease and phosphatase inhibitor (ThermoFisher, A32961) with a Potter-Elvejhem homogenizer for 2 min on ice. The homogenates were centrifuged at 20,000 x g (15,000 rpm) at 4°C for 20 min to separate the supernatant; plasma membrane fraction was prepared by sequential centrifugation as described[202] and the protein concentration was determined by Bradford Assay. Equal amounts of protein, as indicated, were resolved by SDS-PAGE and transferred onto nitrocellulose membranes using a wet transfer system (BioRad) at 20V overnight at 4C. The membranes were blocked in 5% (w/v) bovine serum albumin (BSA) solution for 1 hour at room temperature. For total protein extracts, the membranes were probed with phospho-AMPK, AMPK, GAPDH (Cell Signaling Technologies, 2531, 2793, 2118, respectively), MHC I, MHC IIa, and MHC IIb antibodies (1:100, DSHB, BA-F8, SC-71, 10F5, respectively) at 4°C overnight; for plasma membrane fraction, the membranes were probed with GLUT4 and IRβ (Cell Signaling Technologies, 2213 and 3025, respectively); for mitochondria fraction, the membranes were probed with OXPHOS antibody cocktail (Abcam, ab110413) and VDAC1 antibody (Abcam, ab15895). Primary antibody incubation was followed by IRDye® 800CW and 680RD secondary antibody (LiCOR) for 1 hour, and the detection was done using the 800 channel of Odyssey® Imaging Systems (LiCOR).

Histochemical analyses

Frozen sections (10 µm) were cut in a cryostat, placed on microscope slides, and stored at -80°C for further analysis. On the staining day, slides were allowed to come to room temperature and were then fixed in 4% paraformaldehyde-PBS. Intramuscular triglyceride was stained with a solution of triethyl-phosphate saturated with Oil Red O (Sigma, O0625) as described[203]. Oil red O

stained-sections were examined in brightfield and epifluorescence using a Texas red excitation filter (540–580 nm).

Metabolomics

Metabolomics analysis of frozen livers, plasma and gastrocnemius muscles from WT and LFABP$^{-/-}$ mice was performed by Metabolon (Durham, NC) (n=5 per group for livers and plasma, n=6 per group for muscles). Non-targeted metabolic profiling was conducted using three independent platforms: ultrahigh performance liquid chromatography/tandem mass spectrometry (LC/MS) optimized for basic species, LC/MS optimized for acidic species, and gas chromatography/mass spectrometry as described previously[204,205]. Metabolites were identified by automated matching to chemical reference library standards on the basis of retention time, molecular weight (m/z), preferred adducts, and in-source fragments as well as associated MS spectra, and were curated using software developed at Metabolon[206]. Following log transformation and imputation of missing values with minimum observed values, statistical tests (e.g., t-tests, ANOVA with contrasts, etc.) were used to identify biochemicals that differ significantly between experimental groups. An estimate of the false discovery rate (q-value) was calculated to take into account the multiple comparisons that normally occur in metabolomic-based studies.

Statistics

Pooled data represent mean ± S.E.M. Statistical comparisons were made by two-tailed Student's t test (LFABP$^{-/-}$ vs WT). A p value of less than 0.05 was considered statistically significant.

Results

LFABP$^{-/-}$ mice are protected from high fat feeding-induced decline in exercise capacity

Studies from our laboratory have shown that although there are only modest difference between LFABP$^{-/-}$ and WT mice on low fat diets, LFABP$^{-/-}$ mice become more obese than WT mice when challenged with high fat diets[81,88]. Despite the higher weight gain and fat mass, however, they displayed increased spontaneous activity levels[88]. Here we challenged the mice with an exercise tolerance test, and a surprising exercise phenotype in LFABP$^{-/-}$ mice was observed: On low fat diets, the exercise capacity of WT and LFABP$^{-/-}$ mice was similar. However, in response to high fat feeding, WT mice showed a marked decrease in exercise capacity, whereas LFABP$^{-/-}$ mice maintained their exercise capacity at a comparable level to their low fat-fed counterparts (Fig. 2-1A and B). Similar results were observed with high fat-fed mice in both fed and fasting state, with LFABP$^{-/-}$ mice showing an approximate doubling of total running distance compared with WT (Fig. 2-1C and D). A side-by-side comparison of WT mice and two LFABP$^{-/-}$ substrains, one with mixed J/N background and one >98% J, was performed to examine exercise capacity in the fasting state. Compared with WT, both LFABP$^{-/-}$strains showed significantly higher exercise capacity, with no differences between the two LFABP$^{-/-}$ BL6 strains (Fig. 2-1E and F). Similarly, no consistent differences in weight gain, fat mass, or food intake were observed between the two substrains (data not shown). Initial observations were first reported in abstract form[20].

Figure 2-1

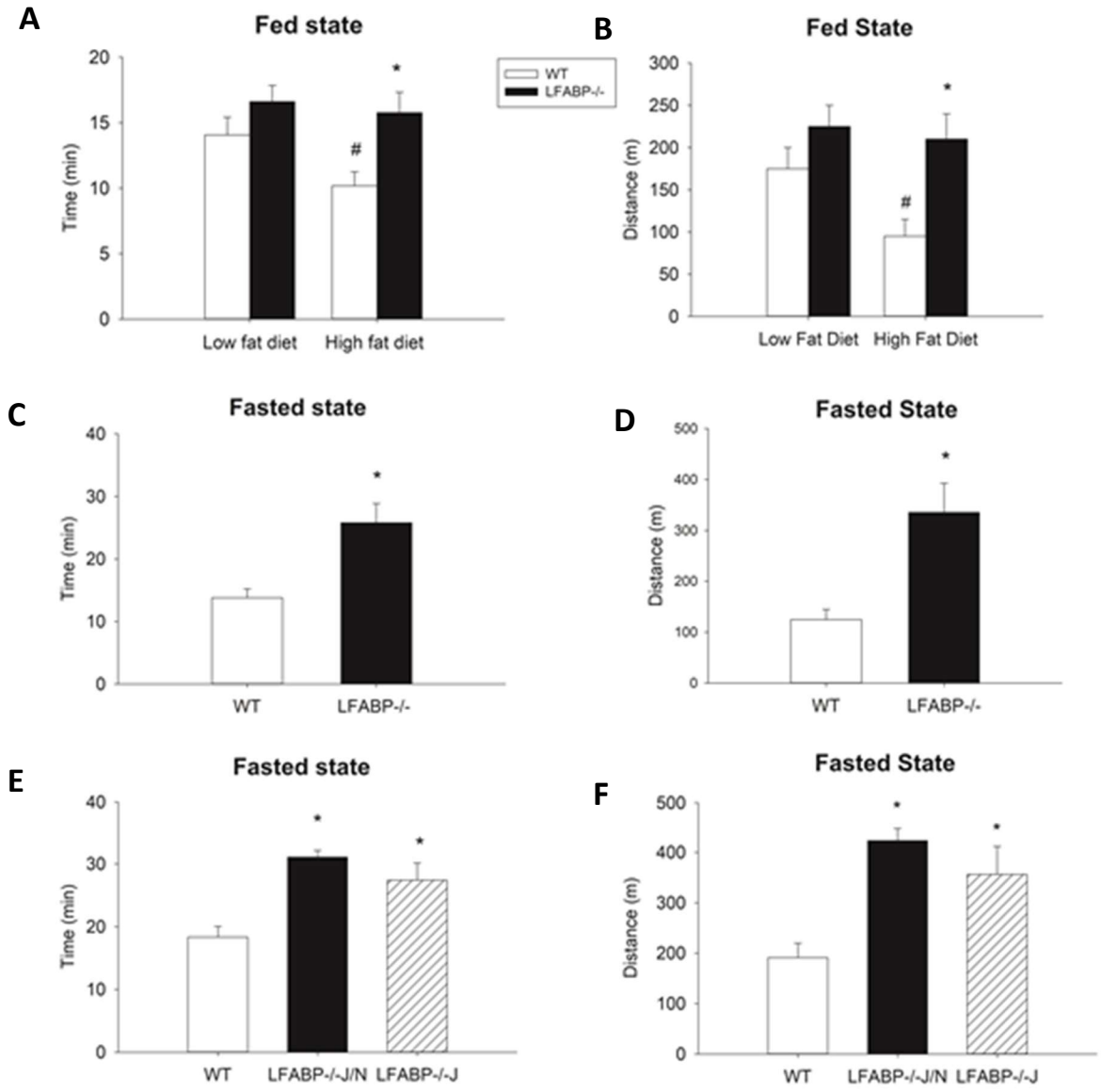

<u>Figure 2-1. Exercise capacity of WT and LFABP$^{-/-}$ mice.</u> (A, B) Running time and distance until exhaustion point of WT and LFABP$^{-/-}$ mice on the low fat and high fat diets at 20 weeks of age in the fed state (n=8-10 per group);(C, D) Running time and distance until exhaustion of high fat-fed WT and LFABP$^{-/-}$ mice in the fasted state (n=8-10 per group). (E, F) Time and running distance

of high fat-fed WT and two strains of LFABP$^{-/-}$ mice in the fasted state (n=6-9 per group). Data are mean ± S.E.M. *$p<0.05$ vs WT, #$p<0.05$ vs Low Fat Diet.

High fat-fed LFABP$^{-/-}$ mice have increased substrate availability

To understand how skeletal muscle energy metabolism in LFABP$^{-/-}$ mice supports a higher exercise capacity, we examined the fuel supply in their skeletal muscles following 12 weeks of high fat feeding. First, we measured the locally stored substrates, including muscle glycogen and intramuscular triglyceride (IMTG), in resting skeletal muscle of high fat-fed LFABP$^{-/-}$ mice. Compared with WT mice, LFABP$^{-/-}$ mice had significantly higher levels of both muscle glycogen and IMTG (Figure 2-2A and B), providing an increased substrate availability for energy production. Oil red O staining of frozen cryosections of gastrocnemius muscle further indicated the higher TG content in LFABP$^{-/-}$ mice, with even distribution among all muscle fibers (Fig 2-2C).

As the mice were in the fasting state, we also examined the potential role of gluconeogenesis in contributing to muscle fuel supply. Glycerol tolerance tests showed a delayed increase in blood glucose in response to glycerol injection in LFABP$^{-/-}$ mice relative to WT, but the peak glucose level was higher in LFABP$^{-/-}$ mice (Fig. 2-2D). After adjusting for baseline levels, LFABP$^{-/-}$ mice had a higher area under the curve (AUC) than the WT mice, suggesting a greater gluconeogenesis capacity (Fig. 2-2E). Using metabolomics approach, we found overall similar levels of gluconeogenic substrates, however the LFABP$^{-/-}$/WT ratios were mostly below 1 and there were significant decreases in liver proline and glycine, and in plasma lactate (Table 2-3). These results suggest that despite the enhanced gluconeogenesis capacity in LFABP$^{-/-}$ mice, their gluconeogenesis level in the fasting state may be restricted by diminished substrate availability.

Figure 2-2

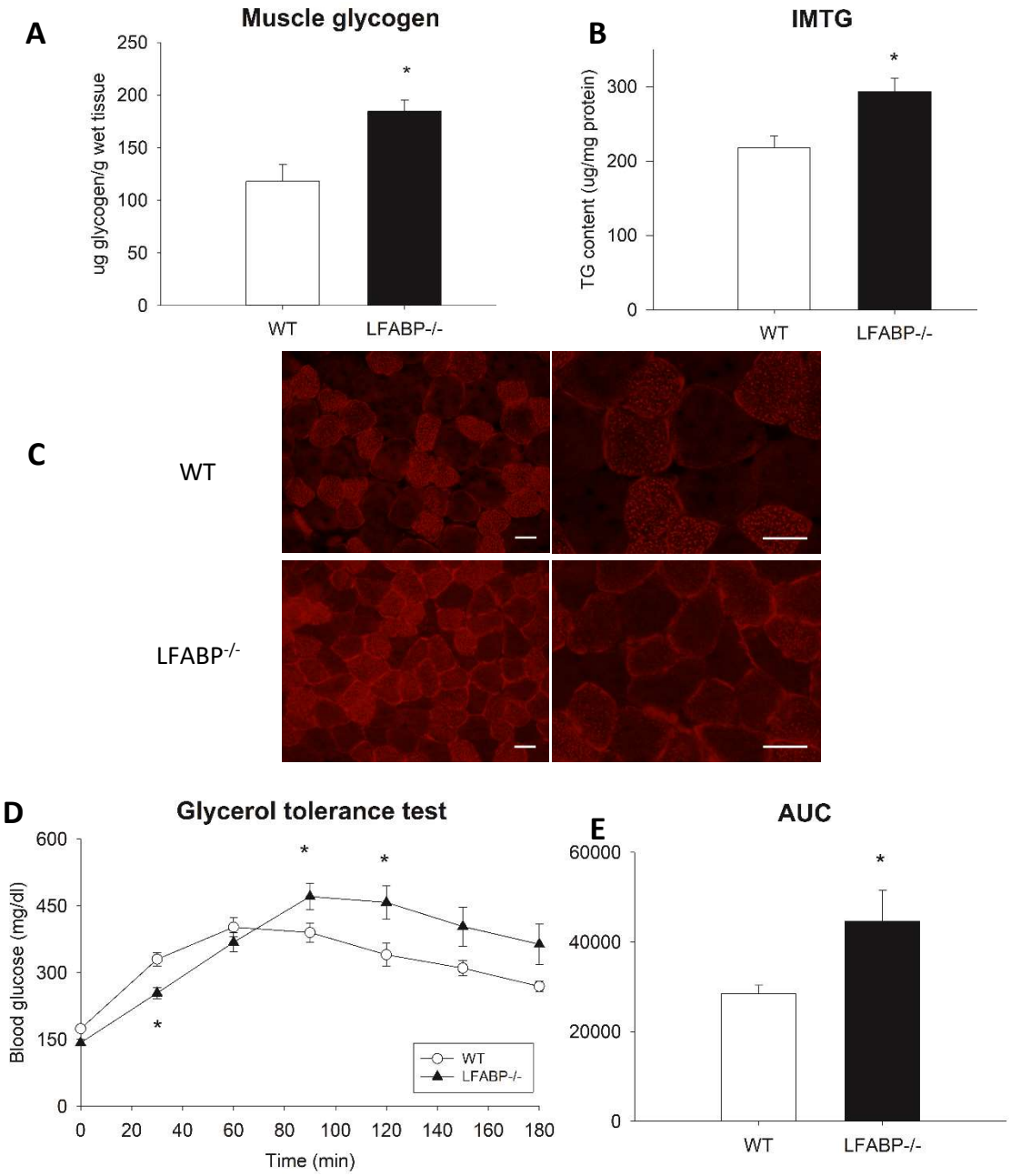

Figure 2-2. Substrate availability in high-fat fed WT and LFABP$^{-/-}$ mice in the fasted state. (A) Muscle glycogen content (n=6-9 per group) and (B) intramuscular triglyceride (n=12 per group). (C) Oil red O staining of frozen cryosections of gastrocnemius muscle (scale bars=50µm). (D) Blood glucose level and (E) area under the curve adjusted for baseline in a glycerol tolerance test in resting mice (n=10-12 per group). Data are mean ± S.E.M. *$p<0.05$ vs WT.

Table2- 3. Glucogenic substrates in the liver and plasma of WT and LFABP$^{-/-}$ mice

Metabolites	LFABP-KO/WT ratio	p value	q value
Glucogenic amino acids			
alanine	0.85	0.16	0.70
aspartate	0.96	0.82	0.72
asparagine	1.6	0.20	0.70
glutamate	0.99	0.89	0.73
glutamine	0.97	0.64	0.71
cysteine	0.99	0.47	0.70
proline	0.85*	0.008	0.67
glycine	0.66*	0.007	0.67
serine	0.8	0.13	0.70
threonine	0.87	0.15	0.70
histidine	0.78	0.16	0.70
valine	0.93	0.53	0.70
methionine	0.92	0.33	0.70
Glucogenic and ketogenic amino acids			
phenylalanine	0.89	0.13	0.70
tyrosine	0.89	0.16	0.70
tryptophan	0.93	0.29	0.70
isoleucine	0.91	0.26	0.70
Other substrates			
glycerol	0.64	0.37	0.70
lactate	1.11	0.85	0.73
Plasma substrates			
glycerol (plasma)	0.99	0.97	0.58
lactate (plasma)	0.69**	0.08	0.34

Comparison of metabolite levels measured from samples of the liver and plasma from LFABP$^{-/-}$ mice and WT controls following 12 weeks of high fat feeding (n=5 per group). Metabolites were determined by liquid chromatography tandem mass spectrometry (LC-MS/MS). *$p<0.05$ between WT and LFABP$^{-/-}$, **$0.05<p<0.1$ between WT and LFABP$^{-/-}$.

High fat-fed LFABP$^{-/-}$ mice have greater mitochondrial function

Sustained energy is needed to maintain muscle contraction in prolonged exercise, and mitochondrial respiration is the major limiting factor in ATP regeneration[94]. Along with the demonstrated increases in glycogen and IMTG availability, we examined mitochondrial function to interrogate the metabolic machinery available to utilize the substrate. Based on the levels of mitochondrial proteins, LFABP$^{-/-}$ mice appear to have a higher mitochondrial quantity in skeletal muscle relative to WT mice (Fig. 2-3A). A marked increase in CS activity and a trend toward higher SDH activity in LFABP$^{-/-}$ mice suggest greater mitochondrial function to support substrate utilization in skeletal muscle (Fig. 2-3B and C), although CCOX activity was similar in both genotypes (Fig. 2-3D). Furthermore, compared with WT mice, LFABP$^{-/-}$ mice had a higher rate of $^{14}CO_2$ production from ^{14}C-oleic acid in skeletal muscle (Fig. 2-3E), indicating greater capacity for complete fatty acid oxidation. The incomplete fatty acid oxidation levels, considered a measure of insulin sensitivity and mitochondrial overload[207], were similar between LFABP$^{-/-}$ and WT mice, as reflected by the unchanged production rate of acid soluble metabolite (ASM) (Fig. 2-3F).

Figure 2-3

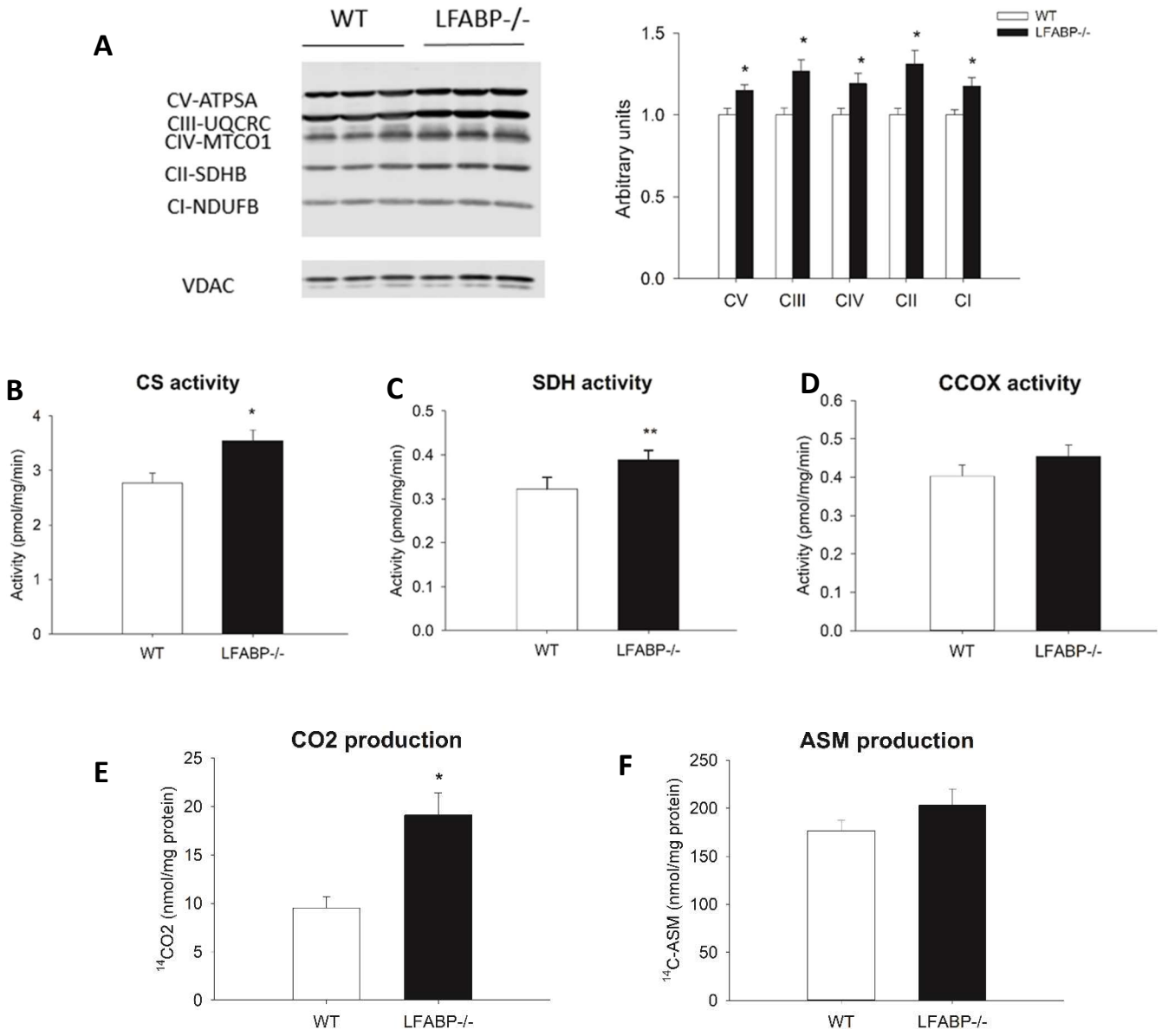

<u>Figure 2-3. Mitochondrial function in resting skeletal muscles of high-fat fed WT and LFABP$^{-/-}$ mice in the fasted state.</u> (A) Mitochondrial content in the muscles and mitochondrial enzyme activities of (B) CS, (C) SDH, (D) CCOX in WT and LFABP$^{-/-}$ skeletal muscle (n=7-9 per group). (E) ^{14}CO2 production and (F) ^{14}C-labeled acid soluble metabolites (ASM) after ^{14}C-Oleic acid administration to muscle homogenates (n=8-9 per group). Data are mean ± S.E.M. *p<0.05 vs WT, **p=0.07 vs WT.

Muscle fiber composition is not altered in skeletal muscle of LFABP$^{-/-}$ mice

To investigate whether the loss of LFABP alters muscle fiber composition in skeletal muscle, we performed real-time quantitative PCR (qPCR) analyses and Western blotting to determine the levels of several markers for type I and type II myofibers in gastrocnemius muscle of LFABP$^{-/-}$ mice. At the mRNA level, there were no significant differences between LFABP$^{-/-}$ and WT mice in markers for oxidative muscle fibers including type I-specific myosin heavy chain 1 (*mhc1*), type IIa-specific mhc 2a, myoglobin (*Mb*) and troponin I slow (*Tnnl*), whereas type IIb-specific mhc2b showed a significant decrease in transcriptional level in LFABP$^{-/-}$ mice (Fig. 2-4A). Western blots confirmed that MHC1 and MHC2a levels were similar between LFABP$^{-/-}$ and WT mice; the decrease in *mhc2b* mRNA levels did not affect its protein abundance in LFABP$^{-/-}$ mice (Fig. 2-4B). Overall, the muscle fiber composition in gastrocnemius muscle appeared unchanged in LFABP$^{-/-}$ relative to WT mice.

Figure 2-4

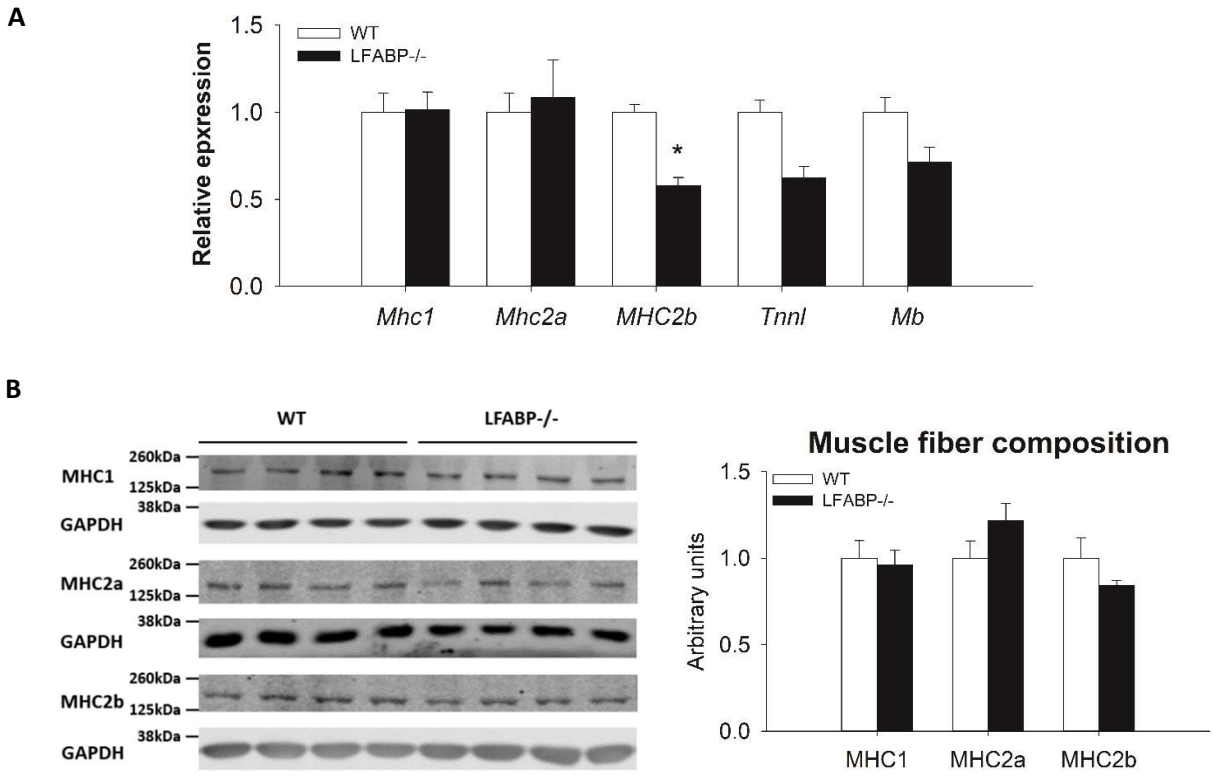

<u>Figure 2-4. Muscle fiber characterization in gastrocnemius muscle of WT and LFABP$^{-/-}$ mice.</u> (A) Relative quantitation of mRNA expression and (B) protein levels of markers for different myofibers (n=7-8 per group), Data are mean ± S.E.M. *p<0.05 vs WT.

LFABP$^{-/-}$ mice show efficient substrate utilization during exercise

As described above, high fat-fed LFABP$^{-/-}$ mice displayed an increased aerobic exercise capacity with a greater mitochondrial function and fatty acid oxidation capacity compared with high fat-fed WT counterparts. Since endurance exercise performance is strongly correlated with aerobic exercise capacity[96], we used indirect calorimetry to examine the substrate utilization of LFABP$^{-/-}$ mice during a 20-min low intensity (endurance type) exercise. The exercise protocol was designed to allow all mice to complete the test, and the mice were fasted overnight before the test to promote fatty acid utilization and keep the condition consistent with the pre-exercise (resting) analysis. LFABP$^{-/-}$ and WT mice did not exhibit markedly different RER values at any single timepoint (Fig. 2-5A), but the average RER of the first and second halves of the 20-minute exercise bout showed different patterns. In the first 10 min, LFABP$^{-/-}$ mice had a higher average RER than WT mice, suggesting relatively more energy production from carbohydrate utilization; in the second half of the exercise, LFABP$^{-/-}$ mice showed a lower average RER compared with WT mice, suggesting a preference for lipid oxidation to provide energy (Fig. 2-5B). Interestingly, while the resting total energy expenditure (EE) during a 16-hour fasting was similar before exercise between the groups (data not shown), LFABP$^{-/-}$ mice displayed a significantly lower EE during exercise than the WT mice (Fig. 2-5C), even without adjusting for body weights, suggesting that LFABP$^{-/-}$ mice may have better muscle efficiency in energy production than WT mice. In keeping with this, AMP-activated kinase (AMPK), an important energy sensor in skeletal muscle, was activated in both genotypes in response to the exercise, but the induction level was lower in LFABP$^{-/-}$ mice, suggesting a lower stress response at the cellular level (Fig. 2-5D).

In the skeletal muscle, the decrease in glycogen content during exercise was significantly greater in LFABP$^{-/-}$ mice than in WT (Fig. 2-4E), supporting the higher carbohydrate utilization in the first

half of exercise. Post-exercise plasma glucose levels were not different between WT and LFABP$^{-/-}$ mice (Fig. 2-5G), suggesting a similar carbohydrate source from the circulation. In terms of muscle lipid utilization, circulating FFA levels were significantly higher in post-exercise LFABP$^{-/-}$ mice (Fig. 2-5H), and the decrease in IMTG during exercise was trending lower (Fig. 2-5F), suggesting that the greater FA supply from the plasma contributes to muscle energy production in LFABP$^{-/-}$ mice during exercise.

Figure 2-5.

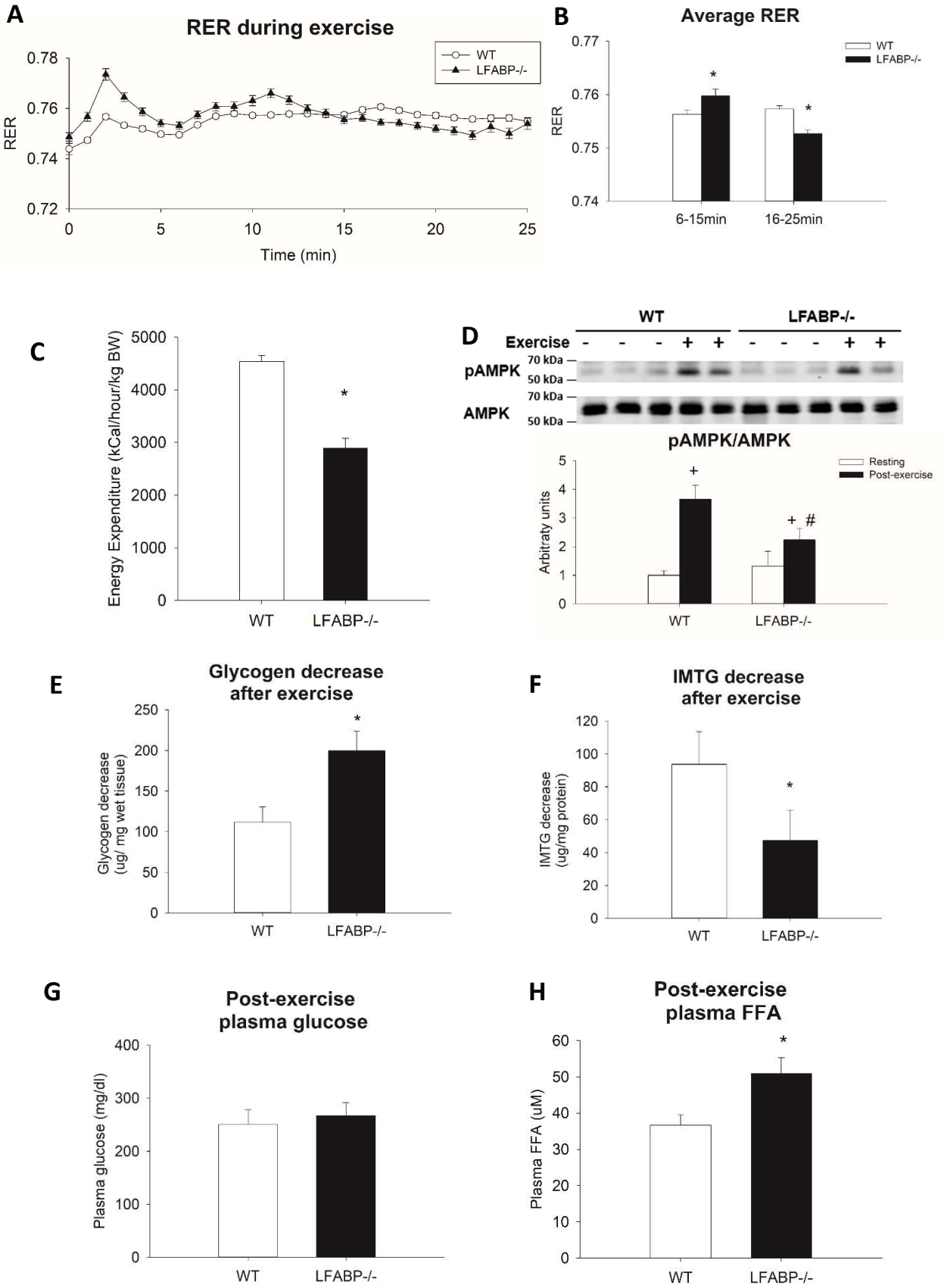
A
RER during exercise
WT
LFABP-/-
RER
Time (min)
B
Average RER
WT
LFABP-/-
RER
6-15min
16-25min
C
Energy Expenditure (kCal/hour/kg BW)
WT
LFABP-/-
D
WT
LFABP-/-
Exercise
pAMPK
AMPK
70 kDa
50 kDa
pAMPK/AMPK
Resting
Post-exercise
Arbitraty units
E
Glycogen decrease after exercise
Glycogen decrease (ug/ mg wet tissue)
F
IMTG decrease after exercise
IMTG decrease (ug/mg protein)
G
Post-exercise plasma glucose
Plasma glucose (mg/dl)
H
Post-exercise plasma FFA
Plasma FFA (uM)

Figure 2-5. Substrate utilization on the whole body level and in skeletal muscle of WT and LFABP$^{-/-}$ mice during low-intensity exercise. (A) RER during a 1 min settlement, 5 min warm-up and a 20 min exercise, (B) average RER for the first half and second half of the exercise, and (C) Energy expenditure during exercise (n=8-10 per group). (D) AMPK activation in skeletal muscle in response to exercise (n=5). Decrease in (E) muscle glycogen content and (F) intramuscular triglyceride after exercise (n=8-10 per group). Plasma (G) glucose and (H) free fatty acid (FFA) after exercise (n=8-10 per group). Data are mean ± S.E.M. *$p<0.05$ vs WT, **$p\approx0.09$ vs WT, +$p<0.05$ vs same genotype on resting state, #$p\approx0.05$ vs WT-EX.

Differential metabolic regulation and basal metabolites in LFABP$^{-/-}$ muscle

To further define the muscle metabolic changes at the molecular level, we analyzed the expression of several genes involved in lipid and glucose metabolism using qPCR (Fig. 2-6A). The mRNA levels of PPARs were not significantly different in the muscle of LFABP$^{-/-}$ mice compared with WT, although we noted a trend toward a higher level of the PPARα target gene long chain acyl-CoA dehydrogenase (*Acadl)* in LFABP$^{-/-}$ mice. Interestingly, carnitine palmitoyl transferase 1 (*Cpt1*) and malonyl-CoA dehydrogenase (*Mcd*) expression were downregulated in LFABP$^{-/-}$ mice, suggesting a suppression of fatty acid transport into the mitochondria. However, similar levels of *Cs* and *Sdh* mRNA expression between the two groups indicated that the *Cpt1* decrease was not associated with impaired metabolic machinery in LFABP$^{-/-}$ muscles. Since both CS and SDH are encoded by the nuclear genome and synthesized in cytosol before being imported into mitochondria, the increase in CS and SDH activities in LFABP$^{-/-}$ muscle (Fig. 2-3B and C) despite their similar mRNA levels suggests improved mitochondrial protein assembly and overall integrity of the mitochondria. Both groups had a similar mRNA expression of *fabp3*, the muscle form of FABP, indicating that the ablation of LFABP did not cause any compensatory FABP overexpression in skeletal muscle. Although LFABP$^{-/-}$ mice showed a significant decrease in muscle *glut1* mRNA level (Fig. 2-6A), there was a higher resting GLUT4 abundance on muscle plasma membrane compared with WT (Fig. 2-6B), which may facilitate glucose transport into the skeletal muscle and promote glycogen synthesis.

We also used non-targeted metabolomics to measure alterations in levels of 522 metabolites associated with major metabolic pathways in the skeletal muscle. We found LFABP$^{-/-}$ muscle had decreased metabolites involved in amino acid signaling (glutamine, asparagine), and specifically in branched chain amino acid catabolism (β-hydroxyisovaleroylcarnitine, α-hydroxyisovalerate,

2-methylbutyrylcarnitine, 3-hydroxyisobutyrate) (Table 2-4). This is consistent with the lower expression levels of BCAA-catabolizing enzymes (Bcat, Bckdk) in LFABP$^{-/-}$ muscle relative to WT (Fig. 2-6C). In addition, LXR signaling was shown to be downregulated, based on the decreased mRNA of Lxrβ and its downstream targets, where a trend toward lower Srebp1c was noted (Fig. 2-6D).

Figure 2-6.

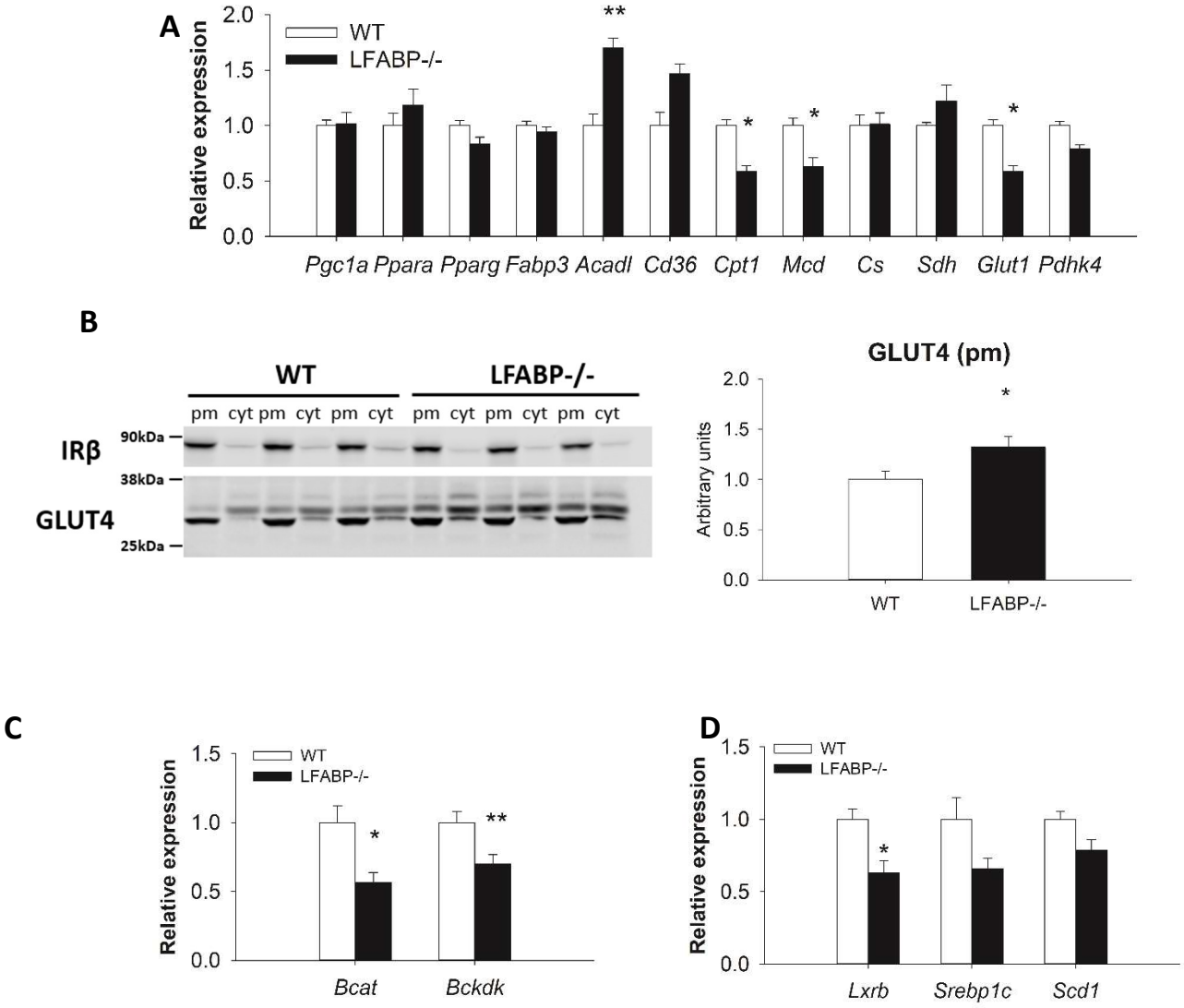

<u>Figure 2-6. Metabolic regulation in resting muscles of high fat-fed WT and LFABP$^{-/-}$ mice.</u> (A) mRNA expression levels of genes involved in lipid metabolism and mitochondrial function (n=6-7). (B) Muscle GLUT4 protein abundance on plasma membrane (pm) and in cytosol (cyt) (n=10). GLUT4 levels on plasma membrane was corrected by the plasma membrane marker insulin receptor β (IRβ). (C) mRNA expression levels of BCAA catabolic genes. (D) mRNA expression levels of transcription factor LXR and its downstream targets in the skeletal muscle (n=6-7). *$p<0.05$ vs WT, **$0.05 \leq p \leq 0.07$.

Table 2-4. Basal metabolites in LFABP$^{-/-}$ and WT muscles.

Metabolites	LFABP$^{-/-}$/WT ratio	p value	q value
AA signaling			
glutamine	0.83*	0.007	0.21
asparagine	0.82*	0.004	0.18
BCAA metabolism			
leucine	0.79	0.18	0.47
4-methyl-2-oxopentanoate	0.92	0.96	0.73
isovalerylcarnitine	0.41	0.11	0.47
beta-hydroxyisovaleroylcarnitine	0.63*	0.02	0.30
alpha-hydroxyisovalerate	0.53*	0.03	0.33
isoleucine	0.82	0.23	0.49
allo-isoleucine	0.55	0.12	0.47
2-methylbutyrylcarnitine (C5)	0.56*	0.04	0.34
valine	0.85	0.34	0.53
isobutyrylcarnitine	0.58	0.23	0.49
3-hydroxyisobutyrate	0.7*	0.03	0.34

Comparison of metabolite levels measured from samples of the gastrocnemius muscle isolated from LFABP$^{-/-}$ mice and WT controls following 12 weeks of high fat feeding (n=6 per group). Metabolites were determined by liquid chromatography tandem mass spectrometry (LC-MS/MS). *$p<0.05$ between WT and LFABP$^{-/-}$; **$0.05<p<0.1$ between WT and LFABP$^{-/-}$.

Discussion

Exercise capacity is affected by many physiological factors that support sustained energy production for muscle contraction, particularly mitochondrial function and substrate availability [94,95,97]. As skeletal muscle is one of the major metabolic engines of the body, obesity and associated conditions like metabolic syndrome have been shown to render impaired energy metabolism in skeletal muscle, including decreased glycogen synthesis, excessive oxidative stress, and mitochondrial dysfunction[101,208,209]. Consequently, physical fitness and exercise capacity are generally limited in obese and insulin-resistant individuals[102,103]. Such impaired energy metabolism in skeletal muscle does not seem to be restricted to the obese population, because even a short-term high fat feeding has been shown to induce a significant decrease in exercise capacity without substantial weight gain[106,107]. Although exercise is well accepted as a major therapeutic intervention for treating obesity and insulin resistance[210,211], it can be very challenging for patients to follow a recommended exercise regimen due to their low fitness level, impeding the benefits of exercise in managing these metabolic diseases. Indeed, inactivity and poor aerobic fitness have been found to be more important than overweight and obesity as mortality predictors[104,105].

In this report, we show that LFABP ablation, when accompanied by lipid overload caused by chronic high fat feeding, is associated with major metabolic alterations in skeletal muscle. These alterations protect LFABP$^{-/-}$ mice from the high fat feeding-induced decline in exercise capacity. It is worth noting that although LFABP$^{-/-}$ mice showed a higher spontaneous activity level than WT mice, the amount of activity was not enough to increase the total energy expenditure and therefore “training effects” did not seem to contribute to the exercise phenotype. We previously reported similar glucose tolerance and blood lipid profiles in resting LFABP$^{-/-}$ mice despite their higher adiposity[88]; given the exercise phenotype and improved energy metabolism

in skeletal muscle shown here, LFABP$^{-/-}$ mice seem to display signs of metabolically healthy obesity (MHO). MHO is characterized by the absence or alleviation of metabolic abnormalities such as dyslipidemia, insulin resistance, hypertension, an unfavorable inflammatory response and poor physical fitness[212-214]. Indeed, a preliminary study shows that LFABP$^{-/-}$ mice have a longer lifespan compared to WT mice on a chow diet (data not shown), suggesting an improved overall health status of LFABP$^{-/-}$ mice. Notably, as a growing body of evidence has supported the reversible transition between MHO and metabolically unhealthy obesity[215,216], MHO is recognized as a dynamic status that needs long term management for sustainable MHO and prevention of progression to the unhealthy stage[217]. Thus, understanding the exercise phenotype in LFABP$^{-/-}$ mice may offer a new perspective on breaking the vicious cycle of physical inactivity and obesity.

Both fuel supply and metabolic machinery are important limiting factors for muscle energy production, and both showed significant changes in high fat-fed LFABP$^{-/-}$ mice, favoring an improved exercise capacity. While we found that plasma glucose and triglyceride levels were similar between fasting LFABP$^{-/-}$ mice and WT mice, free fatty acids showed a trend toward higher levels in LFABP$^{-/-}$ mice[88]. We propose that the increase in IMTG is likely the result of higher FA uptake from the circulation and a decrease in FA β-oxidation as discussed further below, and as evidenced by the lower expression levels of two enzymes involved in FA transport into the mitochondria. The marked adiposity, greater intramuscular triglyceride and possible increase in plasma free fatty acid in LFABP$^{-/-}$ mice also suggest that their inability to process FA in the liver may divert excess FA back to the circulation, leading to FA accumulation, as TG, in other peripheral tissues. The higher muscle glycogen content in LFABP$^{-/-}$ mice does not appear to be secondary to altered insulin sensitivity, as the insulin-responsive cascade regulating glycogen synthase remained unchanged. It is possible that the trend toward higher basal GLUT4 levels at

the plasma membrane may promote glucose uptake. Furthermore, a higher GLUT4 expression is also consistent with the observed lower Glut1 mRNA level, in that GLUT1 has been shown to exert a negative feedback effect on GLUT4 activity by directing glucose into the hexosamine pathway[218].

In addition to the greater skeletal muscle substrate availability, LFABP$^{-/-}$ mice exhibit higher mitochondrial function, as evidenced by the increased mitochondrial quantity, enzyme activities and fatty acid oxidation capacity. Interestingly, however, the increase in mitochondrial respiratory capacity in LFABP$^{-/-}$ muscle is associated with partial suppression of CPT1 and MCD in the resting state. In contrast to the fatty acid oxidation assays with excess substrate, basal FA β-oxidation is dependent on mitochondrial FA import[219]. CPT1 plays a major role in FA transport into the mitochondria and regulates the rate of β-oxidation; MCD regulates CPT1 activity by degrading its natural inhibitor malonyl-CoA. The down regulation of both CPT1 and MCD indicates a potential role of decreased basal mitochondrial FA import in preserving mitochondrial function under high fat feeding conditions. This idea agrees with several reports showing that restricted β-oxidation prevents the mitochondrial dysfunction induced by overnutrition. For example, MCD knockout mice, a genetic model for partial CPT1 inhibition, were protected from the diet-induced glucose intolerance and depletion of TCA cycle intermediates in the skeletal muscle, indicative of compromised mitochondrial status[207]. Moreover, pharmacological inhibition of CPT1 corrected the insulin resistance in mice with muscle-specific PPARα overexpression, where lipid-oxidative genes were genetically upregulated[220]. In contrast, PPARα null mice showed diminished FA oxidation and remained insulin sensitive under high fat diets[221].

The finding of similar insulin sensitivity between LFABP$^{-/-}$ and WT muscle is consistent with other evidence showing that a restricted basal FA oxidation and higher mitochondrial function do not always translate into improved insulin sensitivity. For example, inhibiting MCD activity in isolated human skeletal myocytes resulted in decreased FA oxidation and increased glucose uptake, but no difference in insulin signaling levels[222]. Further, mice with muscle-specific PGC1a overexpression were more prone to diet-induced insulin resistance despite the significant increase in mitochondrial density[223]. Thus, the relationship between mitochondrial function and insulin sensitivity is still inconclusive, with numerous reports suggesting all possible scenarios: decreased, unchanged or increased (compensatory mechanism) mitochondrial function with insulin resistance, as reviewed by Montgomery and Turner [224].

The "crossover" concept for substrate utilization during exercise indicates that relative oxidation of lipid vs. carbohydrate depends on the exercise intensity relative to the maximal oxygen consumption or aerobic exercise capacity[225]. During low-intensity endurance exercise, lipids are the predominant fuel source and peripheral lipolysis is highly stimulated for FA uptake into muscle, whereas IMTG lipolysis is only stimulated at higher exercise intensity. With increasing exercise intensity, there is a shift toward greater carbohydrate metabolism where plasma glucose uptake and muscle glycogen breakdown are increased[225,226]. During the controlled low intensity exercise bout, compared with WT mice, LFABP$^{-/-}$ mice utilized relatively more carbohydrate for energy production in the beginning of the exercise, reflected by the higher RER and increased glycogenolysis. Later on, LFABP$^{-/-}$ mice switched to use more lipids as an energy source, with a lower RER and elevated plasma FFA, likely from lipolysis in adipose tissue. Moreover, although gluconeogenesis may be limited by substrate levels in LFABP$^{-/-}$ mice at rest, their higher gluconeogenesis capacity may contribute to better energy production during exercise with elevated gluconeogenic precursors in circulation[227,228], and particularly, more

glycerol released from adipose tissue along with FFA in LFABP$^{-/-}$ mice. Overall, consistent with their higher aerobic exercise capacity, LFABP$^{-/-}$ mice seem to rely more on FA oxidation for energy production during a controlled treadmill test, suggesting that the exercise for LFABP$^{-/-}$ mice may be at a relatively lower intensity compared with WT mice.

In summary, LFABP ablation in the liver and intestine prevents the high fat feeding-induced decline in exercise capacity, with metabolic reprogramming in the skeletal muscle including improved mitochondrial function and increased storage of muscle glycogen and IMTG. As LFABP is the only FABP highly expressed in the liver, we propose that the lack of LFABP, which diminishes hepatic lipid handling capacity, shunts surplus FA into circulation and to other peripheral tissues including white adipose tissue and skeletal muscle. In the resting state, the restricted mitochondrial FA import in LFABP$^{-/-}$ muscle protects the mitochondria from sustained lipid overload and thereby preserves mitochondria function and aerobic exercise capacity. This restriction in basal mitochondrial FA import does not seem to affect exercise-induced FA oxidation, as LFABP$^{-/-}$ mice preferentially utilized plasma FFA as their fuel source during a low-intensity exercise compared with WT, in keeping with their higher exercise capacity. With similar expression levels of the muscle FABP (FABP3) and insulin sensitivity, the metabolic alterations in the skeletal muscle underlying the exercise phenotype of LFABP$^{-/-}$ mice are likely the results of insulin-independent interorgan signaling that has yet to be identified. Our report provides a model of obesity with unimpaired physical fitness, and the findings on the muscle metabolic profile in the LFABP$^{-/-}$ mouse could have important implications for identifying therapeutic targets to counter obesity and metabolic syndrome by improving exercise capacity.

Chapter 3

Potential Interorgan Signaling Contributing to the Muscle Metabolic Alterations In LFABP$^{-/-}$ Mice

Abstract

Liver fatty acid-binding protein (LFABP, FABP1) is the only FABP highly expressed in the liver, and it also co-expresses with intestinal FABP in the intestine. LFABP is thought to not only function in intracellular lipid trafficking, but also play an important role in regulating systemic energy homeostasis. Previously, we showed that ablation of LFABP (LFABP$^{-/-}$) in mice results in a more obese phenotype in response to high fat feeding. Surprisingly, LFABP$^{-/-}$ mice were protected from a high fat feeding-induced decline in exercise capacity, with increased substrate availability and mitochondrial function in the skeletal muscle compared with WT. Since LFABP is not expressed in the skeletal muscle, it is of interest to find liver- and/or intestine-derived mediators that cause the muscle metabolic changes in LFABP$^{-/-}$ mice. Using cellular bioenergetics measurements, we found similar respiratory capacity in both groups of mice on a chow diet, supporting our previous observation of similar exercise capacity in chow- or low fat-fed WT and LFABP$^{-/-}$ mice. Interestingly, while the cells from chow-fed mice treated with fatty acids did not show significant differences in mitochondrial respiration, there was a significantly higher maximal respiratory capacity in primary myoblasts from high fat-fed LFABP$^{-/-}$ mice compared with WT. This result suggests that in addition to high concentrations of plasma FAs, certain circulating mediators are required for the improved energy metabolism in high fat fed-LFABP$^{-/-}$ muscle. We therefore examined insulin sensitivity and FGF21, as potential interorgan signaling possibilities. Muscle insulin signaling was similar in both groups; further, despite the lower FGF21 expression in liver and plasma of LFABP$^{-/-}$ mice, no difference was found in FGF21 sensitivity in epidydimal adipose tissues between the groups, suggesting a lower FGF21 signaling in LFABP$^{-/-}$ mice. Interestingly, in contrast to their trending higher plasma adiponectin level, LFABP$^{-/-}$ had trending lower expression levels of adiponectin in the epidydimal adipose tissues, suggesting possible adiponectin production and secretion from other fat depots. Overall, the

alterations in muscle energy metabolism of LFABP$^{-/-}$ mice appear to be induced by signaling molecules in the plasma (possibly involving adiponectin), rather than by intrinsic muscle adaptations directly caused by LFABP ablation.

Introduction

Mammalian fatty acid binding proteins (FABPs) are abundant cytoplasmic proteins with high affinities for certain hydrophobic ligands, such as long-chain fatty acid, eicosanoids and monoacylglycerols[1,2]. FABPs are widely expressed in almost all tissues, with some FABPs expressed in more than one tissue and some tissues expressing more than one FABP. There is only one FABP highly expressed in the liver—liver FABP (LFABP, FABP1), and it is thought to be involved in multiple aspects of hepatic lipid metabolism, including facilitating FA uptake[63], fasting-induced triglyceride accumulation and fatty acid oxidation[64,66], and directly interacting with PPARa[8,59]. LFABP also co-expresses with intestinal FABP in the intestine, where it is shown to direct monoacylglycerol towards TG synthesis and FAs towards oxidative pathways[81]. In addition to these local effects, LFABP also plays an important role in whole body energy homeostasis. We have previously reported that although LFABP null (LFABP$^{-/-}$) mice become more obese than WT mice on high fat diets, they exhibit comparable glucose tolerance and insulin sensitivity on a whole body level[88]. More surprisingly, LFABP$^{-/-}$ mice displayed protection against the high fat feeding-induced decline in exercise capacity, with an approximate doubling of running distance compared with the high fat fed-WT counterparts (Chapter 2). We have found several metabolic alterations in skeletal muscle of high fat fed-LFABP$^{-/-}$ mice that likely underlie this exercise phenotype, including increased substrate availability and improved mitochondrial function (unpublished). Since LFABP is only expressed in the liver and intestine, we are interested in how liver/intestine-derived signals may affect energy metabolism in the skeletal muscles of LFABP$^{-/-}$ mice.

Dynamic crosstalk between metabolic organs is crucial in systemic energy homeostasis. Although the direct signaling between liver/intestine and muscle is not well studied, mounting evidence suggests possible links via the adipose tissues and/or brain. It is well established that

the brain integrates peripheral signals from metabolic organs and regulates food intake, energy expenditure and energy metabolism across different tissues[146,147]. Particularly, the gut-brain axis, consisting of enteric and central nervous systems, plays an important role in connecting gastrointestinal function, gut microbiota and higher cognitive function[229]. Bi-directional communications are also found between liver and intestine through nutrients, metabolites and hormones, thereby coordinating the regulation of intestinal microbiota, gut barrier integrity, bile acid synthesis, as well as hepatic glucose and lipid metabolism[148,230,231]. Originally thought of primarily as a major storing site for excessive fat, adipose tissues are now also considered as complex endocrine organs that can secrete many inflammatory cytokines, hormones and adipokines to regulate various aspects of energy metabolism[155]. For example, the adipokines such as leptin, adiponectin and resistin are not only well studied for their important roles in mediating adipose tissue-brain crosstalk[232], but also are involved in signaling muscle and liver to affect their energy metabolism[155,233-236].

As a liver-derived hormone regulating energy homeostasis[158], FGF21 has emerged as an important candidate for mediating muscle metabolic alterations via liver-adipose signaling. FGF21 is predominantly produced in the liver in response to fasting and is a downstream target of PPARa[159,161], which makes it likely to be affected by disruption in LFABP-PPARa interaction. Physiologically, FGF21 has been shown to increase hepatic lipid oxidation, gluconeogenesis and ketogenesis[159-161]; after being secreted into the circulation, FGF21 acts on adipose tissue to stimulate lipolysis, mitochondrial oxidative capacity and glucose uptake independent of insulin signaling[162-164]. FGF21 knockout or knockdown in mice has been associated with increased hepatic triglyceride accumulation on a ketogenic diet[161,166]. Therapeutically, FGF21 has been considered an antidiabetic agent for metabolic disorders; FGF21 administration in mice and nonhuman primates reverses the diabetic symptoms with improved insulin sensitivity and

reduced adiposity and hepatosteatosis [168-170]. Little has been reported on the direct effects of FGF21 on skeletal muscle, though it was recently shown that FGF21 exposure to human myotubes increased glucose uptake and glycogen content, independent of insulin signaling[172,173]. Additionally, FGF21 is shown to indirectly affect muscle metabolism via adiponectin from adipose tissue[174]. In contrast to most other adipokines, decreased adiponectin has been associated with insulin resistance and type 2 diabetes, with visceral adiposity as an independent negative predictor of circulating adiponectin levels[175,237]. Like FGF21, administration of adiponectin has yielded many antidiabetic effects, including improving glucose and lipid metabolism, as well as insulin sensitivity on a whole body level. In liver, adiponectin has been shown to alleviate fatty liver disorders and inhibit gluconeogenesis via AMPK activation[176,238,239]; in skeletal muscle, adiponectin is thought to enhance lipid oxidation, mitochondrial biogenesis and insulin sensitivity via activation of AMPK and MAPK[156,157], as well as induction of CaMK and PGC1a with increased Ca^{2+} influx [177,240]. While FGF21 has promising effects on improving metabolic disorders, obesity has been demonstrated to be associated with FGF21 resistance, with increased endogenous FGF21 levels in plasma but impaired response to exogenous FGF21 treatment in liver and adipose tissue[172,184].

We found a significant decrease in FGF21 mRNA level in liver and lower FGF21 levels in the plasma of LFABP$^{-/-}$ mice relative to WT mice. Interestingly, there was also a trend toward higher adiponectin levels in the plasma of LFABP$^{-/-}$ mice. Given the role of FGF21 in maintaining whole body energy homeostasis, we hypothesized that the lower FGF21 may indicate a higher FGF21 sensitivity in high fat-fed LFABP$^{-/-}$ mice compared with WT. Moreover, the trending higher plasma adiponectin level in LFABP$^{-/-}$ mice despite their greater adiposity, could perhaps result from an FGF21-induced adiponectin production in the adipose tissue. In the present study, we performed cellular bioenergetics analysis with primary myocytes from both groups of mice to

establish an in vitro model to examine the improved exercise phenotype in LFABP$^{-/-}$ mice. We also compared FGF21 sensitivity in liver and epidydimal white adipose tissues (WATs) of WT and LFABP$^{-/-}$ mice. As adiponectin is thought to couple FGF21 actions to liver and skeletal muscle, we also examined the expression levels of adiponectin in WATs, as well as the adiponectin receptors in skeletal muscle.

Experimental procedures

Animal and diets

LFABP$^{-/-}$ mice backcrossed 6 times on a C57BL/6N background were generated by Martin and coworkers[65] and obtained from B. Binas. As described peviously and below, the mice are back-crossed with C57BL/6J mice from Jackson Laboratories (Bar Harbor, ME) for another six generations to generate congenic F12 LFABP$^{-/-}$mice[81] at Rutgers. C57BL/6J mice bred in our facility serve as controls. Mice were maintained on a 12-h light/dark cycle and allowed *ad libitum* access to standard rodent chow (Purina Laboratory Rodent Diet 5015). At 2 months of age, male LFABP$^{-/-}$ and WT (C57BL/6J) mice were housed 2–3 per cage and fed a high saturated fat (45 kcal%) diet (HFS, Research Diets, Inc. #D10080402) for 12 weeks. At the end of the experiment, mice were euthanized by cervical dislocation prior to collection of blood and tissues. The Rutgers University Animal Care and Use Committee approved all animal experiments.

Collagen coating plates

Collagen solution was made by dissolving 0.05g of collagen type I (ThermoFisher Scientific) in 1 L of double-distilled water with 0.02N acetic acid. To coat the plates with collagen, collagen

solution pre-warmed at 37°C was added to the 6-well cell culture plates (1ml/well). The plates were gently rocked until the surface is evenly covered with collagen solution. Plate rocking was repeated frequently over the next 1 hour, and then kept open in culture hood with blower on for a minimum of 2 hours. The excess collagen solution was pipetted off for reuse in future coating. The plates were left partially open in a hood with the blower on overnight to promote drying. Before use, the plates were rinsed 3 times with PBS.

Isolation of primary myoblasts

Primary myoblasts were isolated from gastrocnemius muscles and differentiated as described[241,242] and their respiration capacity was analyzed using the Seahorse XF24 system. Briefly, gastrocnemius muscles were collected from WT and LFABP$^{-/-}$ mice, minced into small pieces and digested in digestion medium containing PBS with 400U/ml collagenase II (ThermoFisher Scientific), 2.5mM CaCl2 and 1% Penicillin-streptomycin (P/S, Thermo Fisher Scientific) for 1h at 37°C. Digested muscle mixtures were passed through a pre-wet 70 µm tissue strainer (VWR) and centrifuged to obtain the cell pellet for resuspension in pre-warmed proliferation medium (PM) consisting of F-10 Nutrient Mix (Thermo Fisher Scientific) supplemented with 10% Fetal Bovine Serum (FBS, Thermo Fisher Scientific), 10ng/ml human fibroblast growth factor (bFGF, PeproTech) and 1% P/S (Thermo Fisher Scientific). The cell mixture (containing myoblasts and fibroblasts) was plated on non-coated tissue culture plates for 2 hours to let the fibroblasts adhere, before transferring the unattached cells to a collagen I-coated plate (pre-plate 1, pp1). After 18-24 hours, the media containing the unattached cells were transferred to another non-coated plate for 2 hours, followed by transferring to another collagen I-coated plate (pp2). After 18-24 hours, the media containing unattached cells were centrifuged to obtain the cell pellet for resuspension in PM and plating onto the third collagen I-

coated plate (pp3). The procedure for pp2 was repeated on the next day to obtain pp4. PM for pp1-pp4 were changed every 48 hours, and myoblast purity was monitored by microscopic visualization and confirmed with Western blotting as describe below. Purified myoblasts (myoblast:fibroblast > 30) were used directly for cellular bioenergetics analyses or differentiated into myotubes.

Differentiating primary myoblasts to myotubes

To differentiate primary myoblasts to myotubes, differentiation medium (DM) containing Dulbecco's modified Eagle's medium (DMEM, Thermo Fisher Scientific) supplemented with 2% horse serum and 1% P/S was added to the myoblasts at 85-95% confluency. After 48 hours of DM incubation, myotubes were visible and ready for fatty acid treatment.

Cellular bioenergetics analysis

After eliminating fibroblasts using the pre-plating techniques, primary myoblasts were seeded (triplicates) on collagen I-coated XF24 microplates (Seahorse Biosciences) and incubated at 37 °C in PM for overnight before analysis. For the fatty acid treatment study, primary myoblasts were differentiated into myotubes after being seeded on XF24 microplates for overnight, followed by treatment with 500 µM fatty acids (1:1 palmitic acid: oleic acid blend) in DM supplemented with 0.5% BSA (75.3 µM, 6.7:1 FA:BSA) and 1mM L-carnitine for 20 hours[207]. Using the mitochondrial stress test procedure with Seahorse XF24 system, oxygen consumption rate (OCR) and extracellular acidification rate (ECAR) were first determined under basal conditions. Through the multi-port drug injection system, ATP production, maximal respiration and non-mitochondrial respiration levels were determined in response to 1µM oligomycin (VWR), 2µM fluoro-carbonyl

cyanide phenylhydrazone (FCCP) (Cayman Chemicals) and 0.5µM rotenone + antimycin A (Sigma), respectively, as depicted in Figure 3-1.

Figure 3-1.

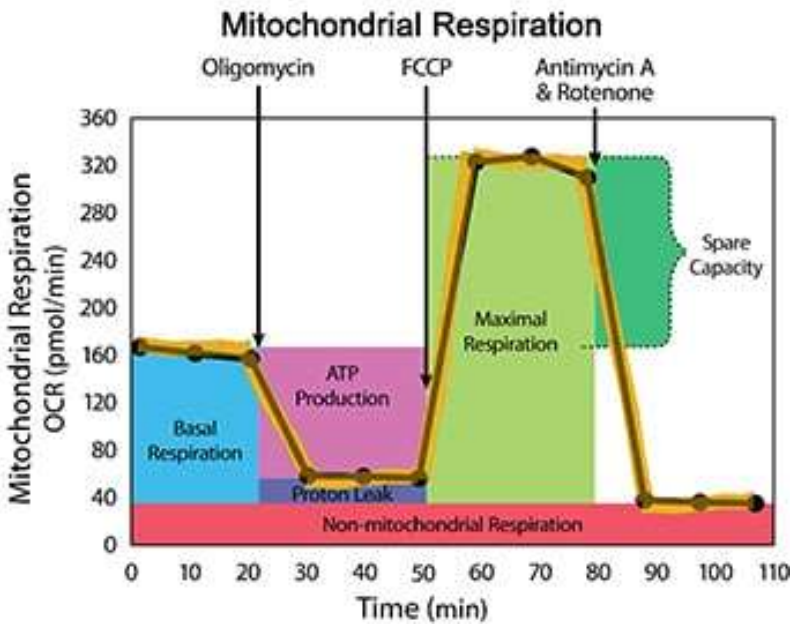

Figure3-1. Schematic of oxygen consumption trace from a mitochondrial stress test (from Aligent.com).

Oligomycin, ATP synthase inhibitor; fluoro-carbonyl cyanide phenylhydrazone (FCCP), ionophore that shuttles hydrogen ions for mitochondrial uncoupling; rotenone and antimycin A, complex I and III inhibitor respectively, are added to cells sequentially to assess mitochondrial respiration.

Insulin signaling

Mice were fasted for 4 hours before intraperitoneal injection with PBS or insulin (Novolin R, Novo Nordisk) at a dose of 2 units/kg body weight. Ten minutes later, mice were sacrificed by cervial dislocation and gastrocnemius muscles were collected for protein extractions and Western bloting of phospho- and total AKT.

in vivo FGF21 signaling

FGF21 sensitivity was measured by the FGF21-induced phosphorylation of ERK1/2 as described by Fisher and colleagues[184]. Briefly, ad libitum-*fed* mice were intravenously injected with saline or recombinant human FGF21 (Raybiotech, GA, solution concentration 50ng/µl) at 0.1mg/kg. Fifteen minutes later, mice are euthanized by cervical dislocation. Liver, epidydimal WAT and gastrocnemius muscles are collected and snap frozen in dry ice for western blot analysis.

Plasma FGF21 analysis

FGF21 ELISA kit (Raybiotech, ELH-FGF21) was used to measure FGF21 in mouse plasma of the mice according to the manufactuer's protocol.

Western blotting

For pp1-pp4 from primary myoblasts isolation, proliferation media was removed from the cells at 80-100% confluency. The plates were kept on ice throughout the lysate preparation. After adding PBS to the plates to wash the cells, PBS was aspirated and RIPA buffer (Cell Signaling, 9806) with protease inhibitors (ThermoFisher Scientific, 88265) was added to the plates (200µl/well in 6-well plates). The plates were incubated on ice for 20 min before scraping the

cells off the surface using a rubber spatula. Cell lysates were centrifuged at 12,000g at 4°C for 10 min. Protein concentration of the supernatant was determined by BCA assay[243] (BCA assay kit, ThermoFisher Scientific, 23227). For tissue lysates, the livers, WATs and gastrocnemius muscles were homogenized in respectively 20×, 1.25× and 12× the weight of the sample of RIPA buffer (Cell Signaling, 9806) supplemented with protease/phosphatase inhibitors (ThermoFisher Scientific, A32959) per gram (wet weight), using a Potter-Elvejhem homogenizer (livers) or a rotor stator homogenizer (WATs and muscles) for 1-2 min on ice. The liver/muscle homogenates were centrifuged at 16,000 g at 4°C for 20 min; the adipose homogenates were centrifuged at 600g at 4°C for 10 min. Protein concentration of the supernatant was determined by Bradford assay. Equal amounts of protein, as indicated, were resolved by SDS-PAGE and transferred onto nitrocellulose membranes using a wet transfer system (BioRad) at 20V overnight at 4°C. The membranes were blocked in 5% (w/v) bovine serum albumin (BSA) solution for 1 hour and probed with primary antibodies at 4°C overnight, followed by IRDye® 680RD and 800CW secondary antibody (LiCOR) for 1 hour. Images were obtained using the 700nm and 800nm channel of Odyssey® Imaging Systems (LiCOR). The following primary antibodies were used in this study: vimentin (Bioss Antibodies, BS-0756R), desmin (Santa Cruz Biotechnology, sc-23879), phosphor-AKT, AKT, phospho-ERK1/2 (Thr202/Tyr204) antibody and total ERK1/2 antibody (Cell Signaling Technologies, 4060, 2920, 4377 and 4696, respectively).

qPCR for mRNA expression analysis

Total RNA was extracted from frozen livers, muscles and WATs (Trizol, Invitrogen) and further purified by RNeasy cleanup kit (Qiagen) along with DNase treatment to minimize genomic DNA contamination. cDNA was synthesized by using a reverse transcription kit (Invitrogen). Primer sequences were retrieved from Primer Bank (Harvard Medical School QPCR primer data base)

and are shown in Table 3-1 below. Efficiency tests were performed for all primers to confirm similar amplification efficiency in both groups. Real time PCR reactions were performed in triplicate using an Applied Biosystems StepOne Plus instrument. Each reaction contained 100ng of cDNA, 250nM of each primer, and 12.5µl of Power SYBR Green Master Mix (ThermoFisher) in a total volume of 25 µl. Relative expression of the target genes was calculated using the comparative Ct method and normalized to endogenous β-actin (for muscle samples) or TBP (for WAT samples).

Table 3-1. Primer sequences for liver/muscle/WAT mRNA expression measurements

genes		Sequences (5'-> 3')
Cd36	forward	GCCAAGCTATTGCGACATGA
	reverse	ATCTCAATGTCCGAGACTTTTCAAC
Pparγ	forward	GAGGACGCGGAAGAAGAGA
	reverse	TTCAGTAAAGGGTAGTCTTGTTTTTAA
Pparα	forward	TATTCGGCTGAAGCTGGTGTAC
	reverse	CTGGCATTTGTTCCGGTTCT
Hmgr	forward	ATTCTGGCAGTCAGTGGGAACT
	reverse	CCTCGTCCTTCGATCCAATTTA
Fasn	forward	TCCTGGAACGAGAACACGATCT
	reverse	GAGACGTGTCACTCCTGGACTTG
Fatp4	forward	GAT GGC CTC AGC TAT CTG TGA
	reverse	GGT GCC CGA TGT GTA GAT GTA
Gk	forward	GCACACGTGGTGCTTTTGAG
	reverse	GCC TTC GGT CCC CAG AGT
Glut1	forward	GGTGTGCAGCAGCCTGTGT
	reverse	CACAGTGAAGGCCGTGTTGA
Pepck	forward	CCACAGCTGCTGCAGAACA
	reverse	GAAGGGTCGCATGGCAAA
Aco	forward	CTT GTT CGC GCA AGT GAG G
	reverse	CAG GAT CCG ACT GTT TAC C
Srebp1c	forward	ATCGGCGCGGAAGCTGTCGGGGTAGCGTC
	reverse	ACTGTCTTGGTTGTTGATGAGCTGGAGCAT
Scd1	forward	TGGGTTGGCTGCTTGTG
	reverse	GCGTGGGCAGGATGAAG
Lxra	forward	GGAGTCATCCGAGCCTACA
	reverse	GCCTTGTCCCCACATACACT

Ucp1	forward	AGGCTTCCAGTACCATTAGGT
	reverse	CTGAGTGAGGCAAAGCTGATTT
Fabp4	forward	AAGGTGAAGAGCATCATAACCCT
	reverse	TCACGCCTTTCATAACACATTCC
Rsp16	forward	CACTGCAAACGGGGAAATGG
	reverse	CACCAGCAAATCGCTCCTTG
Acsl1	forward	CAGAACATGTGGGTGTCCAG
	reverse	GTTACCAACATGGGCTGCTT
AdipoR	forward	TCCCAGGAAGATGAAGGGTTTAT
	reverse	TTCCATTCGTTCGATAGCATGA
Adpn	forward	AGAGAAGGGAGAGAAAGGAGATGC
	reverse	TGAGCGATACACATAAGCGGC
Fgfr1	forward	TGTTTGACCGGATCTACACACA
	reverse	CTCCCACAAGAGCACTCCAA
Fgfr2	forward	CGCCAGCCTGTCACTATACAAA
	reverse	CCAGAGGACCTCGACTCCAA
βKlotho	forward	TGTGGTGAGCGAAGGACTGA
	reverse	GGAGTGGGTTGGGTGGTACA

Results

Primary myoblasts culture and differentiation

Images of pp1-pp4 at day 7 after seeding are shown in Figure 3-2A. At pp1, most of the cells attached to the plate were large and flat triangular-shaped fibroblasts; from pp2-4, more and more small droplet-shaped myoblasts started appearing with less and less adherent fibroblasts on the plates. Vimentin and desmin, markers for fibroblasts and myoblasts, respectively, were used to assess myoblast purity. As shown in Figure 3-2B, Western blots showed that the vimentin: desmin ratio was over 30 on pp4, confirming the purification efficiency. Differentiation media was added to the purified myoblasts on pp4 at 85%-95% confluency. At 48 hours, myotubes were visible and ready for fatty acid treatment (Figure 3-2C).

Figure3-2

A

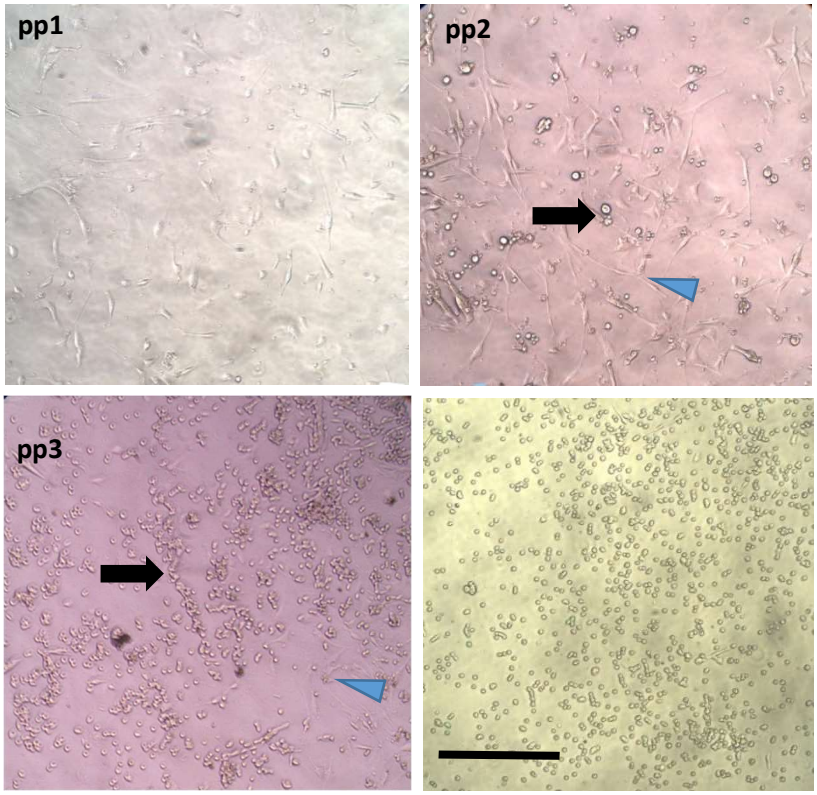

B

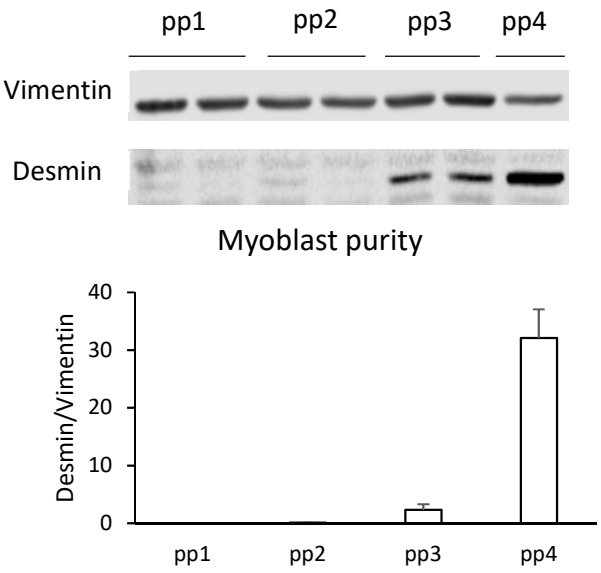

C

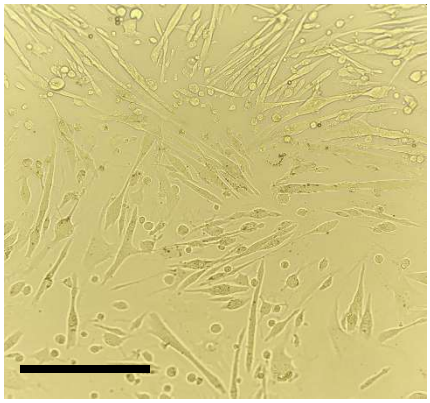

Figure 3-2. Primary myoblast culture and differentiation. (A) Preplates (pp1-pp4) from primary myoblast isolation at day 7 after seeding. Black arrow: myoblasts; blue triangle: fibroblasts. (B) Western blotting of desmin (marker of myoblasts) and vimentin (marker of fibroblasts) from pp1-pp4; the ratio of desmin:vimentin was quantified as an indicator for myoblast purity. (C) 48 hours after adding differentiation media to purified myoblasts. (scale bar=300µm)

Cellular bioenergetics analysis of primary myoblasts

Studies from our laboratory have shown that while there was no difference in exercise capacity between WT and LFABP$^{-/-}$ mice on a low fat diet, LFABP$^{-/-}$ mice were protected from the known high fat feeding-induced decline in exercise capacity, showing an approximate doubling of running distance compared with WT on a high fat diet (Chapter 2, Figure 2-1A). Here we isolated primary myoblasts from both groups of mice on a chow and high fat diet and compared the cellular respiratory levels between WT and LFABP$^{-/-}$ on each diet. In primary myoblasts from chow-fed mice, although the non-mitochondrial respiration trended lower in LFABP$^{-/-}$ mice, basal respiration, proton leak level and maximal reparation were similar between the groups (Figure 3-2A), which is consistent with the similar exercise capacity on low fat feeding condition (Chapter 2, Figure 2-1A). In primary myoblasts from high fat-fed mice, although basal respiration was similar between the groups, LFABP$^{-/-}$ showed a higher maximal respiration compared with WT (Figure 3-2B), in agreement with the improved mitochondrial function in LFABP$^{-/-}$ muscle. We also treated the primary myotubes from chow-fed mice with fatty acids for 20 hours to mimic a chronic high fat feeding condition. In response to FA treatment, primary myotubes from both genotypes showed a significant decrease in maximal respiration, however, there was very modest difference in maximal respiration between the WT and LFABP$^{-/-}$ myotubes treated with FA (Figure 3-3C). This result suggests that the 20h treatment with a high FA concentration alone was not enough to trigger the metabolic adaptations that preserve the mitochondrial function in LFABP$^{-/-}$ muscles.

Figure 3-3

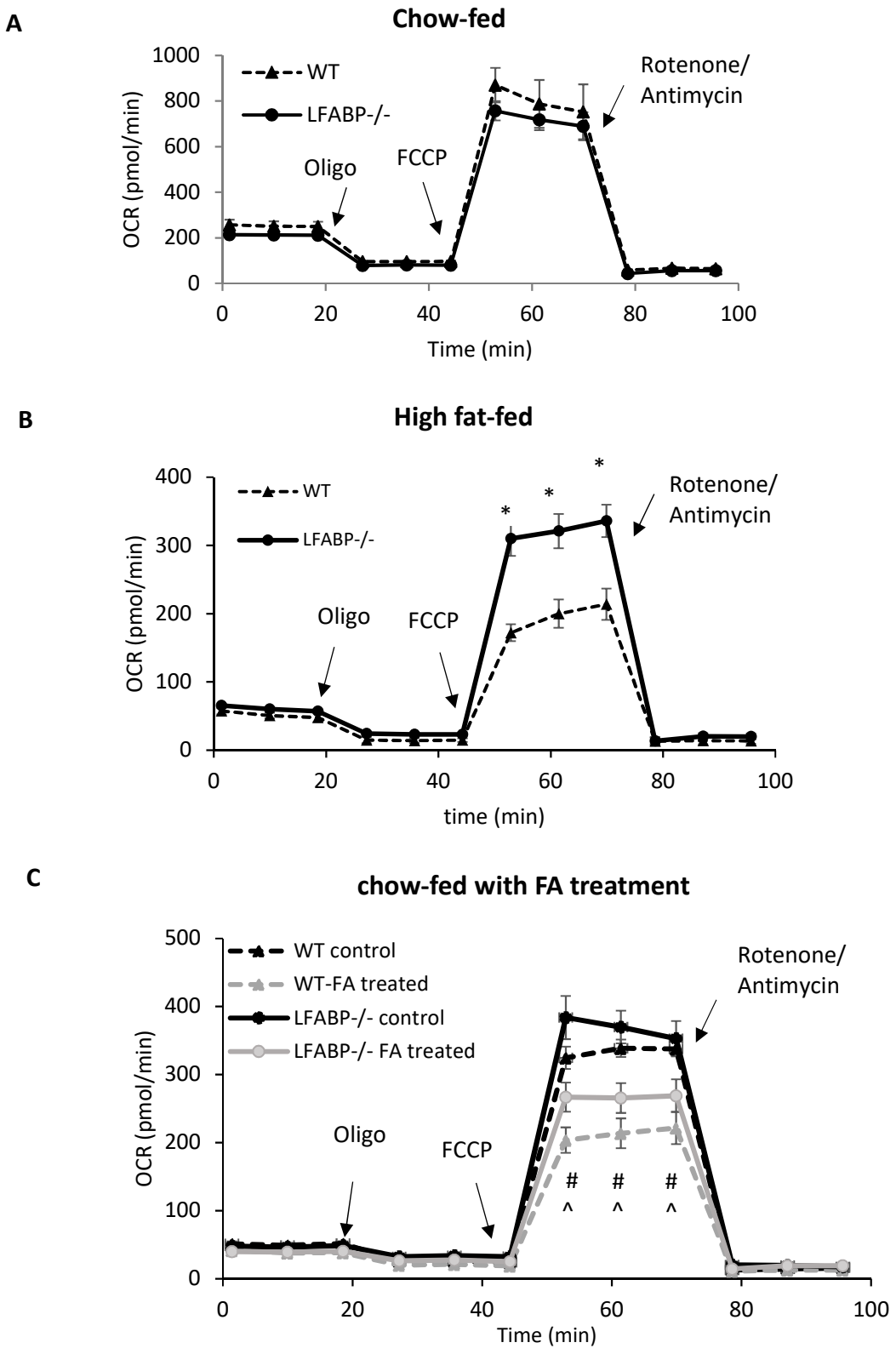
A
Chow-fed
WT
LFABP-/-
Oligo
FCCP
Rotenone/
Antimycin
OCR (pmol/min)
Time (min)
B
High fat-fed
WT
LFABP-/-
Oligo
FCCP
Rotenone/
Antimycin
OCR (pmol/min)
time (min)
C
chow-fed with FA treatment
WT control
WT-FA treated
LFABP-/- control
LFABP-/- FA treated
Oligo
FCCP
Rotenone/
Antimycin
OCR (pmol/min)
Time (min)

Figure 3-3. Cellular respiration analysis of primary myoblasts or myotubes from WT and LFABP$^{-/-}$ mice on a chow or high fat diet. (A) Oxygen consumption rate (OCR) of primary myoblasts from chow-fed mice at baseline and after sequential injections of oligomycin (Oligo), FCCP and mixture of rotenone and antimycin (n=5 per group); (B) OCR of primary myoblasts from mice with 4-week high fat feeding at baseline and after sequential injections of Oligo, FCCP and rotenone/antimycin (n=3-5 per group, *$p<0.05$ vs WT); (C) OCR of primary myotubes from chow-fed mice treated with or without 500µM FA mixture (1:1 Palmitic acid: Oleic acid blend) in DM supplemented with 0.5% BSA (6.7:1 FA:BSA) and 1mM L-carnitine for 20 hours (n=3 per group, ^$p<0.05$ WT FA treated vs WT control, #$p<0.05$ LFABP$^{-/-}$ FA treated vs LFABP$^{-/-}$ control).

Unchanged insulin sensitivity in LFABP$^{-/-}$ muscle

As shown in Chapter 2, we observed higher muscle glycogen concentration in LFABP$^{-/-}$ mice. Since glycogen synthesis is heavily regulated by insulin signaling and circulating insulin was found to be similar between the groups[88], we examined the insulin sensitivity in LFABP$^{-/-}$ muscle. In response to insulin injection, muscle Akt phosphorylation was significantly induced in both groups and the induction level was similar in WT and LFABP$^{-/-}$ mice (Figure 3-4), suggesting an unchanged insulin sensitivity in skeletal muscle of LFABP$^{-/-}$ mice. Therefore, an insulin-independent mechanism may be involved in regulating the muscle glycogen content in LFABP$^{-/-}$ mice.

Figure 3-4

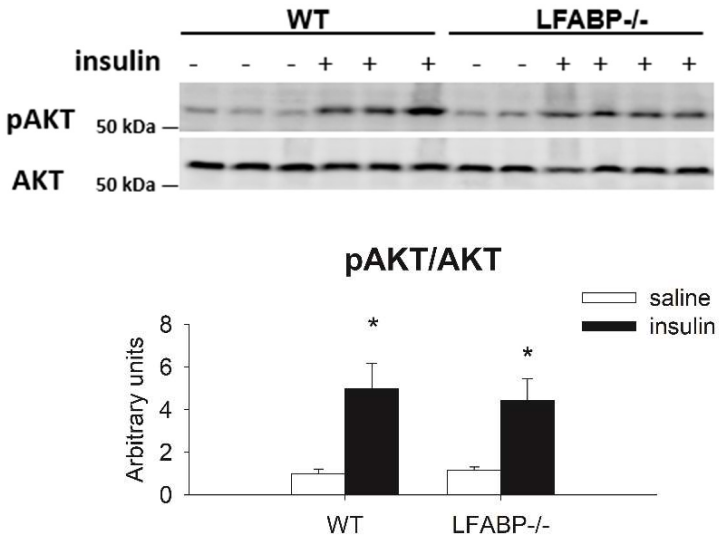

Figure 3-4. Muscle AKT activity in response to insulin injection (i.p.) in WT and LFABP$^{-/-}$ mice on a high fat diet. Representative western blots of insulin-induced AKT phosphorylation and quantification. n=5-6, *p<0.05 vs saline.

Decreased hepatic expression and plasma level of FGF21 in LFABP$^{-/-}$ mice

To examine how the signaling pathways are affected by LFABP ablation, we performed qPCR analyses on several enzymes and transcription factors involved in regulating lipid and glucose metabolism in the liver from WT and LFABP$^{-/-}$ mice. LFABP$^{-/-}$ liver showed a dramatic downregulation in most genes in lipid metabolism, including Ppara, Fasn (fatty acid synthase), Srebp and Aco (Acyl-CoA oxidase) (Figure 3-5A), consistent with previous studies from other labs[64,65]. There was also an increased Gk (Glucokinase) and a decreased Pepck (phosphoenolpyruvate carboxykinase) mRNA levels in the liver, suggesting possible enhanced glycolysis and restricted gluconeogenesis. Additionally, there was a significant decrease in FGF21 expression level in LFABP$^{-/-}$ liver, as well as a trending lower circulating FGF21 level in LFABP$^{-/-}$ mice (Figure 3-5B). Given the important roles of FGF21 in improving systemic energy metabolism, these results suggested the possibility that altered FGF21 signaling associated with LFABP ablation may contribute to the muscle metabolic changes in LFABP$^{-/-}$ mice.

Figure 3-5

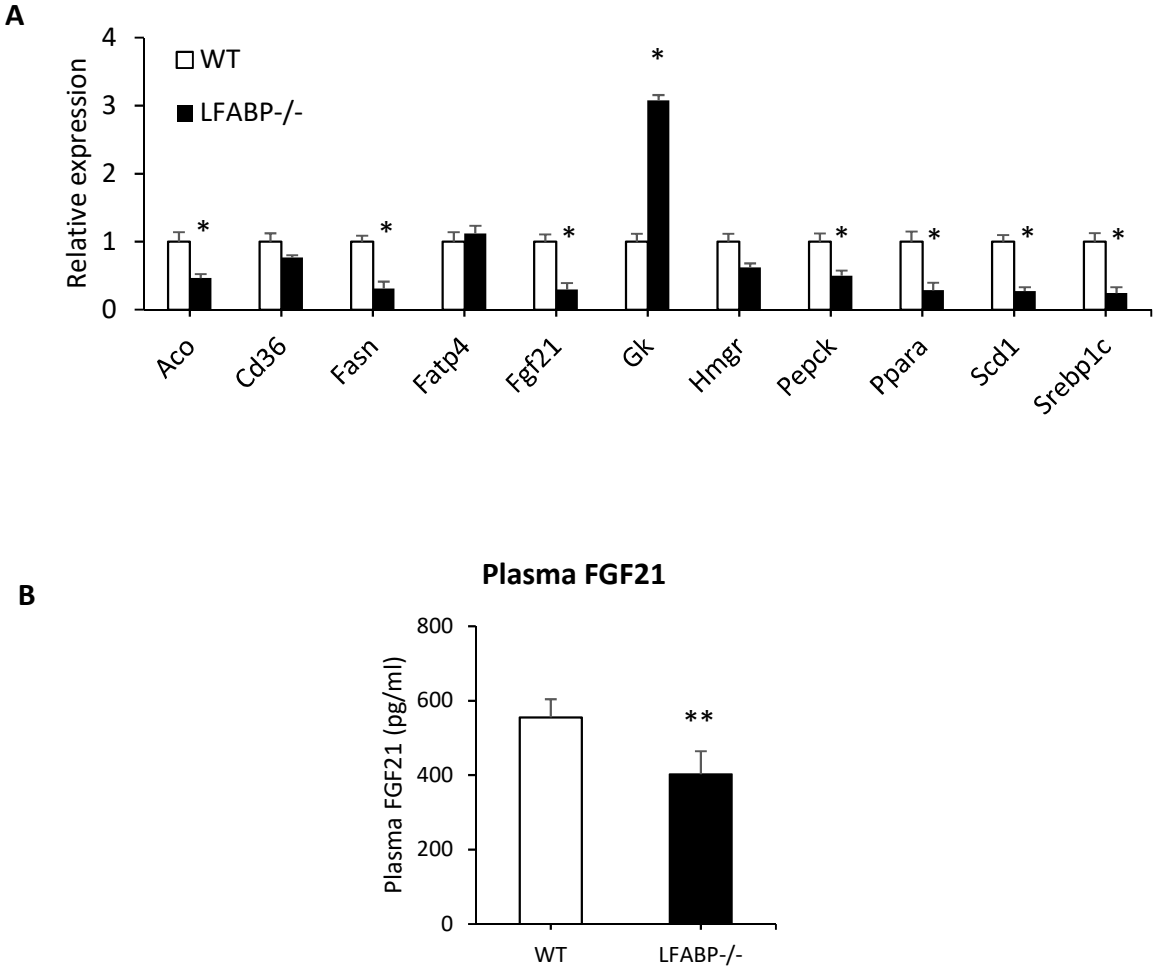

Figure 3-5. Liver qPCR analysis of genes involved in lipid metabolism and plasma FGF21 level of WT and LFABP$^{-/-}$ mice after 12 weeks on a high fat diet. (A) Liver qPCR analysis (n=5-7 per group), *p<0.05 vs WT; (B) Plasma FGF21 level (n=6 per group), **p=0.07 vs WT.

Similar FGF21 sensitivity between WT and LFABP$^{-/-}$ mice

As obesity is considered an FGF21-resistant state, a high endogenous FGF21 level may reflect FGF21 resistance, whereas a decrease in FGF21 may suggest an increased sensitivity[184]. To further determine how FGF21 signaling is affected in LFABP$^{-/-}$ mice, we assessed the FGF21 sensitivity in WAT and liver of WT and LFABP$^{-/-}$ with diet-induced obesity. FGF21 injection was observed to induce ERK1/2 phosphorylation in liver and WAT, and the induction level was similar between WT and LFABP$^{-/-}$ mice in both tissues (Figure 3-6A, 3-6B). As the WAT and liver are the major target tissues of FGF21 signaling, these results indicate that FGF21 sensitivity seems to be unchanged in LFABP$^{-/-}$ mice, despite the decreased circulating FGF21 level.

Figure 3-6

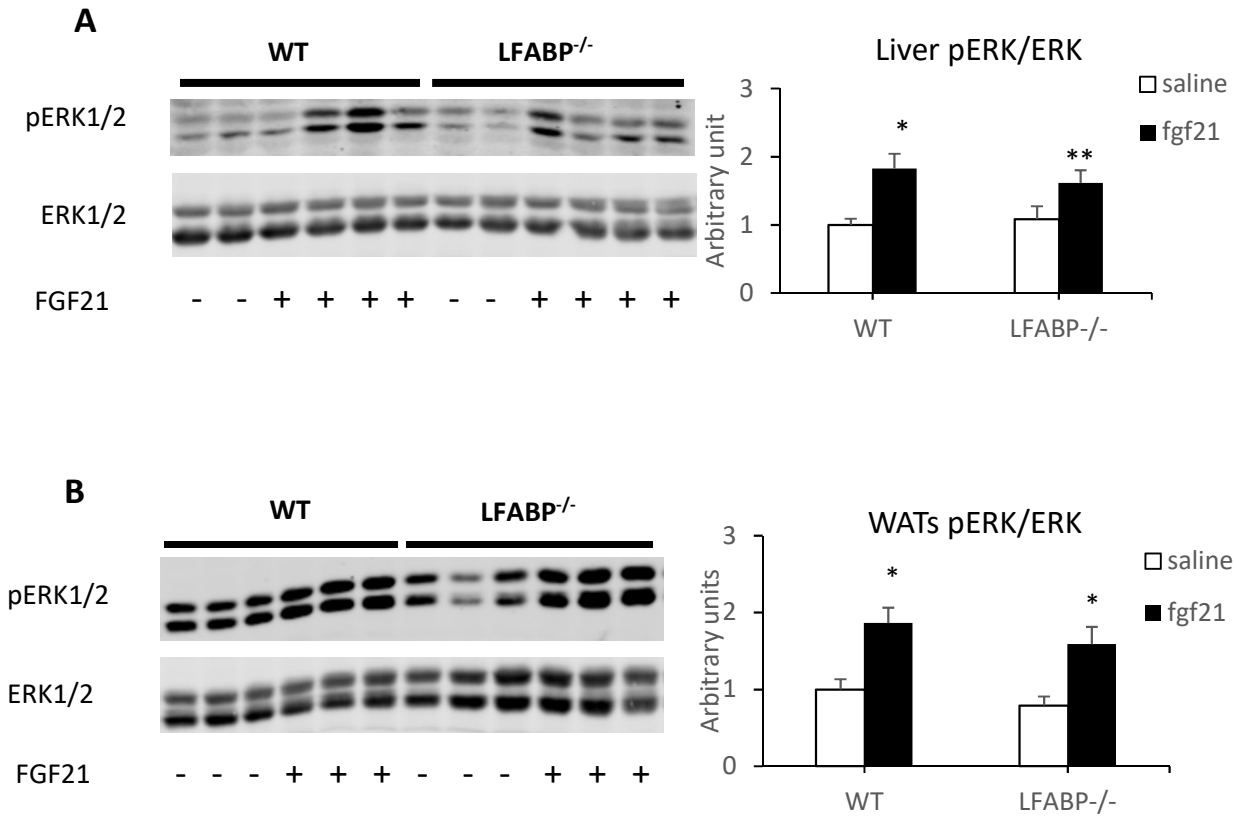

Figure 3-6. FGF21 signaling in the liver and epidydimal adipose tissues (WATs) of WT and LFABP$^{-/-}$ mice after 12 weeks of high fat feeding. (A) Liver ERK1/2 phosphorylation (activation) in response to i.v. FGF21 injection; (B) WAT ERK1/2 phosphorylation in response to i.v. FGF21 injection. Total ERK1/2 in liver/WATs were used as loading controls. n=6, *$p<0.05$ vs saline, **$p=0.07$ vs saline.

Enhanced lipogenesis and trending lower adiponectin expression in epidydimal adipose tissue

We previously showed that LFABP$^{-/-}$ mice displayed a trend towards higher plasma adiponectin levels on a high fat diet, despite their greater adiposity[88]. To elucidate how LFABP ablation affects energy metabolism and adipokine production in adipose tissues, here we examined adiponectin and the genes involved in lipid metabolism, transcriptional regulation and glucose transport in epidydimal WATs of LFABP$^{-/-}$ mice. As an important player in facilitating lipolysis and suppressing lipogenesis[244,245], fabp4 (adipocyte FABP) was found significantly lower in LFABP$^{-/-}$ WAT compared with WT, suggesting enhanced lipogenesis and decreased lipolysis that may explain the greater adiposity of LFABP$^{-/-}$ mice. In keeping with this, Acsl1 trended higher ($p=0.08$) in LFABP$^{-/-}$ WAT, along with a possible increase in Cd36; despite these increases did not reach statistical significance, they may point towards an increased FA uptake due to the trending higher plasma FFA and higher level of CoA modification in LFABP$^{-/-}$ mice. A trend in downregulated Atgl ($p=0.07$) was also observed in LFABP$^{-/-}$ WATs, supporting a restricted basal lipolysis level which may underlie the higher adiposity of LFABP$^{-/-}$ mice. Surprisingly, adiponectin (Adpn) mRNA level was trending lower in LFABP$^{-/-}$ WATs compared with WT (Figure 3-7A), suggesting the trending higher plasma adiponectin in LFABP$^{-/-}$ mice may be derived from other adipose depots (as further discussed below). We also found similar adiponectin receptor levels in skeletal muscles between the genotypes, suggesting similar capacity for adiponectin response (Figure 3-7B). Consistent with the trending lower circulating FGF21 levels in LFABP$^{-/-}$ mice, expression of the crucial FGF21 co-receptor βKlotho was trending lower in LFABP$^{-/-}$ WAT ($p=0.09$), despite the similar expression levels of FGF21 receptors (Fgfr1, Fgfr2) between the groups.

Figure 3-7

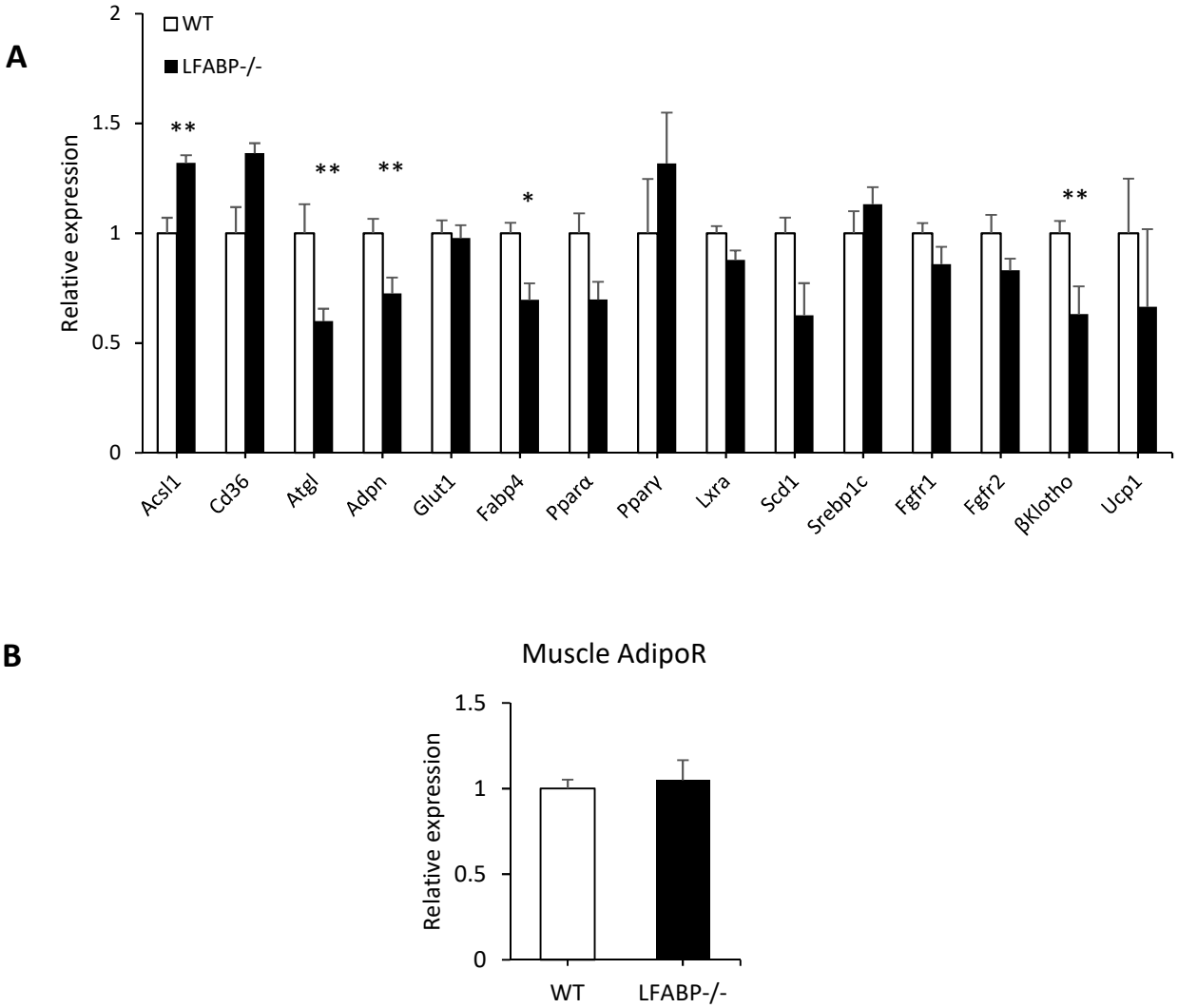

Figure 3-7. qPCR analysis of WAT and skeletal muscle of WT and LFABP$^{-/-}$ mice on a high fat diet. (A) WAT genes involved in lipid metabolism, transcriptional regulation and FGF21 signaling; (B) Gastrocnemius gene expression of adiponectin receptor. n=5-7 per group, *p<0.05 vs WT, **0.05<p<0.1 vs WT.

Discussion

As described in Chapter 2, LFABP$^{-/-}$ mice were protected against a high fat feeding-induced decline in exercise capacity, with a series of muscle metabolic alterations including substrate availability and mitochondrial function that support energy production. In this study, we were interested in examining the potential interorgan signaling pathways connecting LFABP ablation in liver and intestine and the metabolic reprogramming in skeletal muscle. In establishing an in vitro system for testing potential candidates, we found that primary myoblasts from chow-fed mice showed similar mitochondrial respiratory capacity, whereas the myocytes from high fat-fed LFABP$^{-/-}$ mice had significantly higher maximal oxidative capacity compared with WT, supporting the notion that LFABP$^{-/-}$ mice are protected from high fat feeding-induced impairment in skeletal muscle. Interestingly, primary myocytes from chow-fed mice treated with FA showed little difference between the groups, suggesting certain circulating mediators are required for the muscle metabolic adaptations favoring improved energy metabolism in LFABP$^{-/-}$ mice. While treating cells with FAs for 20-24 hours is commonly used to mimic a high fat feeding condition in vitro[207,246,247], one caveat that may complicate interpretation of these data is that cell culture medium supplemented with FAs for ~1 day is not the same as the mouse plasma after 12 weeks of high fat feeding, where the FA composition is dependent on dietary intake and tissue turnover[248]. Therefore, future experiments on effects of exposure to different FA species for varying time periods may provide further explanation for the muscle phenotype in LFABP$^{-/-}$ mice. Notably, we have previously found some evidence of transcriptional regulation in resting muscles of LFABP$^{-/-}$ mice that may be involved in developing improved energy metabolism, including partial inhibition of CPT1 and MCD, and decreased amino acid signaling, branched chain amino acid metabolism and LXR signaling (as shown in Chapter 2). These intrinsic

adaptations in skeletal muscle may be directly or indirectly resulted from LFABP ablation and exert their protective effects, regardless of the high fat feeding.

As a key interorgan signaling mediator targeting skeletal muscle, insulin is a major regulator for muscle glycogen synthesis and energy metabolism[249]. In our study, insulin sensitivity in skeletal muscle was found similar between the groups, suggesting the mechanisms underlying the muscle metabolic changes may be insulin-independent. However, since it is well established that BMI or obesity is positively correlated with indices of insulin resistance[250-252], our finding of similar insulin sensitivity in skeletal muscle and on a whole body level[88] between the groups may be considered a significant improvement given the greater obesity in LFABP$^{-/-}$ mice. In keeping with this, LFABP$^{-/-}$ mice have shown other signs of metabolically healthy obesity, where metabolic abnormalities and poor physical fitness are alleviated[212]. In addition to their improved exercise capacity with higher mitochondrial function relative to the obese WT counterparts, LFABP$^{-/-}$ mice have shown similar blood lipid profile and liver TG content on high fat diets[88], as well as a longer lifespan on a chow diet (unpublished) compared with WT.

As a liver-derived hormone that governs the whole body energy homeostasis, FGF21 is another important candidate for signaling muscle metabolic changes. Although FGF21 was decreased in both liver and plasma in LFABP$^{-/-}$ mice, FGF21 sensitivity in the liver, epidydimal WAT and skeletal muscle was not different between the groups, suggesting a possible downregulation in total FGF21 signaling. Although the FGF21-induced beneficial effects are usually associated with upregulated FGF21 signaling, the roles of specific fat depots in responding to FGF21 have recently been examined in more depth. Li and colleagues found that FGF21 improved systemic insulin sensitivity by healthy expansion of subcutaneous adipose tissue (scWAT)[253] , based on the findings that FGF21 knockout (FGF21KO) mice showed less scWAT mass and more insulin-resistance in response to high fat feeding, but FGF21 administration or transplantation of scWAT

from WT mice to FGF21KO mice rescued the phenotype. Moreover, FGF21 has also been shown to regulate browning of WAT via PGC1a in response to cold exposure or PPARa agonist, with most of the browning effects in subcutaneous inguinal adipose tissue and rarely in epidydimal WAT[254,255]. The FGF21-mediated adaptive thermogenesis is consistent with our observations that LFABP$^{-/-}$ mice had lower body temperature after overnight fasting (unpublished). Therefore, it is of interest to further examine FGF21 sensitivity in scWAT to fully understand how FGF21 signaling may affect downstream targets.

As one of the important downstream targets of FGF21 signaling in WAT, adiponectin is thought to couple the action of FGF21 in WAT to the skeletal muscle[174]. Plasma adiponectin levels have been negatively associated with adiposity, and decreased plasma adiponectin has been shown to increase risk of type 2 diabetes in population studies[256-259]. However, despite their greater obesity, LFABP$^{-/-}$ mice showed a trending higher adiponectin in the plasma, supporting the possibility that FGF21 signaling may be enhanced in scWAT to induce the adiponectin production. Indeed, exogenous FGF21-induced insulin-sensitizing effects in high fat-fed FGF21KO mice has been found to be mediated at least partially by scWAT-derived adiponectin[253]; circulating adiponectin has also been correlated with scWAT rather than visceral (epidydimal) WAT in a population-based study[260]. That may explain why we did not find higher expression levels of adiponectin in epidydimal WAT between the groups, but the trending higher plasma adiponectin in LFABP$^{-/-}$ mice suggests that an enhanced adiponectin signaling may contribute to the improved energy metabolism in skeletal muscle[156,177].

As obesity is now recognized as a chronic, low-grade and systemic inflammatory disease, adiponectin has also been implicated in anti-inflammatory response[261,262]. Interestingly, LFABP$^{-/-}$ mice showed a downregulation in Fabp4 in WAT, which is thought to not only suppress lipogenesis and promote lipolysis, but also affect inflammatory pathways[263]. FABP4 knockout

mice have been shown to be protected from diet-induced insulin resistance despite being more obese, whereas RNAi-mediated FABP4 knockdown in mice has been shown to exacerbate diet-induced obesity without improvement in glucose tolerance[264,265]; this latter effect is consistent with our findings in LFABP$^{-/-}$ mice. Therein, the decreased Fabp4 expression and trending higher plasma adiponectin may suggest an attenuated inflammatory stress response, as an insulin-independent protective mechanism against the high fat feeding-induced disturbance in energy homeostasis.

Overall, LFABP ablation in liver and intestine indirectly result in an improved energy metabolism in skeletal muscle, with consequent protection against high fat feeding-induced decline in exercise capacity. Cellular respiration analyses on primary myocytes from mice on chow and high fat diets suggest the importance of circulating mediators in regulating muscle metabolism. While FGF21 sensitivity and adiponectin expression were not increased in epidydimal WAT, there may be differences in FGF21-adiponectin signaling in scWAT that contribute to metabolic changes in the skeletal muscle of the high fat-fed LFABP$^{-/-}$ mice.

Chapter 4

General Conclusion and Future Directions

LFABP ablation affects high fat feeding-induced modifications in muscle energy metabolism

LFABP is highly expressed in liver and intestine, and thought to not only mediate local lipid trafficking, but also affect systemic lipid homeostasis beyond its expression sites[63,66,81,82,88,266]. Indeed, our laboratory has previously found that mice with whole body LFABP ablation displayed a greater obesity in response to high fat feeding compared with WT, with increased food intake and similar intestinal lipid absorption rate[88]. Surprisingly, despite their obese phenotype, LFABP$^{-/-}$ mice were protected against high fat feeding-induced decline in exercise capacity, with an approximate doubling of running distance compared with WT on a high fat diet. In the present study, we examine different aspects of muscle energy metabolism and found major differences in substrate storage and mitochondrial function in response to high fat feeding.

First of all, high fat-fed LFABP$^{-/-}$ mice showed a significantly higher muscle glycogen concentration in their skeletal muscle than the WT counterparts. As insulin signaling is a major stimulator for glycogen synthesis, high fat feeding has been shown to impair glucose uptake and glycogen synthesis via diet-induced insulin resistance[267,268]. Since there was no difference in whole body or muscle insulin sensitivity between high fat-fed LFABP$^{-/-}$ and WT mice, the increased glycogen content in LFABP$^{-/-}$ muscle may be attributed to their higher GLUT4 expression on the plasma membrane via an insulin-independent mechanism. Moreover, although high fat feeding is expected to increase intramuscular lipid content[268,269], LFABP ablation seemed to have exacerbated the high fat feeding-induced ectopic TG accumulation in skeletal muscle, with a significantly higher IMTG level in LFABP$^{-/-}$ muscle than WT. Consistent with the previous findings of greater adiposity and trending higher plasma FFA in LFABP$^{-/-}$ mice, these results suggest LFABP ablation severely impairs lipid handling capacity in the liver and

thereby direct the excess FAs into circulation and other peripheral tissues, including skeletal muscle.

Diet-induced obesity and insulin resistance have been strongly associated with mitochondrial dysfunction, where β-oxidation and ATP production capacity are restricted and reactive oxygen species production is increased to induce an inflammatory response[124,209,270]. Although LFABP$^{-/-}$ mice were more obese, they displayed comparably insulin resistant compared with WT mice in response to high fat feeding, and showed an improved mitochondrial function with higher mitochondrial quantities, enzyme activities and fatty acid oxidation capacity compared with high fat-fed WT mice. This may be key to the greater exercise capacity in high fat-fed LFABP$^{-/-}$ mice, especially with the increased TG levels in LFABP$^{-/-}$ muscle. Since IMTG is thought to negatively affect insulin action and mitochondrial function[271,272], the concomitant higher TG content and mitochondrial function in LFABP$^{-/-}$ muscle resemble the “athlete’s paradox” phenotype where endurance-trained athletes have high oxidative capacity and greater IMTG, as well as enhanced insulin sensitivity[273].

As there was no difference in muscle fiber composition between LFABP$^{-/-}$ and WT mice, LFABP ablation does not seem to trigger muscle fiber switch to induce metabolic changes. As mentioned before, the increased muscle glycogen and TG storage in LFABP$^{-/-}$ mice are likely to result indirectly from disruptions in hepatic LFABP-mediated lipid metabolism. However, compared with high fat-fed WT, the improved mitochondrial function in high fat-fed LFABP$^{-/-}$ muscle suggests that LFABP ablation not only alters the substrate flux, but also induces metabolic reprogramming in skeletal muscle, possibly via interorgan signaling. So far, we have been focused on liver-derived signals on systemic and muscle metabolism, as there are drastic changes in hepatic lipid metabolism in LFABP$^{-/-}$ mice[39,85,87,266]. However, given the essential role of intestine in lipid absorption and lipid sensing[274], further studies using tissue-specific LFABP

knockout mice are required to specifically examine the intestine- and liver-derived effects on skeletal muscle metabolism. In addition, high fat feeding has been reported to induce greater weight gain and obesity in female LFABP$^{-/-}$ mice than male mice[85], therefore it is also important to examine possible gender differences in the exercise phenotype and muscle metabolic alterations in LFABP$^{-/-}$ mice.

LFABP ablation triggers interorgan signaling to connect liver, adipose and skeletal muscle metabolism

Since LFABP is not expressed in skeletal muscle and LFABP ablation does not cause a compensatory increase in FABP3 expression in skeletal muscle, the underlying mechanisms for the muscle metabolic changes in LFABP$^{-/-}$ mice seem to involve more complicated signaling across different tissues. Direct tissue crosstalk between liver and skeletal muscle is not well studied or understood, but evidence has supported a role of adipose tissue in coordinating liver and muscle metabolism. One of the most studied interorgan signaling pathways is FGF21-adiponectin signaling. FGF21 is predominantly produced in the liver, a physiological response induced by fasting and mediated by PPARα[158,166]. After being released into circulation, FGF21 acts on the adipose tissue via the important co-receptor βKlotho and regulate many metabolic pathways, including stimulating the expression level of adiponectin[162,174,275]. As an adipokine, adiponectin is released from the adipose tissue and becomes an important player in maintaining whole-body energy homeostasis with effects on many tissues, including enhancing lipid oxidation, mitochondrial biogenesis and insulin sensitivity in skeletal muscles[157,175].

In LFABP$^{-/-}$ liver, FGF21 was found to be significantly downregulated at the transcriptional level, which may be related to the disruption in LFABP-PPARα interaction. LFABP has been considered

as a co-factor for PPARα activation for its important roles in facilitating FA trafficking into the nucleus for ligand binding, as well as its direct interaction with PPARα[59,276]. Without LFABP, many downstream targets of PPARα signaling are suppressed, including FGF21. As a liver-derived hormone regulating energy homeostasis on a whole body level[162], FGF21 has been of particular interest to us. Consistent with the mRNA results, circulating FGF21 was trending lower in LFABP$^{-/-}$ mice than WT mice. As the main target tissue of FGF21, white adipose tissues (WATs) from WT and LFABP$^{-/-}$ exhibited similar levels of FGF21-induced ERK1/2 activation, suggesting an unchanged FGF21 sensitivity in LFABP$^{-/-}$. Taken together, LFABP$^{-/-}$ mice showed a downregulated FGF21 signaling, which seemed inconsistent with their improved energy metabolism given the FGF21-mediated benefits in metabolic syndromes[166].

However, in our previous studies, we have found that LFABP$^{-/-}$ mice have trending higher levels of circulating adiponectin, which is a downstream target of FGF21 signaling in WATs[88]. Adiponectin, an adipocyte-derived hormone, has been shown to improve metabolic syndromes with many systemic antidiabetic effects, including increasing insulin sensitivity, glucose uptake and utilization, as well as FA oxidation in the skeletal muscle via AMPK activation and enhanced mitochondrial function[156,157,240,277]. Since circulating adiponectin is thought to be inversely associated with adiposity[256,258], the trending higher adiponectin in the more obese LFABP$^{-/-}$ mice strongly suggests that FGF21 signaling is altered to stimulate adiponectin production in WATs. Indeed, recent findings on the roles of specific fat depots in responding to FGF21 shed light on possible explanations. While we and many other labs have been using epidydimal WATs to study the antidiabetic effects of FGF21[184,275,278] , perhaps due to the strong association between visceral fat and insulin resistance[279], it was recently found that the effect of FGF21 on improving systemic insulin sensitivity and energy metabolism was mediated through subcutaneous WATs (scWATs)[253]. Moreover, not only has circulating adiponectin been correlated with scWATs rather

than epidydimal WATs, but also the insulin-sensitizing effects of FGF21 has been found to be at least partially attributed to scWAT-derived adiponectin[253,260]. This may explain why we found a trending lower expression level of adiponectin in epidydimal WAT of LFABP$^{-/-}$ mice, in spite of their trended higher circulating adiponectin. It is also noteworthy that scWAT transplantation alone has been shown to rescue the diabetic phenotype of FGF21 knockout mice[253], suggesting that adiponectin production from scWAT may be induced by an FGF21-independent pathway. Therefore, further studies on FGF21 signaling and adiponectin expression in scWATs may provide important information on the mechanisms underlying the enhanced adiponectin production in LFABP$^{-/-}$ mice. In addition, FGF21 signaling in scWATs is implicated in adaptive thermogenesis[255]. With our recent observation that LFABP$^{-/-}$ mice may have lower body temperature after overnight fasting (data not shown), it would be interesting to further examine the browning of scWAT in LFABP$^{-/-}$ mice.

LFABP ablation results in metabolic changes associated with improved health status

In our previous study, we have found signs of metabolically healthy obesity (MHO) in LFABP$^{-/-}$ mice. Despite being more obese in response to high fat feeding, LFABP$^{-/-}$ mice did not show exacerbated abnormalities associated with increased adiposity[250], with comparable insulin resistance and similar lipid profiles in plasma[88]. The present study further supports this notion, in that high fat-fed LFABP$^{-/-}$ showed increased spontaneous activity and an improved physical fitness compared with high fat-fed WT counterparts. This exercise phenotype in LFABP$^{-/-}$ mice may have important implications in managing obesity and metabolic syndromes, since poor fitness level is one of the major obstacles for obese or diabetic patients to adhere to an exercise regimen and obtain exercise-induced benefits. It would be of interest to further examine how

exercise training affects whole body energy metabolism and insulin sensitivity in LFABP$^{-/-}$ mice with diet-induced obesity. Moreover, in preliminary studies we found that LFABP$^{-/-}$ mice on a chow diet were also observed to have a longer lifespan compared with WT mice (data not shown). This finding not only supports the improved health status in LFABP$^{-/-}$ mice compared with WT, but also suggests an effect of LFABP ablation on aging modifications, perhaps in a manner similar to high fat challenge, where the impaired lipid handling capacity accumulates to exceed the systemic buffering capacity and exhibit metabolic alterations in multiple organs such as skeletal muscles. In this regard, it may be of interest to examine the skeletal muscles in aging LFABP$^{-/-}$ mice and study the potential of LFABP ablation or inhibition in improving age-related sarcopenia.

In addition to their improved exercise capacity and muscle metabolism, LFABP$^{-/-}$ mice also showed a downregulated expression level of FABP4 in WAT compared with WT. With its major expression site in white and brown adipose tissues, FABP4 ablation has been shown to result in a higher body weight without hyperinsulinemia and insulin resistance in diet-induced and genetic obesity[265,280]. The similar phenotypes between LFABP$^{-/-}$ mice and FABP4 knockdown mice suggest that decreased FABP4 in adipose tissues may contribute to the greater adiposity in LFABP$^{-/-}$ mice. The healthy phenotype in FABP4 null mice is not only associated with reduced lipolysis and increase lipogenesis in adipocytes[265,280,281], but also with suppressed insulin secretory response to β-adrenergic stimulation[244]. Moreover, as FABP4 is also expressed in macrophages (at a lower level than in adipocytes), FABP4 has also been implicated in inflammatory responses. Given that obesity is a chronic, systemic inflammatory disease, the protection against obesity-induced insulin resistance in FABP4 null mice may result from its anti-inflammatory effects[263]. Indeed, FABP4 ablation has been found to reduce macrophage inflammation in diet-induced obesity through monounsaturated fatty acid signaling[282].

Interestingly, mice with RNAi-mediated FABP4 knockdown have been shown to become more obese in response to high fat feeding, but the knockdown has no effects on insulin sensitivity and glucose tolerance[264]. One possible explanation for the discrepancy between FABP4 null mice and FABP4 knockdown mice may involve FABP5, or epidermal FABP, since complete loss of FABP4 has been shown to compensated by increased expression of FABP5 in adipocytes (not in macrophages), whereas the FABP4 knockdown does not induce a compensatory increase in FABP5[264,265]. In keeping with this, adiponectin has also been shown to mediate anti-inflammatory responses. For example, pro-inflammatory cytokines such as IL-6 and TNFα are found to inhibit adiponectin expression and secretion levels in adipocytes[283,284]; plasma adiponectin levels are found to be negatively correlated with not only increased pro-inflammatory cytokines[285], but also C-reactive protein, a pro-inflammatory marker and an independent predictor for cardiovascular disease[262,286]. In addition to its typical definition of excess adiposity, obesity is now considered as a chronic and systemic inflammatory disease[261]. Although LFABP$^{-/-}$ mice are not protected from diet-induced obesity, the anti-inflammatory responses mediated by the trending higher circulating adiponectin and downregulated FABP4 may play an important role in improving the overall health status of high fat-fed LFABP$^{-/-}$ mice.

In summary, we have uncovered a surprising exercise phenotype in LFABP null mice, namely that they are resistant to high fat feeding-induced decline in exercise capacity. Muscle metabolic reprogramming is associated with this exercise phenotype, including increased muscle glycogen and IMTG storage, as well as improved mitochondrial function. FGF21-adipoenctin is found to be a potential interorgan signaling pathway among liver, adipose tissue and skeletal muscle, which may contribute to the muscle metabolic alterations in LFABP$^{-/-}$ mice, since LFABP is not expressed in the skeletal muscle. Lipid metabolism in adipose tissue is also shown to be affected in LFABP$^{-/-}$ mice, possibly via FABP4 downregulation. These results demonstrate the

physiological mechanisms underlying the exercise phenotype of LFABP$^{-/-}$ mice, reveal indirect effects of LFABP in energy metabolism beyond its expression site, and provide information for further identification of interorgan signaling facilitating crosstalks among liver, adipose tissue and skeletal muscle. From a therapeutic standpoint, the “fat and fit” phenotype of LFABP$^{-/-}$ mice could have important implications in combating obesity and other metabolic syndrome disorders through maintained exercise capacity in the face of high-fat feeding.

Literature Cited

Reference

1. Storch J, Corsico B. The emerging functions and mechanisms of mammalian fatty acid–binding proteins. *Annu Rev Nutr.* 2008.
2. Lagakos WS, Guan X, Ho S-Y, et al. Liver fatty acid-binding protein binds monoacylglycerol in vitro and in mouse liver cytosol. *Journal of Biological Chemistry.* 2013;288(27):19805-19815.
3. Furuhashi M, Hotamisligil GS. Fatty acid-binding proteins: role in metabolic diseases and potential as drug targets. *Nature reviews Drug discovery.* 2008;7(6):489.
4. Weisiger RA. Cytoplasmic transport of lipids: role of binding proteins. *Comparative Biochemistry and Physiology Part B: Biochemistry and Molecular Biology.* 1996;115(3):319-331.
5. Haunerland NH, Spener F. Fatty acid-binding proteins–insights from genetic manipulations. *Progress in lipid research.* 2004.
6. Chmurzyńska A. The multigene family of fatty acid-binding proteins (FABPs): function, structure and polymorphism. *Journal of applied genetics.* 2006.
7. Tan N-S, Shaw NS, Vinckenbosch N, et al. Selective cooperation between fatty acid binding proteins and peroxisome proliferator-activated receptors in regulating transcription. *Molecular and cellular biology.* 2002;22(14):5114-5127.
8. Wolfrum C, Borrmann CM, Börchers T, Spener F. Fatty acids and hypolipidemic drugs regulate peroxisome proliferator-activated receptors α-and γ-mediated gene expression via liver fatty acid binding protein: a signaling path to the nucleus. *Proceedings of the National Academy of Sciences.* 2001;98(5):2323-2328.
9. Tontonoz P, Hu E, Graves RA, Budavari AI, Spiegelman BM. mPPAR gamma 2: tissue-specific regulator of an adipocyte enhancer. *Genes & development.* 1994;8(10):1224-1234.
10. Issemann I, Prince R, Tugwood J, Green S. A role for fatty acids and liver fatty acid binding protein in peroxisome proliferation? : Portland Press Limited; 1992.
11. Garin-Shkolnik T, Rudich A, Hotamisligil GS, Rubinstein M. FABP4 attenuates PPARγ and adipogenesis and is inversely correlated with PPARγ in adipose tissues. *Diabetes.* 2014;63(3):900-911.
12. Sawicki LR, Arias NMB, Scaglia N, et al. FABP1 knockdown in human enterocytes impairs proliferation and alters lipid metabolism. *Biochimica et Biophysica Acta (BBA)-Molecular and Cell Biology of Lipids.* 2017;1862(12):1587-1594.
13. Sorof S. Modulation of mitogenesis by liver fatty acid binding protein. *Cancer and Metastasis Reviews.* 1994;13(3-4):317-336.
14. Khan SH, Sorof S. Liver fatty acid-binding protein: specific mediator of the mitogenesis induced by two classes of carcinogenic peroxisome proliferators. *Proceedings of the National Academy of Sciences.* 1994;91(3):848-852.
15. Tang M, Kindler P, Cai D, Chow P, Li M, Lee K. Heart-type fatty acid binding proteins are upregulated during terminal differentiation of mouse cardiomyocytes, as revealed by proteomic analysis. *Cell and tissue research.* 2004;316(3):339-347.
16. Specht B, Bartetzko N, Hohoff C, et al. Mammary derived growth inhibitor is not a distinct protein but a mix of heart-type and adipocyte-type fatty acid-binding protein. *Journal of Biological Chemistry.* 1996;271(33):19943-19949.
17. Huynh HT, Larsson C, Narod S, Pollak M. Tumor suppressor activity of the gene encoding mammary-derived growth inhibitor. *Cancer Research.* 1995;55(11):2225-2231.

18. Yang Y, Spitzer E, Kenney N, et al. Members of the fatty acid binding protein family are differentiation factors for the mammary gland. *The Journal of cell biology.* 1994;127(4):1097-1109.
19. Veerkamp JH, van Moerkerk HTB. Fatty acid-binding protein and its relation to fatty acid oxidation. *Molecular and cellular biochemistry.* 1993;123(1):101-106.
20. Ockner RK, Manning JA, Poppenhausen RB. A binding protein for fatty acids in cytosol of intestinal mucosa, liver, myocardium, and other tissues. *Science.* 1972.
21. Storch J, Thumser AEA. The fatty acid transport function of fatty acid-binding proteins. *Biochimica et Biophysica Acta (BBA)-Molecular and Cell Biology of Lipids.* 2000;1486(1):28-44.
22. Issemann I, Prince R, Tugwood J, Green S. A role for fatty acids and liver fatty acid binding protein in peroxisome proliferation? *Biochemical Society Transactions.* 1992;20(4):824.
23. Tomas J, Mulet C, Saffarian A, et al. High-fat diet modifies the PPAR-γ pathway leading to disruption of microbial and physiological ecosystem in murine small intestine. *Proceedings of the National Academy of Sciences.* 2016;113(40):E5934-E5943.
24. Kannisto K, Chibalin A, Glinghammar B, Zierath JR, Hamsten A, Ehrenborg E. Differential expression of peroxisomal proliferator activated receptors α and δ in skeletal muscle in response to changes in diet and exercise. *International journal of molecular medicine.* 2006;17(1):45-52.
25. Kubota N, Terauchi Y, Miki H, et al. PPARγ mediates high-fat diet–induced adipocyte hypertrophy and insulin resistance. *Molecular cell.* 1999;4(4):597-609.
26. Doktorova M, Zwarts I, Van Zutphen T, et al. Intestinal PPARδ protects against diet-induced obesity, insulin resistance and dyslipidemia. *Scientific reports.* 2017;7(1):846.
27. Zanotti G. Muscle fatty acid-binding protein. *Biochimica et Biophysica Acta (BBA) - Molecular and Cell Biology of Lipids.* 1999;1441(2–3):94-105.
28. Furuhashi M, Hotamisligil GS. Fatty acid-binding proteins: role in metabolic diseases and potential as drug targets. *Nature reviews Drug discovery.* 2008.
29. Hotamisligil GS, Johnson RS, Distel RJ, Ellis R, Papaioannou VE, Spiegelman BM. Uncoupling of obesity from insulin resistance through a targeted mutation in aP2, the adipocyte fatty acid binding protein. *Science.* 1996;274(5291):1377-1379.
30. Furuhashi M, Tuncman G, Gorgun CZ, et al. Treatment of diabetes and atherosclerosis by inhibiting fatty-acid-binding protein aP2. *Nature.* 2007;447(7147):959-965.
31. Makowski L, Hotamisligil GS. The role of fatty acid binding proteins in metabolic syndrome and atherosclerosis. *Current opinion in lipidology.* 2005;16(5):543.
32. Ibrahimi A, Abumrad NA. Role of CD36 in membrane transport of long-chain fatty acids. *Current Opinion in Clinical Nutrition & Metabolic Care.* 2002;5(2):139-145.
33. Hirsch D, Stahl A, Lodish HF. A family of fatty acid transporters conserved from mycobacterium to man. *Proceedings of the National Academy of Sciences.* 1998;95(15):8625-8629.
34. Isola L, Zhou S, Kiang C, Stump D, Bradbury M, Berk P. 3T3 fibroblasts transfected with a cDNA for mitochondrial aspartate aminotransferase express plasma membrane fatty acid-binding protein and saturable fatty acid uptake. *Proceedings of the National Academy of Sciences.* 1995;92(21):9866-9870.
35. Tessari P, Coracina A, Cosma A, Tiengo A. Hepatic lipid metabolism and non-alcoholic fatty liver disease. *Nutrition, Metabolism and Cardiovascular Diseases.* 2009;19(4):291-302.

36. Bechmann LP, Hannivoort RA, Gerken G, Hotamisligil GS, Trauner M, Canbay A. The interaction of hepatic lipid and glucose metabolism in liver diseases. *Journal of hepatology.* 2012;56(4):952-964.
37. Hubbell T, Behnke WD, Woodford JK, Schroeder F. Recombinant liver fatty acid binding protein interacts with fatty acyl-coenzyme A. *Biochemistry.* 1994;33(11):3327-3334.
38. Burrier RE, Manson CR, Brecher P. Binding of acyl-CoA to liver fatty acid binding protein: effect on acyl-CoA synthesis. *Biochimica et Biophysica Acta (BBA)-Lipids and Lipid Metabolism.* 1987;919(3):221-230.
39. Martin GG, Huang H, Atshaves BP, Binas B, Schroeder F. Ablation of the liver fatty acid binding protein gene decreases fatty acyl CoA binding capacity and alters fatty acyl CoA pool distribution in mouse liver. *Biochemistry.* 2003;42(39):11520-11532.
40. Yan S, Yang X-F, Liu H-L, Fu N, Ouyang Y, Qing K. Long-chain acyl-CoA synthetase in fatty acid metabolism involved in liver and other diseases: an update. *World Journal of Gastroenterology: WJG.* 2015;21(12):3492.
41. Mashek DG, Li LO, Coleman RA. Long-chain acyl-CoA synthetases and fatty acid channeling. *Future lipidology.* 2007;2(4):465-476.
42. Coleman RA, Lewin TM, Van Horn CG, Gonzalez-Baró MR. Do long-chain acyl-CoA synthetases regulate fatty acid entry into synthetic versus degradative pathways? *The Journal of nutrition.* 2002;132(8):2123-2126.
43. Listenberger LL, Han X, Lewis SE, et al. Triglyceride accumulation protects against fatty acid-induced lipotoxicity. *Proceedings of the National Academy of Sciences.* 2003;100(6):3077-3082.
44. Postic C, Girard J. Contribution of de novo fatty acid synthesis to hepatic steatosis and insulin resistance: lessons from genetically engineered mice. *The Journal of clinical investigation.* 2008;118(3):829-838.
45. Schönfeld P, Wojtczak L. Short-and medium-chain fatty acids in energy metabolism: the cellular perspective. *Journal of lipid research.* 2016;57(6):943-954.
46. Singh I. Biochemistry of peroxisomes in health and disease. *Molecular and cellular biochemistry.* 1997;167(1-2):1-29.
47. Schrader M, Costello J, Godinho LF, Islinger M. Peroxisome-mitochondria interplay and disease. *Journal of inherited metabolic disease.* 2015;38(4):681-702.
48. Hardwick JP. Cytochrome P450 omega hydroxylase (CYP4) function in fatty acid metabolism and metabolic diseases. *Biochemical pharmacology.* 2008;75(12):2263-2275.
49. Yokoyama S. Assembly of high-density lipoprotein. *Arteriosclerosis, thrombosis, and vascular biology.* 2006;26(1):20-27.
50. Adeli K, Taghibiglou C, Van Iderstine SC, Lewis GF. Mechanisms of hepatic very low-density lipoprotein overproduction in insulin resistance. *Trends in cardiovascular medicine.* 2001;11(5):170-176.
51. Sundaram M, Yao Z. Recent progress in understanding protein and lipid factors affecting hepatic VLDL assembly and secretion. *Nutrition & metabolism.* 2010;7(1):35.
52. Mason TM. The role of factors that regulate the synthesis and secretion of very-low-density lipoprotein by hepatocytes. *Critical reviews in clinical laboratory sciences.* 1998;35(6):461-487.
53. Sato K, Cho Y, Tachibana S, Chiba T, Schneider WJ, Akiba Y. Impairment of VLDL secretion by medium-chain fatty acids in chicken primary hepatocytes is affected by the chain length. *The Journal of nutrition.* 2005;135(7):1636-1641.

54. Tran K, Thorne-Tjomsland G, DeLong CJ, et al. Intracellular assembly of very low density lipoproteins containing apolipoprotein B100 in rat hepatoma McA-RH7777 cells. *Journal of Biological Chemistry.* 2002;277(34):31187-31200.
55. Tran K, Sun F, Cui Z, et al. Attenuated secretion of very low density lipoproteins from McA-RH7777 cells treated with eicosapentaenoic acid is associated with impaired utilization of triacylglycerol synthesized via phospholipid remodeling. *Biochimica et Biophysica Acta (BBA)-Molecular and Cell Biology of Lipids.* 2006;1761(4):463-473.
56. Bandsma RH, Wiegman CH, Herling AW, et al. Acute inhibition of glucose-6-phosphate translocator activity leads to increased de novo lipogenesis and development of hepatic steatosis without affecting VLDL production in rats. *Diabetes.* 2001;50(11):2591-2597.
57. Wiegman CH, Bandsma RH, Ouwens M, et al. Hepatic VLDL production in ob/ob mice is not stimulated by massive de novo lipogenesis but is less sensitive to the suppressive effects of insulin. *Diabetes.* 2003;52(5):1081-1089.
58. Schonfeld G, Pfleger B. Utilization of exogenous free fatty acids for the production of very low density lipoprotein triglyceride by livers of carbohydrate-fed rats. *Journal of lipid research.* 1971;12(5):614-621.
59. Hostetler HA, McIntosh AL, Atshaves BP, et al. L-FABP directly interacts with PPARα in cultured primary hepatocytes. *Journal of Lipid Research.* 2009;50(8):1663-1675.
60. Huang H, McIntosh AL, Martin GG, et al. FABP1: a novel hepatic endocannabinoid and cannabinoid binding protein. *Biochemistry.* 2016;55(37):5243-5255.
61. Prows DR, Murphy EJ, Schroeder F. Intestinal and liver fatty acid binding proteins differentially affect fatty acid uptake and esterification in L-cells. *Lipids.* 1995;30(10):907-910.
62. Murphy EJ. L-FABP and I-FABP expression increase NBD-stearate uptake and cytoplasmic diffusion in L cells. *The American journal of physiology.* 1998;275(2 Pt 1):G244-249.
63. Wolfrum C, Buhlmann C, Rolf B, Börchers T, Spener F. Variation of liver-type fatty acid binding protein content in the human hepatoma cell line HepG2 by peroxisome proliferators and antisense RNA affects the rate of fatty acid uptake. *Biochimica et Biophysica Acta (BBA) - Molecular and Cell Biology of Lipids.* 1999;1437(2):194-201.
64. Newberry EP, Xie Y, Kennedy S, et al. Decreased Hepatic Triglyceride Accumulation and Altered Fatty Acid Uptake in Mice with Deletion of the Liver Fatty Acid-binding Protein Gene. *Journal of Biological Chemistry.* 2003;278(51):51664-51672.
65. Martin GG, Danneberg H, Kumar LS, et al. Decreased Liver Fatty Acid Binding Capacity and Altered Liver Lipid Distribution in Mice Lacking the Liver Fatty Acid-binding Protein Gene. *Journal of Biological Chemistry.* 2003;278(24):21429-21438.
66. Erol E, Kumar LS, Cline GW, Shulman GI, Kelly DP, Binas B. Liver fatty acid-binding protein is required for high rates of hepatic fatty acid oxidation but not for the action of PPAR-α in fasting mice. *The FASEB Journal.* 2003.
67. Francis GA, Fayard E, Picard F, Auwerx J. Nuclear receptors and the control of metabolism. *Annual review of physiology.* 2003;65(1):261-311.
68. Kersten S, Desvergne B, Wahli W. Roles of PPARs in health and disease. *Nature.* 2000;405(6785):421-424.
69. Coe NR, Bernlohr DA. Physiological properties and functions of intracellular fatty acid-binding proteins. *Biochimica et biophysica acta.* 1998;1391(3):287-306.
70. Lee SS, Pineau T, Drago J, et al. Targeted disruption of the alpha isoform of the peroxisome proliferator-activated receptor gene in mice results in abolishment of the pleiotropic effects of peroxisome proliferators. *Molecular and cellular biology.* 1995;15(6):3012-3022.

71. Akiyama TE, Ward JM, Gonzalez FJ. Regulation of the Liver Fatty Acid-binding Protein Gene by Hepatocyte Nuclear Factor 1α (HNF1α): ALTERATIONS IN FATTY ACID HOMEOSTASIS INHNF1α-DEFICIENT MICE. *Journal of Biological Chemistry.* 2000;275(35):27117-27122.
72. Wang G, Chen QM, Minuk GY, Gong Y, Burczynski FJ. Enhanced expression of cytosolic fatty acid binding protein and fatty acid uptake during liver regeneration in rats. *Molecular and cellular biochemistry.* 2004;262(1-2):41-49.
73. Sorof S, Custer RP. Elevated expression and cell cycle deregulation of a mitosis-associated target polypeptide of a carcinogen in hyperplastic and malignant rat hepatocytes. *Cancer research.* 1987;47(1):210-220.
74. Larsen R, Gouveia Z, Soares MP, Gozzelino R. Heme cytotoxicity and the pathogenesis of immune-mediated inflammatory diseases. *Frontiers in pharmacology.* 2012;3:77.
75. Raza H, Pongubala JR, Sorof S. Specific high affinity binding of lipoxygenase metabolites of arachidonic acid by liver fatty acid binding protein. *Biochemical and biophysical research communications.* 1989;161(2):448-455.
76. Samanta A, Das DK, Jones R, George A, Prasad MR. Free radical scavenging by myocardial fatty acid binding protein. *Free radical research communications.* 1989;7(2):73-82.
77. Ek BA, Cistola DP, Hamilton JA, Kaduce TL, Spector AA. Fatty acid binding proteins reduce 15-lipoxygenase-induced oxygenation of linoleic acid and arachidonic acid. *Biochimica et Biophysica Acta (BBA)-Lipids and Lipid Metabolism.* 1997;1346(1):75-85.
78. Ek-von Mentzer BA, Zhang F, Hamilton JA. Binding of 13-HODE and 15-HETE to phospholipid bilayers, albumin andintracellular fatty acid binding proteins (FABP): implications fortransmembrane and intracellular transport, and for protection from lipidperoxidation. *Journal of Biological Chemistry.* 2001.
79. Wang G, Shen H, Rajaraman G, et al. Expression and antioxidant function of liver fatty acid binding protein in normal and bile-duct ligated rats. *European journal of pharmacology.* 2007;560(1):61-68.
80. Smathers RL, Galligan JJ, Shearn CT, et al. Susceptibility of L-FABP$^{-/-}$mice to oxidative stress in early-stage alcoholic liver. *Journal of lipid research.* 2013:jlr. M034892.
81. Lagakos WS, Gajda AM, Agellon L, et al. Different functions of intestinal and liver-type fatty acid-binding proteins in intestine and in whole body energy homeostasis. *American journal of physiology Gastrointestinal and liver physiology.* 2011;300(5):G803-814.
82. Newberry EP, Kennedy SM, Xie Y, Luo J, Davidson NO. Diet-induced alterations in intestinal and extrahepatic lipid metabolism in liver fatty acid binding protein knockout mice. *Molecular and cellular biochemistry.* 2009;326(1):79-86.
83. Newberry EP, Kennedy SM, Xie Y, Sternard BT, Luo J, Davidson NO. Diet-induced obesity and hepatic steatosis in L-Fabp^{−/−} mice is abrogated with SF, but not PUFA, feeding and attenuated after cholesterol supplementation. *American Journal of Physiology - Gastrointestinal and Liver Physiology.* 2008;294(1):G307-G314.
84. Newberry EP, Xie Y, Kennedy SM, Luo J, Davidson NO. Protection against Western diet–induced obesity and hepatic steatosis in liver fatty acid–binding protein knockout mice. *Hepatology.* 2006;44(5):1191-1205.
85. Atshaves BP, McIntosh AL, Storey SM, Landrock KK, Kier AB, Schroeder F. High dietary fat exacerbates weight gain and obesity in female liver fatty acid binding protein gene-ablated mice. *Lipids.* 2010;45(2):97-110.

86. Martin GG, Atshaves BP, McIntosh AL, Mackie JT, Kier AB, Schroeder F. Liver Fatty Acid-Binding Protein Gene-Ablated Female Mice Exhibit Increased Age-Dependent Obesity. *The Journal of nutrition.* 2008;138(10):1859-1865.
87. Martin GG, Atshaves BP, McIntosh AL, Mackie JT, Kier AB, Schroeder F. Liver fatty acid binding protein gene ablation potentiates hepatic cholesterol accumulation in cholesterol-fed female mice. *American journal of physiology Gastrointestinal and liver physiology.* 2006;290(1):G36-48.
88. Gajda AM, Zhou YX, Agellon LB, et al. Direct Comparison of Mice Null for Liver or Intestinal Fatty Acid-binding Proteins Reveals Highly Divergent Phenotypic Responses to High Fat Feeding. *Journal of Biological Chemistry.* 2013;288(42):30330-30344.
89. Brooks GA, Fahey TD, White TP. *Exercise physiology: Human bioenergetics and its applications.* Mayfield publishing company; 1996.
90. Robergs RA, Roberts SO. *Exercise physiology: exercise, performance, and clinical applications.* Mosby St. Louis; 1997.
91. Mclester JR. Muscle contraction and fatigue. *Sports Medicine.* 1997;23(5):287-305.
92. Green H. Mechanisms of muscle fatigue in intense exercise. *Journal of sports sciences.* 1997;15(3):247-256.
93. Wan J-j, Qin Z, Wang P-y, Sun Y, Liu X. Muscle fatigue: general understanding and treatment. *Experimental & molecular medicine.* 2017;49(10):e384.
94. Kravitz L, Dalleck LC. Physiological factors limiting endurance exercise capacity. *IDEA Health & Fitness Association Advanced sports conditioning for enhanced performance IDEA Resource Series.* 2002:21-27.
95. Bassett Jr DR, Howley ET. Limiting factors for maximum oxygen uptake and determinants of endurance performance. *Medicine & Science in Sports & Exercise.* 2000;32(1):70.
96. Costill DL. Metabolic responses during distance running. *Journal of Applied Physiology.* 1970;28(3):251-255.
97. Robergs RA, Roberts S. *Exercise physiology: exercise, performance, and clinical applications.* Mosby St. Louis; 1997.
98. Davies KJA, Packer L, Brooks GA. Biochemical adaptation of mitochondria, muscle, and whole-animal respiration to endurance training. *Archives of Biochemistry and Biophysics.* 1981;209(2):539-554.
99. Brooks GA, Mercier J. Balance of carbohydrate and lipid utilization during exercise: the "crossover" concept. *Journal of Applied Physiology.* 1994;76(6):2253-2261.
100. Romijn JA, Coyle EF, Sidossis LS, et al. Regulation of endogenous fat and carbohydrate metabolism in relation to exercise intensity and duration. *American Journal of Physiology - Endocrinology And Metabolism.* 1993;265(3):E380-E391.
101. Petersen KF, Dufour S, Savage DB, et al. The role of skeletal muscle insulin resistance in the pathogenesis of the metabolic syndrome. *Proceedings of the National Academy of Sciences of the United States of America.* 2007;104(31):12587-12594.
102. Regensteiner JG, Sippel J, McFarling ET, Wolfel EE, Hiatt WR. Effects of non-insulin-dependent diabetes on oxygen consumption during treadmill exercise. *Med Sci Sports Exerc.* 1995;27(5):661-667.
103. Salvadori A, Fanari P, Fontana M, et al. Oxygen uptake and cardiac performance in obese and normal subjects during exercise. *Respiration.* 1999;66(1):25-33.
104. Blair SN, Brodney S. Effects of physical inactivity and obesity on morbidity and mortality: current evidence and research issues. *Medicine and science in sports and exercise.* 1999;31:S646-S662.

105. Wei M, Gibbons LW, Kampert JB, Nichaman MZ, Blair SN. Low cardiorespiratory fitness and physical inactivity as predictors of mortality in men with type 2 diabetes. *Annals of internal medicine.* 2000;132(8):605-611.
106. Murray AJ, Knight NS, Cochlin LE, et al. Deterioration of physical performance and cognitive function in rats with short-term high-fat feeding. *The FASEB Journal.* 2009;23(12):4353-4360.
107. Xiao Y, Wang W, Chen L, et al. The effects of short-term high-fat feeding on exercise capacity: multi-tissue transcriptome changes by RNA sequencing analysis. *Lipids in health and disease.* 2017;16(1):28.
108. Schiaffino S, Reggiani C. Fiber types in mammalian skeletal muscles. *Physiological reviews.* 2011;91(4):1447-1531.
109. Egan B, Zierath Juleen R. Exercise Metabolism and the Molecular Regulation of Skeletal Muscle Adaptation. *Cell metabolism.* 2013;17(2):162-184.
110. Lee SR, Khamoui AV, Jo E, Park BS. Effects of chronic high-fat feeding on skeletal muscle mass and function in middle-aged mice. *Aging clinical and ….* 2015.
111. Lin J, Wu H, Tarr PT, et al. Transcriptional co-activator PGC-1 alpha drives the formation of slow-twitch muscle fibres. *Nature.* 2002;418(6899):797-801.
112. Reyes NL, Banks GB, Tsang M, et al. Fnip1 regulates skeletal muscle fiber type specification, fatigue resistance, and susceptibility to muscular dystrophy. *Proceedings of the National Academy of Sciences of the United States of America.* 2015;112(2):424-429.
113. Phillips SM, Green HJ, Tarnopolsky MA, Heigenhauser GJ, Grant SM. Progressive effect of endurance training on metabolic adaptations in working skeletal muscle. *The American journal of physiology.* 1996;270(2 Pt 1):E265-272.
114. Leblanc PJ, Howarth KR, Gibala MJ, Heigenhauser GJ. Effects of 7 wk of endurance training on human skeletal muscle metabolism during submaximal exercise. *Journal of applied physiology (Bethesda, Md : 1985).* 2004;97(6):2148-2153.
115. Stuart CA, McCurry MP, Marino A, et al. Slow-twitch fiber proportion in skeletal muscle correlates with insulin responsiveness. *The Journal of clinical endocrinology and metabolism.* 2013;98(5):2027-2036.
116. Oberbach A, Bossenz Y, Lehmann S, et al. Altered fiber distribution and fiber-specific glycolytic and oxidative enzyme activity in skeletal muscle of patients with type 2 diabetes. *Diabetes care.* 2006;29(4):895-900.
117. Tanner CJ, Barakat HA, Dohm GL, et al. Muscle fiber type is associated with obesity and weight loss. *American journal of physiology Endocrinology and metabolism.* 2002;282(6):E1191-1196.
118. DeNies MS, Johnson J, Maliphol AB, et al. Diet‐induced obesity alters skeletal muscle fiber types of male but not female mice. *Physiological reports.* 2014;2(1):e00204.
119. Hua N, Takahashi H, Yee GM, et al. Influence of muscle fiber type composition on early fat accumulation under high-fat diet challenge. *PloS one.* 2017;12(8):e0182430.
120. Shortreed KE, Krause MP, Huang JH, et al. Muscle-specific adaptations, impaired oxidative capacity and maintenance of contractile function characterize diet-induced obese mouse skeletal muscle. *PloS one.* 2009;4(10):e7293.
121. Chanseaume E, Malpuech-Brugère C, Patrac V, et al. Diets High in Sugar, Fat, and Energy Induce Muscle Type–Specific Adaptations in Mitochondrial Functions in Rats. *The Journal of nutrition.* 2006;136(8):2194-2200.

122. Trajcevski KE, O'Neill HM, Wang DC, et al. Enhanced lipid oxidation and maintenance of muscle insulin sensitivity despite glucose intolerance in a diet-induced obesity mouse model. *PLoS One.* 2013;8(8):e71747.
123. de Wilde J, Mohren R, van den Berg S, et al. Short-term high fat-feeding results in morphological and metabolic adaptations in the skeletal muscle of C57BL/6J mice. *Physiological genomics.* 2008;32(3):360-369.
124. Turner N, Bruce CR, Beale SM, et al. Excess lipid availability increases mitochondrial fatty acid oxidative capacity in muscle: evidence against a role for reduced fatty acid oxidation in lipid-induced insulin resistance in rodents. *Diabetes.* 2007;56(8):2085-2092.
125. Eshima H, Tamura Y, Kakehi S, et al. Long‐term, but not short‐term high‐fat diet induces fiber composition changes and impaired contractile force in mouse fast‐twitch skeletal muscle. *Physiological reports.* 2017;5(7):e13250.
126. Almond RE, Cawthorne MA, Enser M. Muscles of diabetic (db/db) mice: fibre size, fibre type and the effects of a thermogenic, beta-adrenoceptor agonist. *International journal of obesity.* 1988;12(1):81-91.
127. Warmington SA, Tolan R, McBennett S. Functional and histological characteristics of skeletal muscle and the effects of leptin in the genetically obese (ob/ob) mouse. *International journal of obesity and related metabolic disorders : journal of the International Association for the Study of Obesity.* 2000;24(8):1040-1050.
128. Bayley JS, Pedersen TH, Nielsen OB. Skeletal muscle dysfunction in the db/db mouse model of type 2 diabetes. 2016;54(3):460-468.
129. Hardie DG. Energy sensing by the AMP-activated protein kinase and its effects on muscle metabolism. *Proceedings of the Nutrition Society.* 2011;70(1):92-99.
130. Narkar VA, Downes M, Ruth TY, et al. AMPK and PPARδ agonists are exercise mimetics. *Cell.* 2008;134(3):405-415.
131. Ventura-Clapier R, Garnier A, Veksler V. Transcriptional control of mitochondrial biogenesis: the central role of PGC-1α. *Cardiovascular research.* 2008;79(2):208-217.
132. Gowans GJ, Hardie DG. AMPK: a cellular energy sensor primarily regulated by AMP. Portland Press Limited; 2014.
133. Jornayvaz FR, Shulman GI. Regulation of mitochondrial biogenesis. *Essays in biochemistry.* 2010;47:69-84.
134. Gervois P, Kleemann R, Pilon A, et al. Global suppression of IL-6-induced acute phase response gene expression after chronic in vivo treatment with the peroxisome proliferator-activated receptor-α activator fenofibrate. *Journal of Biological Chemistry.* 2004;279(16):16154-16160.
135. Schoonjans K, Staels B, Auwerx J. The peroxisome proliferator activated receptors (PPARS) and their effects on lipid metabolism and adipocyte differentiation. *Biochimica et Biophysica Acta (BBA)-Lipids and Lipid Metabolism.* 1996;1302(2):93-109.
136. Rosen ED, Walkey CJ, Puigserver P, Spiegelman BM. Transcriptional regulation of adipogenesis. *Genes & development.* 2000;14(11):1293-1307.
137. Gavrilova O, Haluzik M, Matsusue K, et al. Liver peroxisome proliferator-activated receptor γ contributes to hepatic steatosis, triglyceride clearance, and regulation of body fat mass. *Journal of Biological Chemistry.* 2003;278(36):34268-34276.
138. Luquet S, Gaudel C, Holst D, et al. Roles of PPAR delta in lipid absorption and metabolism: a new target for the treatment of type 2 diabetes. *Biochimica et Biophysica Acta (BBA)-Molecular Basis of Disease.* 2005;1740(2):313-317.

139. Kidani Y, Bensinger SJ. Liver X receptor and peroxisome proliferator‐activated receptor as integrators of lipid homeostasis and immunity. *Immunological reviews.* 2012;249(1):72-83.
140. Peet DJ, Turley SD, Ma W, et al. Cholesterol and bile acid metabolism are impaired in mice lacking the nuclear oxysterol receptor LXRα. *Cell.* 1998;93(5):693-704.
141. Janowski BA, Willy PJ, Devi TR, Falck J, Mangelsdorf DJ. An oxysterol signalling pathway mediated by the nuclear receptor LXRα. *Nature.* 1996;383(6602):728.
142. Luo Y, Tall AR. Sterol upregulation of human CETP expression in vitro and in transgenic mice by an LXR element. *The Journal of clinical investigation.* 2000;105(4):513-520.
143. Venkateswaran A, Laffitte BA, Joseph SB, et al. Control of cellular cholesterol efflux by the nuclear oxysterol receptor LXRα. *Proceedings of the National Academy of Sciences.* 2000;97(22):12097-12102.
144. Repa JJ, Liang G, Ou J, et al. Regulation of mouse sterol regulatory element-binding protein-1c gene (SREBP-1c) by oxysterol receptors, LXRα and LXRβ. *Genes & development.* 2000;14(22):2819-2830.
145. Yoshikawa T, Ide T, Shimano H, et al. Cross-talk between peroxisome proliferator-activated receptor (PPAR) α and liver X receptor (LXR) in nutritional regulation of fatty acid metabolism. I. PPARs suppress sterol regulatory element binding protein-1c promoter through inhibition of LXR signaling. *Molecular Endocrinology.* 2003;17(7):1240-1254.
146. Kim JB. Dynamic cross talk between metabolic organs in obesity and metabolic diseases. Nature Publishing Group; 2016.
147. Roh E, Song DK, Kim M-S. Emerging role of the brain in the homeostatic regulation of energy and glucose metabolism. *Experimental & molecular medicine.* 2016;48(3):e216.
148. Tripathi A, Debelius J, Brenner DA, et al. The gut–liver axis and the intersection with the microbiome. *Nature Reviews Gastroenterology & Hepatology.* 2018:1.
149. Kong B, Wang L, Chiang JY, Zhang Y, Klaassen CD, Guo GL. Mechanism of tissue‐specific farnesoid X receptor in suppressing the expression of genes in bile‐acid synthesis in mice. *Hepatology.* 2012;56(3):1034-1043.
150. Kim I, Ahn S-H, Inagaki T, et al. Differential regulation of bile acid homeostasis by the farnesoid X receptor in liver and intestine. *Journal of lipid research.* 2007;48(12):2664-2672.
151. Watanabe M, Houten SM, Wang L, et al. Bile acids lower triglyceride levels via a pathway involving FXR, SHP, and SREBP-1c. *The Journal of clinical investigation.* 2004;113(10):1408-1418.
152. Kamada Y, Tamura S, Kiso S, et al. Enhanced carbon tetrachloride-induced liver fibrosis in mice lacking adiponectin. *Gastroenterology.* 2003;125(6):1796-1807.
153. Park P-H, Sanz-Garcia C, Nagy LE. Adiponectin as an anti-fibrotic and anti-inflammatory adipokine in the liver. *Current pathobiology reports.* 2015;3(4):243-252.
154. Balmer ML, Joneli J, Schoepfer A, Stickel F, Thormann W, Dufour J-F. Significance of serum adiponectin levels in patients with chronic liver disease. *Clinical science.* 2010;119(10):431-436.
155. R Moschen A, Wieser V, Tilg H. Adiponectin: key player in the adipose tissue-liver crosstalk. *Current medicinal chemistry.* 2012;19(32):5467-5473.
156. Yamauchi T, Kamon J, Minokoshi Ya, et al. Adiponectin stimulates glucose utilization and fatty-acid oxidation by activating AMP-activated protein kinase. *Nature medicine.* 2002;8(11):1288.

157. Yoon MJ, Lee GY, Chung J-J, Ahn YH, Hong SH, Kim JB. Adiponectin Increases Fatty Acid Oxidation in Skeletal Muscle Cells by Sequential Activation of AMP-Activated Protein Kinase, p38 Mitogen-Activated Protein Kinase, and Peroxisome Proliferator–Activated Receptor α. *Diabetes.* 2006;55(9):2562-2570.
158. Potthoff MJ, Kliewer SA, Mangelsdorf DJ. Endocrine fibroblast growth factors 15/19 and 21: from feast to famine. *Genes & development.* 2012;26(4):312-324.
159. Inagaki T, Dutchak P, Zhao G, et al. Endocrine regulation of the fasting response by PPARα-mediated induction of fibroblast growth factor 21. *Cell metabolism.* 2007;5(6):415-425.
160. Potthoff MJ, Inagaki T, Satapati S, et al. FGF21 induces PGC-1α and regulates carbohydrate and fatty acid metabolism during the adaptive starvation response. *Proceedings of the National Academy of Sciences.* 2009;106(26):10853-10858.
161. Badman MK, Pissios P, Kennedy AR, Koukos G, Flier JS, Maratos-Flier E. Hepatic fibroblast growth factor 21 is regulated by PPARα and is a key mediator of hepatic lipid metabolism in ketotic states. *Cell metabolism.* 2007;5(6):426-437.
162. Adams AC, Yang C, Coskun T, et al. The breadth of FGF21's metabolic actions are governed by FGFR1 in adipose tissue. *Molecular metabolism.* 2013;2(1):31-37.
163. Véniant MM, Hale C, Helmering J, et al. FGF21 promotes metabolic homeostasis via white adipose and leptin in mice. *PloS one.* 2012;7(7):e40164.
164. Chau MD, Gao J, Yang Q, Wu Z, Gromada J. Fibroblast growth factor 21 regulates energy metabolism by activating the AMPK–SIRT1–PGC-1α pathway. *Proceedings of the National Academy of Sciences.* 2010;107(28):12553-12558.
165. Chen W, Hoo RL-c, Konishi M, et al. Growth hormone induces hepatic production of fibroblast growth factor 21 through a mechanism dependent on lipolysis in adipocytes. *Journal of Biological Chemistry.* 2011;286(40):34559-34566.
166. Kharitonenkov A, Shiyanova TL, Koester A, et al. FGF-21 as a novel metabolic regulator. *Journal of Clinical Investigation.* 2005;115(6):1627.
167. Kharitonenkov A, Shiyanova TL, Koester A, et al. FGF-21 as a novel metabolic regulator. *Journal of Clinical Investigation.* 2005;115(6):1627-1635.
168. Kharitonenkov A, Wroblewski VJ, Koester A, et al. The metabolic state of diabetic monkeys is regulated by fibroblast growth factor-21. *Endocrinology.* 2007;148(2):774-781.
169. Coskun T, Bina HA, Schneider MA, et al. Fibroblast growth factor 21 corrects obesity in mice. *Endocrinology.* 2008;149(12):6018-6027.
170. Xu J, Lloyd DJ, Hale C, et al. Fibroblast growth factor 21 reverses hepatic steatosis, increases energy expenditure, and improves insulin sensitivity in diet-induced obese mice. *Diabetes.* 2009;58(1):250-259.
171. Jimenez V, Jambrina C, Casana E, et al. FGF21 gene therapy as treatment for obesity and insulin resistance. *EMBO molecular medicine.* 2018;10(8):e8791.
172. Jeon JY, Choi S-E, Ha ES, et al. Association between insulin resistance and impairment of FGF21 signal transduction in skeletal muscles. *Endocrine.* 2016;53(1):97-106.
173. Mashili FL, Austin RL, Deshmukh AS, et al. Direct effects of FGF21 on glucose uptake in human skeletal muscle: implications for type 2 diabetes and obesity. *Diabetes/Metabolism Research and Reviews.* 2011;27(3):286-297.
174. Lin Z, Tian H, Lam Karen SL, et al. Adiponectin Mediates the Metabolic Effects of FGF21 on Glucose Homeostasis and Insulin Sensitivity in Mice. *Cell metabolism.* 2013;17(5):779-789.

175. Yamauchi T, Kamon J, Waki H, et al. The fat-derived hormone adiponectin reverses insulin resistance associated with both lipoatrophy and obesity. *Nature medicine.* 2001;7(8):941.
176. Xu A, Wang Y, Keshaw H, Xu LY, Lam KS, Cooper GJ. The fat-derived hormone adiponectin alleviates alcoholic and nonalcoholic fatty liver diseases in mice. *Journal of Clinical Investigation.* 2003;112(1):91.
177. Civitarese AE, Ukropcova B, Carling S, et al. Role of adiponectin in human skeletal muscle bioenergetics. *Cell metabolism.* 2006;4(1):75-87.
178. Dutchak PA, Katafuchi T, Bookout AL, et al. Fibroblast growth factor-21 regulates PPARγ activity and the antidiabetic actions of thiazolidinediones. *Cell.* 2012;148(3):556-567.
179. Nawrocki AR, Rajala MW, Tomas E, et al. Mice lacking adiponectin show decreased hepatic insulin sensitivity and reduced responsiveness to peroxisome proliferator-activated receptor γ agonists. *Journal of Biological Chemistry.* 2006;281(5):2654-2660.
180. Zhang X, Yeung DC, Karpisek M, et al. Serum FGF21 levels are increased in obesity and are independently associated with the metabolic syndrome in humans. *Diabetes.* 2008;57(5):1246-1253.
181. Muise ES, Kuo DW, El-Sherbeini M, et al. Adipose fibroblast growth factor 21 is up-regulated by PPARγ and altered metabolic states. *Molecular pharmacology.* 2008.
182. Nygaard EB, Møller CL, Kievit P, Grove KL, Andersen B. Increased Fibroblast Growth Factor 21 expression in high-fat diet sensitive non-human primates (Macaca mulatta). *International journal of obesity (2005).* 2014;38(2):183.
183. Berglund ED, Li CY, Bina HA, et al. Fibroblast growth factor 21 controls glycemia via regulation of hepatic glucose flux and insulin sensitivity. *Endocrinology.* 2009;150(9):4084-4093.
184. Fisher fM, Chui PC, Antonellis PJ, et al. Obesity Is a Fibroblast Growth Factor 21 (FGF21)-Resistant State. *Diabetes.* 2010;59(11):2781-2789.
185. Hale C, Chen MM, Stanislaus S, et al. Lack of Overt FGF21 Resistance in Two Mouse Models of Obesity and Insulin Resistance. *Endocrinology.* 2012;153(1):69-80.
186. Savage DB, Petersen KF, Shulman GI. Disordered lipid metabolism and the pathogenesis of insulin resistance. *Physiological reviews.* 2007;87(2):507-520.
187. Unger RH. Minireview: weapons of lean body mass destruction: the role of ectopic lipids in the metabolic syndrome. *Endocrinology.* 2003;144(12):5159-5165.
188. Thompson J, Winter N, Terwey D, Bratt J, Banaszak L. The crystal structure of the liver fatty acid-binding protein. A complex with two bound oleates. *The Journal of biological chemistry.* 1997;272(11):7140-7150.
189. Lagakos WS, Guan X, Ho S-Y, et al. Liver fatty acid-binding protein binds monoacylglycerol in vitro and in mouse liver cytosol. *Journal of Biological Chemistry.* 2013;288(27):19805-19815.
190. Kersten S, Desvergne B, Wahli W. Roles of PPARs in health and disease. *Nature.* 2000;405(6785):421.
191. Martin GG, Atshaves BP, Mcintosh AL, Mackie JT, Kier AB, Schroeder F. Liver fatty-acid-binding protein (L-FABP) gene ablation alters liver bile acid metabolism in male mice. *Biochemical Journal.* 2005;391(3):549-560.
192. McLean J, Tobin G. *Animal and human calorimetry.* Cambridge University Press; 1987.
193. Leonardi R, Rehg JE, Rock CO, Jackowski S. Pantothenate kinase 1 is required to support the metabolic transition from the fed to the fasted state. *PloS one.* 2010;5(6):e11107.

194. Folch J, Lees M, Sloane-Stanley G. A simple method for the isolation and purification of total lipids from animal tissues. *The Journal of biological chemistry.* 1957;226(1):497-509.
195. Passonneau JV, Lauderdale VR. A comparison of three methods of glycogen measurement in tissues. *Analytical biochemistry.* 1974;60(2):405-412.
196. Xu K, Zheng X, Sehgal A. Regulation of Feeding and Metabolism by Neuronal and Peripheral Clocks in Drosophila. *Cell metabolism.* 2008;8(4):289-300.
197. Spinazzi M, Casarin A, Pertegato V, Salviati L, Angelini C. Assessment of mitochondrial respiratory chain enzymatic activities on tissues and cultured cells. *Nature protocols.* 2012;7(6):1235.
198. O'Neill HM, Maarbjerg SJ, Crane JD, et al. AMP-activated protein kinase (AMPK) β1β2 muscle null mice reveal an essential role for AMPK in maintaining mitochondrial content and glucose uptake during exercise. *Proceedings of the National Academy of Sciences.* 2011;108(38):16092-16097.
199. Huynh FK, Green MF, Koves TR, Hirschey MD. Measurement of Fatty Acid Oxidation Rates in Animal Tissues and Cell Lines. *Methods in enzymology.* 2014;542:391-405.
200. Hirschey MD, Verdin E. Measuring fatty acid oxidation in tissue homogenates. 2010.
201. Garcia-Cazarin ML, Snider NN, Andrade FH. Mitochondrial isolation from skeletal muscle. *Journal of visualized experiments: JoVE.* 2011(49).
202. Nishiumi S, Ashida H. Rapid preparation of a plasma membrane fraction from adipocytes and muscle cells: application to detection of translocated glucose transporter 4 on the plasma membrane. *Bioscience, biotechnology, and biochemistry.* 2007;71(9):2343-2346.
203. Koopman R, Schaart G, Hesselink MK. Optimisation of oil red O staining permits combination with immunofluorescence and automated quantification of lipids. *Histochemistry and Cell Biology.* 2001;116(1):63-68.
204. Evans AM, DeHaven CD, Barrett T, Mitchell M, Milgram E. Integrated, nontargeted ultrahigh performance liquid chromatography/electrospray ionization tandem mass spectrometry platform for the identification and relative quantification of the small-molecule complement of biological systems. *Analytical chemistry.* 2009;81(16):6656-6667.
205. Boudonck KJ, Mitchell MW, Német L, et al. Discovery of metabolomics biomarkers for early detection of nephrotoxicity. *Toxicologic pathology.* 2009;37(3):280-292.
206. DeHaven CD, Evans AM, Dai H, Lawton KA. Organization of GC/MS and LC/MS metabolomics data into chemical libraries. *Journal of cheminformatics.* 2010;2(1):9.
207. Koves TR, Ussher JR, Noland RC, et al. Mitochondrial overload and incomplete fatty acid oxidation contribute to skeletal muscle insulin resistance. *Cell metabolism.* 2008;7(1):45-56.
208. Lee-Young RS, Ayala JE, Fueger PT, Mayes WH, Kang L, Wasserman DH. Obesity impairs skeletal muscle AMPK signaling during exercise: role of AMPKα2 in the regulation of exercise capacity in vivo. *International journal of obesity (2005).* 2011;35(7):982-989.
209. Yokota T, Kinugawa S, Hirabayashi K, et al. Oxidative stress in skeletal muscle impairs mitochondrial respiration and limits exercise capacity in type 2 diabetic mice. *American Journal of Physiology - Heart and Circulatory Physiology.* 2009;297(3):H1069-H1077.
210. Borghouts L, Keizer H. Exercise and insulin sensitivity: a review. *International journal of sports medicine.* 2000;21(01):1-12.
211. Hawley JA. Exercise as a therapeutic intervention for the prevention and treatment of insulin resistance. *Diabetes/metabolism research and reviews.* 2004;20(5):383-393.

212. Phillips CM. Metabolically healthy obesity: definitions, determinants and clinical implications. *Reviews in Endocrine and Metabolic Disorders.* 2013;14(3):219-227.
213. Blüher M. MECHANISMS IN ENDOCRINOLOGY: Are metabolically healthy obese individuals really healthy? *European journal of endocrinology.* 2014:EJE-14-0540.
214. Stefan N, Häring H-U, Hu FB, Schulze MB. Metabolically healthy obesity: epidemiology, mechanisms, and clinical implications. *The lancet Diabetes & endocrinology.* 2013;1(2):152-162.
215. Appleton SL, Seaborn CJ, Visvanathan R, et al. Diabetes and cardiovascular disease outcomes in the metabolically healthy obese phenotype: a cohort study. *Diabetes care.* 2013:DC_121971.
216. Soriguer F, Gutiérrez-Repiso C, Rubio-Martín E, et al. Metabolically healthy but obese, a matter of time? Findings from the prospective Pizarra study. *The Journal of Clinical Endocrinology & Metabolism.* 2013;98(6):2318-2325.
217. Jung CH, Lee WJ, Song K-H. Metabolically healthy obesity: a friend or foe? *The Korean journal of internal medicine.* 2017;32(4):611.
218. Ebeling P, Koistinen HA, Koivisto VA. Insulin‐independent glucose transport regulates insulin sensitivity. *FEBS letters.* 1998;436(3):301-303.
219. Eaton S. Control of mitochondrial β-oxidation flux. *Progress in lipid research.* 2002;41(3):197-239.
220. Finck BN, Bernal-Mizrachi C, Han DH, et al. A potential link between muscle peroxisome proliferator-activated receptor-α signaling and obesity-related diabetes. *Cell metabolism.* 2005;1(2):133-144.
221. Guerre-Millo M, Rouault C, Poulain P, et al. PPAR-α–null mice are protected from high-fat diet–induced insulin resistance. *Diabetes.* 2001;50(12):2809-2814.
222. Bouzakri K, Austin R, Rune A, et al. Malonyl coenzyme A decarboxylase regulates lipid and glucose metabolism in human skeletal muscle. *Diabetes.* 2008.
223. Choi CS, Befroy DE, Codella R, et al. Paradoxical effects of increased expression of PGC-1α on muscle mitochondrial function and insulin-stimulated muscle glucose metabolism. *Proceedings of the National Academy of Sciences.* 2008:pnas. 0810339105.
224. Montgomery MK, Turner N. Mitochondrial dysfunction and insulin resistance: an update. *Endocrine connections.* 2014:EC-14-0092.
225. Brooks GA, Mercier J. Balance of carbohydrate and lipid utilization during exercise: the" crossover" concept. *Journal of applied physiology.* 1994;76(6):2253-2261.
226. Romijn J, Coyle E, Sidossis L, et al. Regulation of endogenous fat and carbohydrate metabolism in relation to exercise intensity and duration. *American Journal of Physiology-Endocrinology And Metabolism.* 1993;265(3):E380-E391.
227. Wasserman DH, Lacy DB, Bracy D, Williams PE. Metabolic regulation in peripheral tissues and transition to increased gluconeogenic mode during prolonged exercise. *American Journal of Physiology-Endocrinology And Metabolism.* 1992;263(2):E345-E354.
228. Lewis GD, Farrell L, Wood MJ, et al. Metabolic signatures of exercise in human plasma. *Science translational medicine.* 2010;2(33):33ra37-33ra37.
229. Carabotti M, Scirocco A, Maselli MA, Severi C. The gut-brain axis: interactions between enteric microbiota, central and enteric nervous systems. *Annals of gastroenterology: quarterly publication of the Hellenic Society of Gastroenterology.* 2015;28(2):203.
230. Kirpich IA, Marsano LS, McClain CJ. Gut–liver axis, nutrition, and non-alcoholic fatty liver disease. *Clinical biochemistry.* 2015;48(13):923-930.
231. Poeta M, Pierri L, Vajro P. Gut–liver axis derangement in non-alcoholic fatty liver disease. *Children.* 2017;4(8):66.

232. Yi C-X, Tschöp MH. Brain–gut–adipose-tissue communication pathways at a glance. *Disease models & mechanisms.* 2012;5(5):583-587.
233. Pravenec M, Kazdová L, Landa V, et al. Transgenic and recombinant resistin impair skeletal muscle glucose metabolism in the spontaneously hypertensive rat. *Journal of Biological Chemistry.* 2003.
234. Calabro P, Samudio I, Willerson JT, Yeh ET. Resistin promotes smooth muscle cell proliferation through activation of extracellular signal–regulated kinase 1/2 and phosphatidylinositol 3-kinase pathways. *Circulation.* 2004;110(21):3335-3340.
235. Sabio G, Das M, Mora A, et al. A stress signaling pathway in adipose tissue regulates hepatic insulin resistance. *Science.* 2008;322(5907):1539-1543.
236. Nov O, Shapiro H, Ovadia H, et al. Interleukin-1β regulates fat-liver crosstalk in obesity by auto-paracrine modulation of adipose tissue inflammation and expandability. *PloS one.* 2013;8(1):e53626.
237. Lihn A, Pedersen SB, Richelsen B. Adiponectin: action, regulation and association to insulin sensitivity. *Obesity reviews.* 2005;6(1):13-21.
238. Ahima RS, Flier JS. Adipose tissue as an endocrine organ. *Trends in Endocrinology & Metabolism.* 2000;11(8):327-332.
239. Yamauchi T, Kamon J, Ito Y, et al. Cloning of adiponectin receptors that mediate antidiabetic metabolic effects. *Nature.* 2003;423(6941):762.
240. Iwabu M, Yamauchi T, Okada-Iwabu M, et al. Adiponectin and AdipoR1 regulate PGC-1α and mitochondria by Ca 2+ and AMPK/SIRT1. *Nature.* 2010;464(7293):1313.
241. Lavasani M, Lu A, Thompson SD, Robbins PD, Huard J, Niedernhofer LJ. Isolation of muscle-derived stem/progenitor cells based on adhesion characteristics to collagen-coated surfaces. *Stem Cells and Aging: Methods and Protocols.* 2013:53-65.
242. Hindi L, McMillan JD, Afroze D, Hindi SM, Kumar A. Isolation, Culturing, and Differentiation of Primary Myoblasts from Skeletal Muscle of Adult Mice. *Bio-protocol.* 2017;7(9).
243. Smith Pe, Krohn RI, Hermanson G, et al. Measurement of protein using bicinchoninic acid. *Analytical biochemistry.* 1985;150(1):76-85.
244. Scheja L, Makowski L, Uysal KT, et al. Altered insulin secretion associated with reduced lipolytic efficiency in aP2$^{-/-}$mice. *Diabetes.* 1999;48(10):1987-1994.
245. Hertzel AV, Smith LA, Berg AH, et al. Lipid metabolism and adipokine levels in fatty acid-binding protein null and transgenic mice. *American Journal of Physiology-Endocrinology and Metabolism.* 2006;290(5):E814-E823.
246. Deng Y-T, Chang T-W, Lee M-S, Lin J-K. Suppression of free fatty acid-induced insulin resistance by phytopolyphenols in C2C12 mouse skeletal muscle cells. *Journal of agricultural and food chemistry.* 2012;60(4):1059-1066.
247. Yang M, Wei D, Mo C, et al. Saturated fatty acid palmitate-induced insulin resistance is accompanied with myotube loss and the impaired expression of health benefit myokine genes in C2C12 myotubes. *Lipids in health and disease.* 2013;12(1):104.
248. Buettner R, Parhofer K, Woenckhaus M, et al. Defining high-fat-diet rat models: metabolic and molecular effects of different fat types. *Journal of molecular endocrinology.* 2006;36(3):485-501.
249. Petersen KF, Dufour S, Savage DB, et al. The role of skeletal muscle insulin resistance in the pathogenesis of the metabolic syndrome. *Proceedings of the National Academy of Sciences.* 2007;104(31):12587-12594.

250. Abbasi F, Brown BW, Lamendola C, McLaughlin T, Reaven GM. Relationship between obesity, insulin resistance, and coronary heart disease risk. *Journal of the American College of Cardiology.* 2002;40(5):937-943.
251. Esteghamati A, Khalilzadeh O, Anvari M, Ahadi MS, Abbasi M, Rashidi A. Metabolic syndrome and insulin resistance significantly correlate with body mass index. *Archives of medical research.* 2008;39(8):803-808.
252. Chung JO, Cho DH, Chung DJ, Chung MY. Associations among body mass index, insulin resistance, and pancreatic β-cell function in Korean patients with new-onset type 2 diabetes. *The Korean journal of internal medicine.* 2012;27(1):66.
253. Li H, Wu G, Fang Q, et al. Fibroblast growth factor 21 increases insulin sensitivity through specific expansion of subcutaneous fat. *Nature communications.* 2018;9(1):272.
254. Goto T, Hirata M, Aoki Y, et al. The hepatokine FGF21 is crucial for peroxisome proliferator-activated receptor-α agonist-induced amelioration of metabolic disorders in obese mice. *Journal of Biological Chemistry.* 2017:jbc. M116. 767590.
255. Kleiner S, Douris N, Fox EC, et al. FGF21 regulates PGC-1α and browning of white adipose tissues in adaptive thermogenesis. *Genes & development.* 2012;26(3):271-281.
256. Snehalatha C, Mukesh B, Simon M, Viswanathan V, Haffner SM, Ramachandran A. Plasma adiponectin is an independent predictor of type 2 diabetes in Asian Indians. *Diabetes care.* 2003;26(12):3226-3229.
257. Duncan BB, Schmidt MI, Pankow JS, et al. Adiponectin and the development of type 2 diabetes: the atherosclerosis risk in communities study. *Diabetes.* 2004;53(9):2473-2478.
258. Ukkola O, Santaniemi M. Adiponectin: a link between excess adiposity and associated comorbidities? *Journal of molecular medicine.* 2002;80(11):696-702.
259. Arita Y, Kihara S, Ouchi N, et al. Paradoxical decrease of an adipose-specific protein, adiponectin, in obesity. *Biochemical and biophysical research communications.* 1999;257(1):79-83.
260. Frederiksen L, Nielsen T, Wraae K, et al. Subcutaneous rather than visceral adipose tissue is associated with adiponectin levels and insulin resistance in young men. *The Journal of Clinical Endocrinology & Metabolism.* 2009;94(10):4010-4015.
261. Rocha VZ, Folco EJ. Inflammatory concepts of obesity. *International journal of inflammation.* 2011;2011.
262. Ouchi N, Walsh K. Adiponectin as an anti-inflammatory factor. *Clinica chimica acta.* 2007;380(1-2):24-30.
263. Furuhashi M, Saitoh S, Shimamoto K, Miura T. Fatty acid-binding protein 4 (FABP4): pathophysiological insights and potent clinical biomarker of metabolic and cardiovascular diseases. *Clinical Medicine Insights: Cardiology.* 2014;8:CMC. S17067.
264. Yang R, Castriota G, Chen Y, et al. RNAi-mediated germline knockdown of FABP4 increases body weight but does not improve the deranged nutrient metabolism of diet-induced obese mice. *International journal of obesity.* 2011;35(2):217.
265. Hotamisligil GS, Johnson RS, Distel RJ, Ellis R, Papaioannou VE, Spiegelman BM. Uncoupling of obesity from insulin resistance through a targeted mutation in aP2, the adipocyte fatty acid binding protein. *Science.* 1996;274(5291):1377-1379.
266. Martin GG, Atshaves BP, Huang H, et al. Hepatic phenotype of liver fatty acid binding protein gene-ablated mice. *American Journal of Physiology-Gastrointestinal and Liver Physiology.* 2009;297(6):G1053-G1065.

267. Oakes ND, Cooney GJ, Camilleri S, Chisholm DJ, Kraegen EW. Mechanisms of liver and muscle insulin resistance induced by chronic high-fat feeding. *Diabetes.* 1997;46(11):1768-1774.
268. Chalkley SM, Hettiarachchi M, Chisholm DJ, Kraegen EW. Five-hour fatty acid elevation increases muscle lipids and impairs glycogen synthesis in the rat. *Metabolism.* 1998;47(9):1121-1126.
269. Chen M-T, Kaufman LN, Spennetta T, Shrago E. Effects of high fat-feeding to rats on the interrelationship of body weight, plasma insulin, and fatty acyl-coenzyme A esters in liver and skeletal muscle. *Metabolism.* 1992;41(5):564-569.
270. Kim J-a, Wei Y, Sowers JR. Role of mitochondrial dysfunction in insulin resistance. *Circulation research.* 2008;102(4):401-414.
271. Pan D, Lillioja S, Kriketos A, et al. Skeletal muscle triglyceride levels are inversely related to insulin action. *Diabetes.* 1997;46(6):983-988.
272. Perseghin G, Scifo P, De Cobelli F, et al. Intramyocellular triglyceride content is a determinant of in vivo insulin resistance in humans: a 1H-13C nuclear magnetic resonance spectroscopy assessment in offspring of type 2 diabetic parents. *Diabetes.* 1999;48(8):1600-1606.
273. Goodpaster BH, He J, Watkins S, Kelley DE. Skeletal muscle lipid content and insulin resistance: evidence for a paradox in endurance-trained athletes. *The Journal of Clinical Endocrinology & Metabolism.* 2001;86(12):5755-5761.
274. DiPatrizio NV, Piomelli D. Intestinal lipid–derived signals that sense dietary fat. *The Journal of clinical investigation.* 2015;125(3):891-898.
275. Ding X, Boney-Montoya J, Owen BM, et al. βKlotho is required for fibroblast growth factor 21 effects on growth and metabolism. *Cell metabolism.* 2012;16(3):387-393.
276. McIntosh AL, Atshaves BP, Hostetler HA, et al. Liver type fatty acid binding protein (L-FABP) gene ablation reduces nuclear ligand distribution and peroxisome proliferator-activated receptor-α activity in cultured primary hepatocytes. *Archives of biochemistry and biophysics.* 2009;485(2):160-173.
277. Kadowaki T, Yamauchi T, Kubota N, Hara K, Ueki K, Tobe K. Adiponectin and adiponectin receptors in insulin resistance, diabetes, and the metabolic syndrome. *Journal of Clinical Investigation.* 2006;116(7):1784.
278. Kurosu H, Choi M, Ogawa Y, et al. Tissue-specific Expression of βKlotho and Fibroblast Growth Factor (FGF) Receptor Isoforms Determines Metabolic Activity of FGF19 and FGF21. *Journal of Biological Chemistry.* 2007;282(37):26687-26695.
279. Frayn KN. Visceral fat and insulin resistance—causative or correlative? *British Journal of Nutrition.* 2000;83(S1):S71-S77.
280. Uysal KT, Scheja L, Wiesbrock SM, Bonner-Weir S, Hotamisligil GkS. Improved glucose and lipid metabolism in genetically obese mice lacking aP2. *Endocrinology.* 2000;141(9):3388-3396.
281. Coe NR, Simpson MA, Bernlohr DA. Targeted disruption of the adipocyte lipid-binding protein (aP2 protein) gene impairs fat cell lipolysis and increases cellular fatty acid levels. *Journal of lipid research.* 1999;40(5):967-972.
282. Xu H, Hertzel AV, Steen KA, Bernlohr DA. Loss of fatty acid binding protein 4/aP2 reduces macrophage inflammation through activation of SIRT3. *Molecular endocrinology.* 2016;30(3):325-334.
283. Fasshauer M, Kralisch S, Klier M, et al. Adiponectin gene expression and secretion is inhibited by interleukin-6 in 3T3-L1 adipocytes. *Biochemical and biophysical research communications.* 2003;301(4):1045-1050.

284. Kappes A, Löffler G. Influences of ionomycin, dibutyryl-cycloAMP and tumour necrosis factor-alpha on intracellular amount and secretion of apM1 in differentiating primary human preadipocytes. *Hormone and Metabolic Research.* 2000;32(11/12):548-554.
285. Choi K, Ryu O, Lee K, et al. Serum adiponectin, interleukin-10 levels and inflammatory markers in the metabolic syndrome. *Diabetes research and clinical practice.* 2007;75(2):235-240.
286. Ouchi N, Kihara S, Funahashi T, et al. Reciprocal association of C-reactive protein with adiponectin in blood stream and adipose tissue. *Circulation.* 2003;107(5):671-674.